IOWA STATE UNIVERSITY
Digital Repository

Retrospective Theses and Dissertations

Iowa State University Capstones, Theses and Dissertations

2004

Photocatalytic degradation of organic contaminants in water

Youn-Chul Oh
Iowa State University

Follow this and additional works at: https://lib.dr.iastate.edu/rtd

 Part of the Inorganic Chemistry Commons, and the Organic Chemistry Commons

Recommended Citation
Oh, Youn-Chul, "Photocatalytic degradation of organic contaminants in water " (2004). *Retrospective Theses and Dissertations*. 1115.
https://lib.dr.iastate.edu/rtd/1115

This Dissertation is brought to you for free and open access by the Iowa State University Capstones, Theses and Dissertations at Iowa State University Digital Repository. It has been accepted for inclusion in Retrospective Theses and Dissertations by an authorized administrator of Iowa State University Digital Repository. For more information, please contact digirep@iastate.edu.

www.manaraa.com

Photocatalytic degradation of organic contaminants in water

by

Youn-Chul Oh

A dissertation submitted to the graduate faculty

in partial fulfillment of the requirements for the degree of

DOCTOR OF PHILOSOPHY

Major: Chemistry

Program of Study Committee:
William S. Jenks, Major Professor
Mark S. Gordon
Victor S.-Y. Lin
Jacob W. Petrich
Xueyu Song

Iowa State University

Ames, Iowa

2004

UMI Number: 3145675

INFORMATION TO USERS

The quality of this reproduction is dependent upon the quality of the copy submitted. Broken or indistinct print, colored or poor quality illustrations and photographs, print bleed-through, substandard margins, and improper alignment can adversely affect reproduction.

In the unlikely event that the author did not send a complete manuscript and there are missing pages, these will be noted. Also, if unauthorized copyright material had to be removed, a note will indicate the deletion.

UMI®

UMI Microform 3145675

Copyright 2004 by ProQuest Information and Learning Company.

All rights reserved. This microform edition is protected against unauthorized copying under Title 17, United States Code.

ProQuest Information and Learning Company
300 North Zeeb Road
P.O. Box 1346
Ann Arbor, MI 48106-1346

Graduate College
Iowa State University

This is to certify that the doctoral dissertation of

Youn-Chul Oh

has met the dissertation requirements of Iowa State University

Signature was redacted for privacy.

Major Professor

Signature was redacted for privacy.

For the Major Program

TABLE OF CONTENTS

ABSTRACT

This dissertation concerns the elucidation of degradation mechanisms of organic contaminants in aqueous suspension of TiO_2, and extending understanding of photo catalysis condition to optimize degradation efficiency.

The degradation mechanism of maleic acid, an important intermediate from the photocatalytic degradation of aromatic contaminants, was investigated via product distribution study and control experiments. The understanding of the mechanism of degradation of these compounds can assist us for the ascertaining of the better conditions to perform the mineralization of recalcitrant organic compounds.

The challenge to degrade cyanuric acid, a recalcitrant species by modifying TiO_2 suspension was carried out. The addition of fluoride to aqueous suspensions of TiO_2 has proved to be an important mechanistic tool in unraveling a long-standing conundrum in photocatalytic degradation. By using this method in parallel with other methods for producing homogeneous hydroxyl-type reagents, it is shown that cyanuric acid is susceptible to degradation under easily accessible conditions.

There are isotope studies of photocatalysis of dimethyl phenylphosphonate, a simple and safe form of organic phosphonate. The oxidative degradation of phosphonate has received significant attention because of the presence of this group in warfare agents and pesticides. An important unsettled mechanistic point is

the mechanism by which the methyl is removed. Through the isotope studies of TiO_2-mediated photocatalytic degradation of phosphonates, now we can understand removal of the alkyl ester portion of the compounds to produce phosphonic acid monoesters among the primary steps. The retention of ^{18}O in the formation of MMPP clearly demonstrates that the dealkylation mechanism involves degradation of the methyl group exclusively, and neither attack at phosphorus by $HO\bullet_{ads}$ nor a related species, nor photoinduced hydrolysis.

As an attempt to activate modified TiO_2 photocatalysts with visible light and to decrease the rapid recombination of excited electrons/holes during photoreaction, WO_x-TiO_2 powder was prepared by a sol-gel method. The WO_x-TiO_2 catalysts were characterized by X-ray Diffraction (XRD), X-ray Photoelectron spectrometry (XPS), and Scanning Electron Microscopy-Energy Dispersive X-ray Spectroscopy (SEM-EDX). The degradation of 4-methoxyresorcinol and 4-chlororesorcinol by using WO_x-TiO_2 under visible light irradiation was observed. The modification of TiO_2 by W shows its benefit of utilizing visible light for photocatalytic degradation of organic compounds. Differently prepared (incipient wetness method for P25 Degussa and PC 50 Millennium Chemical) WO_x-TiO_2 also shows similar effect of photo-activation by visible light. This is the first report that directly compared the photocatalytic degradation efficiency between WO_x-TiO_2 prepared by traditional incipient wetness method and WO_x-TiO_2 by sol-gel method. WO_x-TiO_2 by sol-gel method consistently shows higher degradation efficiency (c.a. 20 %). It is difficult to explain thoroughly this result at this point because photocatalytic activity is affected by much more

factors than simply particle size i.e., agglomerate size, crystallization condition, surface property also affect to photocatalytic activity. One possible speculation for better photocatalytic activity of WO_x-TiO_2 by sol-gel method may due to less formation of aggregate by WO_x-TiO_2 from sol-gel method. Future work could refine the degradation efficiency precisely by controlling the particle sizes, defective sites of TiO_2, agglomerate size etc.

Chapter 1

General Introduction

1.1 Introduction

With the increasing demands of higher living standard accompanied by exploitation of nature and mass productions, natural self-cleaning processes have not been able anymore to remedy the environmental load caused by the ever-increasing world population and industrial processes. Water is an indispensable element for both existence and living of human. Thus, our main concern has to focus on our water reserves, because pollution from both the atmosphere and soil will eventually enter the aqueous phase by deposition and penetration respectively [1].

Pollution by mankind is caused by variety of activity for sustaining life for e.g. nutrition, transportation, accommodation, synthesis, and energy exploitation. Although probably not always acknowledged, chemical activity is indispensable to sustain life; also it is needed to comply with a high standard of living. Examples are medicines, cleaning and disinfecting products, cosmetics, stabilizers, artificial fertilizers, fuel, batteries, polymers, paints, and dyes. Both synthesis and application of these product classes inevitably yield pollution. In addition to biological waste like carbohydrates, proteins, urea, fats, food & vegetation residues and carbon dioxide, we also encounter priority compounds ((The Environmental Protection Agency has

identified approximately 129 priority pollutants. These pollutants were selected on the basis of their known or suspected carcinogenicity (cancer causing), teratogenicity (the production of malformations in an embryo or fetus), or high acute toxicity (poisonous)) of hazardous effects. Moreover, priority compounds can be highly persistent. Some organic priority compounds are for instance: halogenated dioxins/benzofurans/xanthenes from the incineration of halogenated phenols, polychlorinated biphenyls (PCB's) used as dielectric media, fire retardants, polycyclic aromatic hydrocarbons (benzene, nitrobenzene, *p*-dichlorobenzene, *o*-phenylenediamine) used as precursors in organic synthesis, chlorinated aliphatics (chloroform, tetrachloromethane, trichloroethylene) applied as solvent and/or stain remover; pesticides (DDT, kepone, lindane) for crop protection and pest control; ammunition (TNT, picric acid, nitroanilines); monmers (acrylonitrile, vinylchloride, urethane) from the synthesis, processing and incomplete combustion of polymers, dyes (benzidine based) for colorization for e.g. textile, leather and polymers [1, 2].

Another big threat to water is caused by hazardous wastes. Both most advanced industrialized nations and underdeveloped countries are faced with a tremendous set of environmental problems related to the remediation of hazardous wastes. Problems with hazardous wastes at military installations are related in part to the disposal of chemical wastes in lagoons, underground storage tanks, and dump sites. As a consequence of these disposal practices, the surrounding soil and underlying groundwater aquifers have become contaminated with a variety of

hazardous chemicals. In the civilian sector, the elimination of toxic and hazardous chemical substances such as halogenated hydrocarbons from waste effluents and previously contaminated sites has become a major concern. More than 540 million metric tons of hazardous solid and liquid wastes are generated annually by more than 14000 installations in the United States. A significant fraction of these wastes are disposed on the land each year. Some of these wastes eventually contaminate groundwater and surface water. Groundwater contamination is likely to be the primary source of human contact with toxic chemicals emanating from more than 70% of the hazardous waste sites in the United States [3]. General classes of compounds of concern include: solvents, volatile organics, chlorinated volatile organics, dioxins, dibenzofuran, pesticides, PCB's, chlorophenols, asbestos, heavy metals, and arsenic compounds. Some specific compounds of interest are 4-chlorophenol, pentalchlorophenol, trichloroethylene (TCE), perchloroethylene (PCE), CCl_4, $HCCl_3$, CH_2Cl_2, ethylene dibromide, vinyl chloride, ethylene dichloride, methyl chloroform, p-chlorobenzene, and hexachlorocyclopentadiene [3].

In order to address this significant problem, extensive research is underway to develop advanced analytical, biochemical, and physicochemical methods for the characterization and elimination of hazardous chemical compounds from air, soil, and water. Although we left the ages of unprincipled operation long ago, we inherit innumerous highly polluted waste sites of former generations. Natural process or conventional microbiological degradation desperately needs the assistance of new

technologies, like for instance advanced oxidation processes (AOPs), to destruct hazardous persistent materials by chemical oxidation. Advanced physicochemical processes such as semiconductor photocatalysis are intended to be both supplementary and complementary to some of the more conventional approaches to the destruction or transformation of hazardous chemical wastes such as high temperature incineration, anaerobic digestion, and conventional physicochemical treatment. Treatment of contaminated surface water and groundwater as well as of wastewaters is part of a long-term strategy to improve the quality of our life by elimination of toxic material from drinking water resources and other sources of water for sustaining our necessities.

Photochemical processes have emerged as valuable techniques for water purification. Fundamental and applied research on this subject has been performed extensively during the last 20 years all over the world. Direct photochemical processes require an artificial light source, high-pressure mercury or a xenon arc lamp, and a long time to decompose the organic compounds. In order to overcome these shortcomings, the combination of UV irradiation and other oxidizing agents were considered, which led to the development of Advanced Oxidation Processes (AOPs) [4].

AOPs include thermal processes with H_2O_2 or ozone, UV/H_2O_2 photolysis, UV/ozone photolysis, the photo-Fenton process, semiconductor-based photocatalysis, sonolysis, radiolysis and indirect electrolysis, etc [5]. The AOPs such

as UV/H_2O_2, UV/ozone, and photo-Fenton processes have already been proved useful to carry out the mineralization of organic compounds [4, 6, 7]. The other AOPs, semiconductor-based photocatalysis, sonolysis, and radiolysis have also emerged as viable processes in recent years [3, 8-11].

Although extensive research is being performed on semiconductor-based photocatalysis, there are still many unsolved parts in the chemistries and mechanisms of semiconductor-based photocatalysis processes. The photodegradation reactions of organic pollutants may take place through the formation of harmful intermediates that are more toxic than the original compounds. Therefore, the identification of the intermediates is necessary in photocatalytic degradation process. This thesis contains study of degradation mechanisms of characteristic model organic contaminants in aqueous systems under photo-catalysis condition. It also covers modified photocatalysts to enhance the efficiency of destructing pollutant and the study of degradation mechanisms of model organic pollutants under modified photocatalysis systems.

1.2. Dissertation Organization

This dissertation is organized into five chapters. Chapter 1 is a general introduction based on a literature review on the Advanced Oxidation Processes (AOPs) and photocatalysis for organic contaminants in aqueous systems. The main emphasis is on the TiO_2 mediated photocatalytic degradation of organic

contaminants in water. However, other major AOPs are discussed too. Chapter 2 presents the degradation mechanism studies of an important intermediate from the photocatalytic degradation of aromatic organic contaminants. The challenge to degrade cyanuric acid, a recalcitrant species, by modifying the surface of TiO_2 by fluoride is covered in chapter 3. The emphasis of chapter 4 is on isotope studies to clarify the unsettled mechanistic point from the degradation of organic phosphonate. Chapter 5 focuses on the modification of TiO_2 to increase activity with an attempt to activate the modified TiO_2 photocatalysts by visible light and decrease the rapid recombination. Following the last chapter is general conclusion.

Chapter 2 presents the photocatalytic degradation of maleic acid in aqueous TiO_2 suspensions. Maleic acid is one of major four carbon intermediates from the photocatalysis of 4-chlorophenol and other aromatic organic contaminants. The aliphatic intermediates most frequently encountered during the degradation of aromatic compounds are short-chain carboxylic diacids, as maleic, fumaric and oxalic acids, which have been detected during the mineralization of a variety of organic chemicals. Thus, the understanding of the mechanism of degradation of these compounds can assist us in ascertaining better conditions to perform the mineralization of persistent organic compounds.

Chapter 3 discusses the photocatalytic degradation of a cyanuric acid, a recalcitrant species, in TiO_2/F aqueous suspensions. The addition of fluoride to aqueous suspensions of titania has proved to be an important mechanistic tool in unraveling a long-standing conundrum in photocatalytic degradation. By using this

method in parallel with other methods for producing homogeneous hydroxyl-type reagents, it is shown that cyanuric acid is susceptible to degradation under easily accessible conditions.

In chapter 4, there are isotope studies of photocatalysis of dimethyl phenyl phosphonate, a simple and safe form of organic phosphonate such as VX, a nerve gas. Because of the hazards associated with VX, Soman, and Sarin, most study has been done with model compounds, such as dimethyl methylphosphonate (DMMP). Exposure of DMMP and related simple phosphonates to TiO_2-mediated photocatalytic conditions results first in the loss of one of the methyl esters. An important unsettled mechanistic point is the mechanism by which the methyl is removed [12, 13]. The question is whether attack occurs at the methyl or at the phosphorus or both. Through the isotope studies of TiO_2-mediated photocatalytic degradation of phosphonates, now we can well understand including removal of the alkyl ester portion of the compounds to produce phosphonic acid monoesters among the primary steps.

Chapter 5 contains photocatalytic degradation of 4-methoxy resorcinol and 4-chlororesorcinol by using composite semiconductor photo catalyst, WO_x-TiO_2. There has been recent interest in WO_3-coated DeGussa P25 TiO_2 because it has higher activity than native material. With an attempt to activate the modified TiO_2 photocatalysts by the visible light and decrease the rapid recombination of excited electrons/holes during photoreaction, WO_x-TiO_2 powder was prepared by a sol-gel

method. This method is distinct from the incipient wetness method, and grafting methods, which deposit the tungsten coating over the surface of P 25 DeGussa and other titania. The sol-gel method can provide a true composite semiconductor catalyst by binding the W to every possible site of titania. The modification of TiO_2 by W shows its benefit of utilizing visible light for photocatalytic degradation of organic compounds. Differently prepared (incipient wetness method for P25 Degussa and PC 50 Millennium Chemical) WO_x-TiO_2 show similar effect of photo-activation by visible light. This is the first report that directly compared the photocatalytic degradation efficiency between WO_x-TiO_2 prepared by traditional incipient wetness method and WO_x-TiO_2 by sol-gel method. WO_x-TiO_2 by sol-gel method consistently shows higher degradation efficiency (c.a. 20 %). It is difficult to explain thoroughly this result at this point because photocatalytic activity is affected by much more factors than simply particle size i.e., agglomerate size, crystallization condition, and surface property also affect to photocatalytic activity. One possible speculation for better photocatalytic activity of WO_x-TiO_2 by sol-gel method may due to less formation of aggregate by WO_x-TiO_2 from sol-gel method. Future work could refine the degradation efficiency precisely by controlling the particle sizes, defective sites of TiO_2, agglomerate size etc.

1.3. Advanced Oxidation Processes (AOPs)

Advanced oxidation Processes (AOPs) aim at the in-situ production of strong oxidizers. The oxidizing power is reflected by the standard reduction potential E° values. Table 1.1 shows some oxidizers in power order and E° values, expressed for reduction half-cell reactions [14, 15]. The potential is defined relative to the standard hydrogen electrode (SHE) potential. The Gibbs free energy change ΔG for the redox-reaction is calculated from the resulting electromotive force of both half-cell reactions corrected for activity dependence (E), the number of electrons involved (n) and Faraday constant (F = 94685 C/mol); $\Delta G = -nFE$

The strongest oxidizers known are xenon fluoride (XeF) and possibly H_4RnO_6, but these oxidizers are not commercially attractive for water treatment because of both extreme reactivity and remaining toxicity in reduced form. Also, halogen-based oxidizers are not acceptable as oxidizer, because they halogenated organic materials for e.g. trihalomethanes that are very harmful compounds; in addition their reaction leads to salt formation. It is obvious that heavy metal-based oxidizers like permanganate (MnO_4^-) and dichromate (CrO_7^{2-}) also are not desirable due to their toxicity. Of interest are thus oxygen-based halogen/heavy metal-free oxidizers like the hydroxyl radical (•OH), atomic oxygen (O), ozone (O_3) and hydrogen peroxide (H_2O_2) [2].

Table 1.1 Standard reduction potential values for some oxidizers at T=298.15 K, for acidic conditions pH=0 applies [14, 15].

Reduction half-cell reaction	E° (V) vs. SHE
$XeF + e^- \rightarrow Xe + F^-$	3.40
$2OF_2\ (g) + 4H^+ + 4\ e^- \rightarrow O_2\ (g) + 4HF$	3.29
$OH + H^+ + e^- \rightarrow H_2O$	2.56
$O\ (g) + 2H^+ + 2e^- \rightarrow H_2O$	2.43
$O_3 + 2H^+ + 2e^- \rightarrow O_2 + H_2O$	2.08
$H_2O_2 + 2H^+ + 2e^- \rightarrow 2\ H_2O$	1.76
$HClO_2 + 2H^+ + 2e^- \rightarrow HClO + H_2O$	1.67
$HO_2 + H^+ + e^- \rightarrow H_2O_2$	1.44
$Cl_2 + 2e^- \rightarrow 2\ Cl^-$	1.40

H_2O_2/UV process

Hydroxyl radical can be generated in the photolysis of hydrogen peroxide process by the cleavage of the hydrogen peroxide molecule into hydroxyl radicals under the radiation (equation 1.1).

$$H_2O_2 \xrightarrow{h\nu} 2HO\bullet \qquad (1.1)$$

Hydroxyl radical can react with hydrogen peroxide to generate hydroperoxyl radical, which is also an oxidation reagent (equation 1.2).

$$H_2O_2 + HO\bullet \longrightarrow H_2O + HOO\bullet \qquad (1.2)$$

Hydrogen peroxide is also known to decompose to hydroxyl radical by a dismutation reaction with a maximum rate at the pH of its pK_a value of 11.6 (equation 1.3) [16]

$$H_2O_2 + HO_2\bullet \longrightarrow H_2O + O_2 + HO\bullet \qquad (1.3)$$

After the generation of hydroxyl radical, hydroxyl radicals can further react with organic substrates by hydrogen abstraction, electrophilic addition and electron transfer mechanisms. There is wide research on utilization of H_2O_2/UV oxidation process to remove the toxic organic pollutants [4, 17-20]. The advantage of this process includes that hydrogen peroxide is a cheap and easy to handle oxidant, infinitely miscible with water, and there are no separation requirements after the treatment of water. However, the absorption coefficient of hydrogen peroxide and quantum efficiency of hydroxyl radical production is very low at λ>250 nm [4].

Ozone/UV process

The higher standard reduction potential of ozone (2.07 V at pH=1) makes ozone a powerful oxidant used for the degradation of organic pollutants in water [21, 22]. Additionally, ozone/UV process generates HO• radicals by the light-induced homolysis O_3 and the subsequent by the interaction of O (^1D) with water (equation 1.4) [23].

$$O_3 \xrightarrow{h\nu<310\ nm} O_2 + O(^1D)$$
$$O(^1D) + H_2O \longrightarrow HO\bullet + HO\bullet \qquad (1.4)$$

A second explanation for the production of hydroxyl radical in photolysis of ozone dissolved in water involves the formation of H_2O_2 (equation 1.5). The resulting H_2O_2 is then a source of HO• radicals via a photohomolysis. The disadvantage of this ozone/UV process is the expensive production of ozone.

$$O_3 + H_2O + h\nu < 310\ nm \longrightarrow H_2O_2 + O_2 \qquad (1.5)$$

In the ozone/UV process [7, 8], hydroxyl radicals are produced from ozone, water and UV photons; high-pressure mercury or xenon lamps deliver the photons. Ozone is produced on location by ozonizer, which converts atmospheric or pure oxygen into ozone by corona discharges [9, 10]. These electrical discharges are separated by a dielectric material e.g. glass or ceramics at a thickness of about 0.5-3nm. Commercial ozone generators are based on different electrode configurations, e.g. fluid-cooled shell & tube type generators for generation of large ozone amounts

and air-cooled plate type generators for small amounts. A cooling system is very important, to prevent decomposition of ozone.

Photo-Fenton Reactions

Fenton reagent Fe^{2+} is a well-known oxidant, generating the hydroxyl radical as the following equation (equation 1.6) [24].

$$Fe^{2+} + H_2O_2 \longrightarrow Fe^{3+} + HO^- + HO\bullet \qquad (1.6)$$

Fenton reagent has been applied for water and soil treatment. Furthermore it was found that a more effective system for oxidative degradation could be realized by applying near UV/Vis irradiation to the basic Fenton reaction (equation 1.7) [7, 25, 26].

$$Fe^{2+} + H_2O + h\nu \longrightarrow Fe^{3+} + H^+ + HO\bullet \qquad (1.7)$$

Usually, complete degradation can be realized in a short period during the photo-Fenton process. However the iron salts constitute a pollution source and its removal is recommended. Since the reaction takes place at pH 2-3, neutralization is necessary to precipitate the dissolved iron as $Fe(OH)_3$.

Sonolysis

Sonochemical degradation methods are relative new and involve acoustic cavitations, the cyclical growth and collapse of gas bubble [27]. Propagation of an ultrasound wave in aqueous solution leads to the formation of cavitations bubbles. The cavitations process involves the oscillation of the radii of pre-existing gas cavities by periodically changing pressure field of the ultrasonic waves. The rapid implosion of the eventually unstable gas bubbles causes adiabatic heating of the bubble vapor phase. The collapse of these bubbles spawns extreme conditions on the microscopic scale such as very high temperatures and pressures, which in turn lead to the dissociation of H_2O and the production of radical species such as HO•, HOO•, etc. These can be subsequently used for the transformation and/or destruction of organic substrates. Evidence has accumulated indicating that higher ultrasound frequencies at ~400 KHz are more favorable for the production of HO• radicals [28]. The O'Shea group has used sonolysis to destruct the hazards orgaophosphorus compounds to CO_2, H_2O and H_3PO_4 [9, 13]. The generation of ultrasound energy can be performed by electrochemical (piezoelectric or magnetostrictive) or liquid-driven (liquid whistle = low intensity) tranceducers.

Radiolysis

Radiolysis refers bond cleavage or any chemical process brought about by high-energy radiation [29]. The decay of radioactive nuclei (α, β, γ radiation), beam of accelerated charged particles (electrons, protons, deuterons, helium and heavier nuclei), and short-wavelength radiation (X or Bremsstrahlung radiation) are most commonly used as the types of radiation for the radiolysis process.

Organic contaminants in aqueous solutions can be destroyed either by a "direct" or "indirect" interaction with the incident radiation. Because of the low concentration of organic contaminants in aqueous solution, the decomposition of organic contaminant takes place by "indirect" radiolysis, i.e. by interacting with the radicals e^-_{aq}, H•, and HO• and the hydrogen peroxide generated by radiation-induce reaction with the water (equation 1.8) [30]:

$$H_2O \xrightarrow{\text{radiation}} [2.6]\, e^-_{aq} + [0.6]\, H^\bullet + [2.7] HO^\bullet + [0.7]\, H_2O_2 + [2.6]\, H_3O^+ + [0.45]\, H_2 \qquad (1.8)$$

The number in brackets is the radiation chemical yield (G value) defined as the number of species generated per 100 eV absorbed energy or the approximate micromolar concentration per 10 J of absorbed energy [30].

Semiconductor-based photocatalysis

Semiconductor photocatalysis with a primary focus on TiO_2 as a durable photocatalyst has been applied to a variety of problems of environmental interest in addition to water and air purification. It has been shown to be useful for destruction of microorganisms such as bacteria and viruses, for odor control, for the photosplitting of water to produce hydrogen gas, for the fixation of nitrogen, and for the clean up of oil spills.

Semiconductors (e.g., TiO_2, ZnO, Fe_2O_3, CdS and ZnS) can act as sensitizers for light-induced redox processes due to their electronic structure, which is characterized by filled valence band and an empty conduction band. When a photon with a energy of $h\nu$ matches or exceeds the band gap energy, E_g, of the semiconductor, an electron, is promoted from the valence band, VB, into conduction band, CB, leaving a hole, h_{vb}^+ behind. Excited state conduction-band electrons (e^-_{cb}) and valence-band holes can recombine and dissipate the input energy as heat, get trapped in meta-stable surface states, or react with electron donors and electron acceptors adsorbed on the semiconductor surface or within the surrounding electrical double layer of the charged particles.

In the absence of suitable electron and hole scavengers, the stored energy is dissipated within few nanoseconds by recombination. If a suitable scavenger or surface defect site is available to trap the electron or hole, recombination is prevented and subsequent redox reaction may occur. The valence-band holes are

powerful oxidants (+1.0 to 3.5 V vs NHE depending on the semiconductor and pH), while the conduction-band electrons are good reductants (+0.5 to –1.5 V vs NHE). Most organic photodegradation reactions utilize the oxidizing power of the holes directly or indirectly; however, to prevent a buildup of charge one must also provide a reducible species to react with the electrons. In contrast, on bulk semiconductor electrodes only one species, either the hole or the electron, is available for reaction due to band bending. However, in very small semiconductors particle suspensions both species are present on the surface. Therefore, careful consideration of both the oxidative and the reductive paths is required [3].

Mineralization of organic pollutants in water and air steams to CO_2, H_2O and inorganic ions can be realized by using certain semiconductors as photocatalyts [3-5, 31-35]. There are a lot of different semiconducting materials which are readily available, but only a few are suitable for photodegradation of organic pollutants, such as WO_3, TiO_2, $SrTiO_3$, CdSe, CdTe, ZnO, CdS and ZnS. In order to a semiconductor suitable for mineralizing organic waste products, the redox potential of the photogenerated valence band hole must be sufficient positive to generated absorbed HO• radical, and the redox potential of photogenerated conductance band electron must be sufficiently negative to be able to reduce adsorbed O_2 to superoxide [36]. Of all the different semiconductor photocatalysts, TiO_2 seems to be the most active [37]. In addition, TiO_2 is a very cheap catalyst and can be recycled. Furthermore, the suspended photocatalyst TiO_2 is stable to the photolysis conditions

and a large number of oxidative conversions per active site on the catalyst can be attained without significant degradation of the semiconductor's redox catalytic capacity. Thus, TiO_2 photocatalysis is an active field of research and commercial interest. In the section 1.4, TiO_2-based photolysis will be discussed in detail.

Widely applied AOP comparison (adapted from ref. 1)

Hydrogen peroxide/UV

Pro: Hydrogen peroxide is a pure source of hydroxyl radicals. Activation can be applied by UV photons and/or iron (II, III) salts. The quantum yield for generation of hydroxyl radicals from photolysis of hydrogen peroxide is about 1.0.

Contra: The transport, storage and handling of hydrogen peroxide require special safety precautions. Hydrogen peroxide shows only weak absorption in the range 200-300 nm and also absorption at the wavelengths higher than 300 nm is not significant; by addition of iron salts the hydroxyl radical production efficiency is greatly enhanced, but a high iron salt concentration is required according to stoichiometry. The application of other salts than iron hydroxo/carboxyl chelate causes unnecessary release of anions like e.g. sulfate, chloride or nitrate. Lamp power efficiency and lamp life are limited. Turbid wastewater is problematic.

Ozone/UV

Pro: Ozone is powerful oxidizer that can be produced from a simple ozonizer setup and air. Also, hydrogen peroxide is produced from the oxidation of water by ozone.

Contra: The reactions of ozone in aqueous solution are mass transfer limited. Molecular ozone reacts much slowly than hydroxyl radicals. Unreacted/undecomposed ozone left in the reactor has to be detoxified e.g. by chemical reduction. The UV-lamp power efficiency and lamp life are limited; the penetration depth of UV radiation in turbid aqueous solution is low

Sonolysis

Pro: with a simple setup, vigorous conditions can be created in aqueous solution. Continuous flow operation is possible.

Contra: A main issue is the fact that the scale-up procedure is complex. The shielding of ultrasound is important, because the intense first subharmonic of the applied driving frequency and white noise cause hearing impairment; also, potential hazard is the formation of aerosols from the harmful solution by surface wave activity. The transducer device undergoes erosion by intense cavitation.

Photocatlysis

Pro: Dirt cheap, nontoxic, robust, can be immobilized, absorbs some of the solar spectrum, extremely effective and versatile *vis a vis* substrates. A simple setup is required.

Contra: The quantum yield for the generation for hydroxyl radicals on the surface of the most generally applied photocatalyst titanium dioxide is low. Indicated numbers are only 4-8% for titanium dioxide slurries or even lower for immobilized

photocatalyst particles. Also, the quantum yield is dependent on the light intensity. Mainly for these reasons, the scale-up procedure from laboratory setup to industrial application is problematic. Mass transfer limitation occurs for immobilized photocatalysts. After reaction, suspended photocatalyst particle have to be separated from the oxidation product mixture. UV-lamp power efficiency and lamp life are limited. Turbid wastewater is problematic.

General Remarks

It is sensible to state that one particular ideal AOP does not exist. The applicability depends on e.g. the nature of the target compound(s), the pollution magnitude and concentration, geographical location of the pollution and AOP performance stability. With regard to high quantities, continuous-flow operation is preferable to bath-wise processing. Treatment of low concentration intermediate toxic waste flow should be performed with maximum efficiency.

1.4. Semiconductor photocatalysis

TiO_2 is considered a promising photodegradation catalysis because it posses five basic characteristics: 1) photoactive, 2) able to utilize visible and/or near UV-light, 3) biologically and chemically inert, 4) photo-stable, and 5) inexpensive [38]. In order to improve the reproducibility of the results between groups, many have

chosen to use a particular source of TiO_2, Degussa P25, produced through the high temperature (greater than 1200 °C) flame hydrolysis of $TiCl_4$ in the presence of hydrogen and oxygen, which continue to be treated with steam to remove HCl. The two crystal structures of TiO_2 utilized in photocatalysis are rutile and anatase. DeGussa P25 is approximately 70% anatase and 30% rutile. This brand TiO_2 was used in this study. In order to have the insight of the TiO_2 photodegradation, the initial events of TiO_2 photocatalytic system are going to be discussed first.

Chemical mechanism of initial steps [3]

Typical photodegradation is performed with oxygen or air saturated aqueous suspensions of TiO_2 (Degussa P25). The energy bandgaps of anatase is 3.23 eV (384 nm) and rutile is 3.02 eV (411 nm) [39]. The band gap of DeGussa P25 is roughly 3.2 eV [40]. When ultraviolet radiation equaling or exceeding the energy of the bandgap (<400 nm) is absorbed, an electron is promoted from the valence band to the conduction band leaving an electron hole (h_{VB}^+) in the valence band. This process is shown in equation 1.9 of Figure 1.1. Adsorbed water on the surface of TiO_2 can continue to react with the hole to generate the hydroxyl radical shown in equation 1.10 of Figure 1.1. This process is the main mode for adsorbed hydroxyl radical formation. Hydroxyl radicals are believed to be the main oxidation reagents from TiO_2 and it is supposed that the reactions take place on the TiO_2 surface, but electron transfer is another important mechanism [8, 41-49]. Photocatalytic

degradations are carried out in aqueous solution and with oxygen. The main role of oxygen is an electron consumer reacting with a conduction band electron to form superoxide as seen in equation 1.11 of Figure 1.1 and preventing electron-hole recombination, and another main role of oxygen is as the oxidant [50]. Hydrogen peroxide may then undergo fragmentation to a hydroxyl radical and a hydroxide anion, as seen in equation 1.14 of Figure 1.1.

It has also been reported that organic molecules may interact directly with an electron in the conduction band or an electron hole in the valence band. These steps are represented in equation 1.15 and 1.16 of Figure 1.1. The symbol A represents a general electron acceptor molecule while D signifies an electron donor molecule. Of course, there exists an important charge and hole recombination reaction in the initial steps.

$$TiO_2 + h\nu \longrightarrow e^-_{cb} + h^+_{vb} \quad (1.9)$$

$$H_2O_{ads} + h^+_{vb} \longrightarrow HO\bullet_{ads} + H^+ \quad (1.10)$$

$$O_2 + e^-_{cb} \longrightarrow O_2^{\bullet -} \quad (1.11)$$

$$O_2^{\bullet -} + H^+ \longrightarrow HO_2\bullet \quad (1.12)$$

$$2HO_2\bullet \longrightarrow H_2O_2 + O_2 \quad (1.13)$$

$$H_2O_2 + e^-_{cb} \longrightarrow HO\bullet + HO^- \quad (1.14)$$

$$A + e^-_{cb} \longrightarrow A^{\bullet -} \quad (1.15)$$

$$D + h^+_{vb} \longrightarrow D^{\bullet +} \quad (1.16)$$

Figure 1.1. Reactions at TiO_2 surface

Debate on the oxidizing species

In aqueous solution, two main oxidizing species are considered involving TiO_2 photocatalytic degradation process: the hydroxyl radical or the irradiation-induced hole. There exists a significant body of literature that oxidation may occur by either indirect oxidation via the surface-bound hydroxyl radical or directly via valence-band hole before it is trapped either within the particle or at the particle surface [8, 41-49].

The results of detailed laser flash photolysis experiments have obtained the characteristic time scales of the processes associated with the reaction mechanism [3]. The charge-carrier generation (equation 1.9 in Figure 1.1) occurs on the femtosecond time scale. Charge carrier trapping (equation 1.10 in Figure 1.1) is at picosecond to nanosecond time scale. The charge-carrier recombination is on the picosecond to nanosecond time scale, while the direct oxidation (equation 1.16 in Figure 1.1) is on microsecond to millisecond time scale. Direction oxidation competes with two other processes, charge-carrier recombination and trapping. In the general mechanism and from the time scale, it is assumed that the substrate does not undergo direct hole transfer and that oxidative electron transfer occurs exclusively through a surface-bound hydroxyl radical or equivalent trapped hole species.

Hydroxyl radical as the principal reactive oxidant in photoactivated TiO_2 is supported by the observation of the hydroxylated structure intermediates during the photocatalytic degradation of aromatic compounds. When those compounds react

with a known source of hydroxyl radicals, similar intermediates are generated as those during the photocatalytic degradation. For example, Li *et al.* studied the decomposition of anisole by using photoactivated TiO_2 system, direct H_2O_2/UV system and Fenton system [51]. The intermediates distribution observed in the different systems are similar and the *para*- and the *ortho*-hydroxyl anisole are the main intermediates. This phenomenon shows that during primary photodegradation of anisole the hydroxyl radical is very possible the main oxidation reagent. . In addition, ESR studies and indirect kinetic evidence have verified the existence of hydroxyl and hydroperoxyl radicals in aqueous solutions of illuminated TiO_2 [52, 53].

On the other hand, Li *et al.* suggested that the ring-opening on TiO_2 photocatalytic degradation of 4-chlorophenol is induced by direct single electron transfer, rather than hydroxyl radical reaction [54, 55]. Mao *et al.* have observed that trichloroacetic acid and oxalic acid are oxidized primarily by valence-band holed on TiO_2 via a photo-Kolbe process [56]. Likewise, Draper and Fox were unable to find evidence of any hydroxyl radical adducts for the TiO_2-sensitized reaction of potassium iodide, etc [44]. They observed only the products of the direct electron-transfer oxidation. Carraway *et al.* have provided experimental evidence for the direct hole oxidation of tightly bound electron donors such as formate, acetate, and glyoxylate at the semiconductor surface [57].

Richard has argued that both holes and hydroxyl radicals are involved in the photooxidation of 4-hydroxylbenzyl alcohol (HBA) on ZnO or TiO_2 [58]. His results

suggest positive holes and hydroxyl radicals have different regioselectivities in the phtocatalytic tansformation of HBA. Hydroquinone (HQ) is thought to result mainly from the direct oxidation of HBA by h_{vb}^{+}, dihydroxybenzyl alcohol (DHBA) mainly from the reaction with hydroxyl radical, while 4-hydroxybenzaldehyde (HBZ) is produced by both pathways. In the presence of isopropyl alcohol, which is used as a hydroxyl radical quencher, the formation of DHBA is completely inhibited and the formation of HBZ is inhibited.

Kinetic view

In general, the kinetics of TiO_2 photomineralization of organic substrates in the presence of oxygen and under steady state illumination fit a Langmuir-Hinshelwood kinetic scheme. The Langmuir-Hinshelwood model suggests that the organic reagent is pre-adsorbed on the photocatalyst surface prior to UV illumination. The rate of degradation is proportional to the surface coverage (θ) (equation 1.16) [53].

$$\text{Rate} = k\,\theta \tag{1.16}$$

After insert the formulation of θ, the above equation can be converted into the common Langmuir-Hinshelwood kinetic model (equation 1.17).

$$\frac{dC}{dt} = \frac{k_{obs}K_L C}{(K_L C + 1)} \tag{1.17}$$

Where k_{obs} is an apparent reaction rate constant, and K_L is the Langmuir constant reflecting the adsorption/desorption equilibrium between the reagent and

the surface of the photocatalyst. There are two extreme cases. For high concentration of the pollutant, where saturation coverage of the surface is achieved (i.e. $K_L C >> 1$), the equation can be simplified to a zero-order rate equation (equation 1.18).

$$\frac{dC}{dt} = k_{obs} \tag{1.18}$$

For the low concentration ($K_L C << 1$), the equation can be simplified to a pseudo-first-order kinetic equation (equation 1.19).

$$\frac{dC}{dt} = k_{obs} K_L C \tag{1.19}$$

The solvent and reaction intermediates compete with the reacting substrate for the active surface, thus the Langmuir-Hinshelwood kinetic model can be characterized by equation (equation 1.20):

$$\frac{dC}{dt} = \frac{k_{obs} K_L C}{(K_L C + \Sigma K_i C_i + 1)} \tag{1.20}$$

When the concentration of the reacting substrate is high, this equation can be similarly transferred into the zero-order equation.

When the concentration of the reacting substrate is low, the Langmuir-Hinshelwood equation into its inverse function results in a linear relationship with an intercept of k_{obs}^{-1} and a slope of $(k_{obs}^{-1} K^{-1})$ (equation 1.21).

$$\frac{dt}{dC} = \frac{1}{k_{obs}} + \frac{1}{k_{obs} K_L C} \tag{1.21}$$

The process, in which a surface-generated catalytic species diffuses to the bulk solution where the primary catalytic conversion occurs can also be described by an Eley-Ridel pathway [59]. It was shown by Turchi and Ollis that the rate of photo-oxidation of an organic substrate on irradiated TiO_2 presents the same kinetic behavior as L-H kinetic model [53]. Unfortunately, an experimental distinction between Langmuir-Hinshelwood kinetic model and Eley-Ridel pathway, based on kinetics alone, is not possible because of the kinetic ambiguities [60, 61].

The kinetic expression can be same irrespective of (1) the oxidizing species and the substrate are both adsorbed, (2) both species are in solution, (3) the oxidizing species is adsorbed and the substrate is in solution, or (4) the substrate is adsorbed and the oxidant is in solution.

Effects on the TiO_2 photocatalytic degradation process

Adsorption effect

It has been suggested that preliminary adsorption is a prerequisite for highly efficient detoxification [62]. Because recombination of the photogenerated electron and hole is so rapid, interfacial electron transfer is kinetically competitive only when the relevant donor or acceptor is preadsorbed before photolysis. The correlation between degradation rates and concentration of the organic pollutant adsorbed to

surface is reported often [63-65]. However, dark adsorption properties do not always correlate with reactivity [66].

Our group studied the photodegradation of 4-chlorophenol [54, 55]. The interesting result is that the ring is opened easily until there is two hydroxyl groups are in the *ortho* position on the phenyl ring. This result may be explained in that two *ortho* hydroxyl groups can anchor the substrate on TiO_2 surface. Then, the substrate can react with a hole to generate the radical species further reacting with the superoxide to occur the ring opening. Isopropanyl alcohol was used as the competitive absorption materials that can compete with the weak absorbed species on TiO_2 [67]. When there are more methoxy groups on the ring, the rate inhibition effects of isopropanol are more obvious, while more hydroxyl group substitutes on benzene ring, the effect of isopropanol is less obvious.

Effect of pH

The particle size, surface charge and band edge positions of TiO_2 are strongly influenced by pH. The isoelectric point for TiO_2 in water is about pH=6.6 [68], and positive surface charge is expected at lower pH and negative surface charge is predicted at higher pH values. This surface charge is due to protonation or deprotonation of the surface HO groups. A second charge layers is formed in the electrolyte near the interface to the surface charge. For negative charges accumulate at the interface of n-type semiconductor (semiconductor in which

concentration of electrons is much higher then concentration of holes; electrons are majority carriers and dominate conductivity). The space charge layer formed is a depletion layer and the bands bend upward toward the surface. Thus, the concentration of holes on the surface is larger than electrons. The higher concentration of holes may react with a high concentration of HO- on the surface. Therefore, increased surface density of OH^- adsorbed thereon [8]. Therefore, a higher concentration of hydroxyl radical is produced by the neutralization of adsorbed OH^- ion by photogenerated holes. However, it was found out that the change in the rate of photocatalytic degradation rate is generally less than one order of magnitude from pH 2 to pH 12 [69-72].

Effect of the amount of TiO_2

Usually, the rate of reaction is almost linearly dependent on the increased concentration of TiO_2 [73, 74]. This behavior is consistent with the complete absorption of light near the surface of the semiconductor [73, 74]. In some cases, with the increased concentration of TiO_2, the rate of degradation increases up to a certain point, then, begins to decrease slowly [75, 76]. The reason is that when the amount of TiO_2 increase, there are more active sites for the reaction, thus the reaction rate increases. When the amount of TiO_2 is more than the optimum concentration, the aggregation of TiO_2 becomes a serious problem and the reaction rate slows. The increase in opacity and light scattering by the particles may be the

other reasons for the decrease of the rate. In a commercial system, TiO_2 can be fixed on Nafion film, ceramic film, silica gel, and glass surface.

Effect of the concentration of the substrate

As discussed earlier in the section 1.4.4, the concentration of organic substrate affects the kinetic rate of the degradation. It is also clear that the kinetics of photodegradation will depend on the ease with which the substrate can be oxidized and how well it absorbs and how well its products absorb on the surface TiO_2. For most of organic pollutants tested, the relationship of degradation rate and the concentration of pollutants comply with Langmuir-Hinshelwood kinetic model [55, 67]. However, this is not always true: San et al found the decrease of initial degradation rate with the increase of the initial concentration of pollutant due to strong absorption of the products [76]. It is also worth noting that the absorption spectrum of the pollutant can drastically affect the kinetics of photocatalysis. In particular, if the pollutant is a strong UV absorber, then, as its concentration is increased it will eventually begin significantly to screen the TiO_2 from the ultra–bandgap light and the kinetic of the light will be affected.

Effect of the concentration of the oxygen

Since oxygen is the electron consumer inhibiting the recombination of the electron/hole pair the concentration of dissolved oxygen in solution also affect the

degradation rate. It is found that the rate degradation is proportional to the fraction of O_2 (equation 1.14) [36].

$$\text{Rate} \propto \frac{K_{O_2}[O_2]}{1 + K_{O_2}[O_2]} \tag{1.14}$$

Where K_{O_2} is the Langmuir adsorption coefficient for O_2.

Effect of reaction temperature

Photochemical reactions are often not very temperature sensitive. The reactant is converted into product through an excited state surface funnel crossing an excited-state surface to ground-state surface [77]. The overall process of TiO_2 photo-degradation is only slightly temperature sensitive. The activation energies of photo-catalytic degradation reactions usually have the values of 5 –16 kJ mol^{-1} [36], because the photocatalytic degradation process involves potentially temperature-dependent steps, such as adsorption, desorption, surface migration, and rearrangement. In principle, it is possible to sort the temperature dependence into (1) adsorption contribution (by alteration of the Langmuir adsorption isotherm), (2) stabilization of intermediates (by alteration of kinetics for formation or decay of different transients), and environmental effects (by alteration of solvent, electrolytes, etc.) [78].

Application of TiO_2 photocatalysis

The semiconductor-sensitized photomineralization of organic substrate by oxygen can be summarized as follows (equation 1.15).

$$\text{Organic pollutant} + O_2 \xrightarrow[h\nu \geq E_{bg}]{TiO_2} CO_2 + H_2O + \text{Mineral acid} \qquad (1.15)$$

The degradation of a variety of organic molecules has been investigated. For an exhaustive review of these publications please refer to Hoffman [3] and Mills [38]. The various examples of photo-mineralization of organic pollutants by TiO_2 was summarized in Table 1. The research related to degradation of organic compounds by photocatalysis and or AOPs progressed very fast. Mills suggests that it is necessary to define a standard test system [36]. 4-Chlorophenol has become a standard for evaluating various experimental parameters [11, 54, 55, 61, 79-94].

Table1. 2 Photomineralization of organic pollutants by TiO_2: Examples of compounds studied [31]

Class	Examples
Alkanes	methane; isobutane; pentane; isooctane; heptane; *n*-dodecane; cyclohexane; methylcyclohexane; 1,4-methylcyclohexane; paraffin
Haloalkanes	mono-,di-, tri-, and tetra-chloromethane; fluorotrichloromethane;

	1,1-and 1,2-dichloroethane; tetrachloroethane, pentachloroethane; dibromoethane; tribromoethane; 1,2-dichloropropane; 1-bromododecane; 1,1-difluoro-1,2-dichloroethane;1,1-difluoro-1,2,2-trichloroethane;
Aliphatic alcohols	methanol; ethanol; *iso*propyl alcohol; cyclobutanol; *n*-propyl alcohol; propan-2-ol; butanol; penta-1,4-diol; 2-elloxyethanol; 2-butoxylethanol; dodecanol; benzyl alcohol; glucose; sucrose
Aliphatic carboxylic acid	formic; ethanoic; dimethylethanoic; mono-, di-, and tri-chloroethanoic; propanoic; butanoic; dodecanoic; oxalic
Alkenes	Propene; cyclohexene
Haloalkenes	perchloroethene; 1,2-dichloroethene; 1,1,1- and 1,1,2-trichloroethene; tetrachloroethene; mono-, di-, and tetra-fluoroethene; hexafluoropropene
Aromatics	Benzene; naphthalene
Haloaromatics	chlorobenzene; bromobenzene; 2,3,4-chlorophenol; 2,4- and 3,4-dichlorophenol; 2,4,5- and 2,4,6-trichlorophenol; pentachlorophenol; 2,3-, and 4-fluorophenol; 2,4- and 3,4-dichloronitrobenzene; 1,2-dichlornitrobenzene
Phenol	phenol; hydroquinone; methylhydroquinone; catechol; 4-methyl

	catechol; 4-nitrocatechol; resorcinol; 2-naphthol; *o*-, *m*-, and *p*-cresol
Aromatic carboxylic acid	benzoic; 4-amino benzoic; 3-chloro-4-hydroxylbenzoic; phthalic; salicyclic; *m*-, and *p*-hydroxybenzoic; 3-chlorohydroxylbenzoic
polymers	polyethylene; PVC
surfactants	SDS; *p*-nonyl phenyl polyoxyetheylene ether; polyethylene glycol; *p*-nonyl phenyl ether; sodium dodecyl benzene sulfonate; benzyl dodecyl dimethyl ammonium chloride; p-nonyl phenyl poly(oxyethylene)esters; sodium benzene sulfonate; paraxon; malathion; 4-nitrophenyl ethyl phosphinate; 4-nitrophenyl isopropyl phosphinate; 1-hydroxy ethane-1,1-diphosphonate; 4-nitrophenyl diethyl phosphate; trimethyl phosphate; trimethyl phosphite; dimethyl ammonium phosphodithionate; tetrabutyl ammonium phosphate
Herbicides	methyl viologen; atrazine; simazine; prometon; propetryne; bentazon
pesticides	DDT; parthion; lindane
Dyes	methylene blue; rhodamine B; methyl orange; fluorescerin; umbelliferone

Modified TiO_2 based photocatalysts

TiO_2 has been shown to be an excellent photocatalyst for the degradation of organic contaminants in water and air. Nearly every organic molecule ever tested (as introduced in Table 1. 2) was degraded to CO_2, H_2O, and appropriate inorganic ions when exposed to TiO_2-mediated photocatalytic degradation conditions in oxygenated water. However, it has two typical limitations. Firstly, TiO_2 is a wide band gap (3.2 eV) semiconductor that can be excited by high energy UV irradiation (with a wavelength of 385 nm for anatase and 410 nm for rutile). This allows only no more than 5 % of sunlight can be utilized for photocatalytic degradation. Secondly, a low rate of electron transfer to oxygen and a high rate of recombination between excited electron/hole pair results in a limited photocatalytic degradation [95-97].

Semiconductor-metal composite nanoparticles facilitate charge rectification (i.e. directing the flow of electrons and holes in opposite directions) and improve the photocatalytic efficiency in the system [98]. Accumulation of electrons on the TiO_2 and acceleration of the radiationless electron-hole recombination due to insufficient O_2 reduction (scavenging electron) exhibit relatively poor photocatalytic efficiency. Application of transition metals as co-catalyst can improve the efficiency of the photocatalysis; the noble metal, which acts as a sink for photo-induced charge carriers, promotes interfacial charge-transfer processes. Modified photo-catalyst systems not only rectify the flow of photo-generated charge carriers [99-101] but

also extend the photo-response of large band-gap semiconductors [95] and improve the efficiency of dye sensitization [101, 102].

In this study, WO_x-TiO_2 samples were prepared by a sol-gel process with the aims of extending the light absorption spectrum toward the visible region, and hindering the recombination of electron/hole pairs [95]. We are particularly interested in a recent report by Li *et al.* that describe the preparation and characterization of WO_x-dispersed TiO_2 by the sol-gel method [95]. These catalysts have relatively featureless absorption spectra that extend well into the visible, potentially making them extremely valuable photocatalysts because they will absorb a greater fraction of sunlight. Its photocatalytic effectiveness was tested by measuring the disappearance of methylene blue under visible light irradiation [95]. They proposed that tungsten oxides doping into TiO_2 could shift the light absorption band from near UV range to visible range. This could also hinder the fast recombination rate of excited electrons/holes. Hence, we tried to prepare some of this material and assess it with more typical substrates, especially our standard probes, to understand if the same general mechanism will apply for organic degradation, despite the narrower band gap. Probes such as 4-methoxyresorcinol should be good indicators for the types of chemistry occurring at modified or alternative photocatalysts. Our previous experiments with 4-methoxyresorcinol have been carried out with DeGussa P25 TiO_2 [67].

1.5. Reference:

[1] W. F. L. M. Hoben, Pulsed Corona-Induced Degradation of Organic Materials in Water, in Ph.D. Dissertation (2000) Technishe Universiteit Eindhoven.

[2] P. Patnaik, A comprehensive guide to the hazardous properties of chemical substances. 2nd ed. (1999) New York: Wiley 835.

[3] M. R. Hoffmann, S. T. Martin, W. Choi, D. W. Bahnemann, Chem. Rev. 95 (1995) 69.

[4] O. Legrini, E. Oliveros, A.M. Braun, Chem. Rev. 93(1993) 671.

[5] P. V. Kamat, L. K. Vinodgopal, Molecular and Supramolecular Photochemistry: Organic and Inorganic Chemistry, ed. V. Ramanmurthy and K. Schanze Eds (1998) New York: Marcel Dekker. 307.

[6] T. Mill, C.W. Gould, Environ. Sci. Technol. 13 (1979) 205.

[7] R. Bauer, H. Fallmann, Res. Chem. Intermed. 23 (1997) 341-354.

[8] A. L. Linsebigler, G. Lu, J. T. Yates, Jr., Chem. Rev. 95 (1995) 735.

[9] K. E. O'Shea, A. Aguila, L. K. Vinodgopal, P. V. Kamat, Res. Chem. Intermed. 24 (1998) 695.

[10] S. C. Choure, M. Bamatraf, B. S. M. Rao, R. Das, H. Mohan, J. P. Mittal, J. Phys. Chem. 101 (1997) 9837.

[11] U. Stafford, K. A. Gray, P. V. Kamat, Chem. Oxid. 4 (1997) 193.

[12] K. E. O'Shea, S. Beightol, I. Garcia, M. Auguilar, D. V. Kalen, W. J. Cooper, J. Photochem. Photobiol. A 107 (1997) 221.

[13] K. E. O'Shea, I. Garcia, M. Auguilar, Res. Chem. Intermed. 23 (1997) 325.

[14] S. G. Bratsh, Phys. Chem. 18 (1989) 1.

[15] D. R. Lide, Handbook of Chemistry and Physics. 79th ed. Electrochemical Series (1999) Cleaveland, OH: Chemical Rubber Co. 21.

[16] W. H. Koppenol, Bioelectrochemistry and Bioenergetics 18 (1987) 3.

[17] M. Sorensen, F.H. Frimmel, Z. Naturforsch. B 50 (1995) 1845.

[18] M. Sorensen, F.H. Frimmel, Water Res. 31 (1997) 2885.

[19] F. J. Benitez, J. Beltran-Heredia, J. L. Acero, Toxicol. Environ. Chem. 56 (1996) 199.

[20] M. I. Stefan, A. R. Hoy, J. R. Bolton, Environ. Sci. Technol. 30 (1996) 2382.

[21] R. M. Lelacheur, W. H. Glaze, Environ. Sci. Technol. 30 (1996) 1072.

[22] R. Hausler, F. G. Briere, P. Beron, Ozone Sci. Eng. (1993) 15.

[23] G. R. Peyton, W.H. Glaze, Environ. Sci. Technol. 22 (1988) 761.

[24] C. WallingAcc. Chem. Res. 8 (1975) 125.

[25] R. G. Zepp, B. C. Faust, J. Hoigné, Environ. Sci. Technol. 26 (1992) 313.

[26] J. J. Plgnatello, Y. Sun, Water Res. 29 (1995) 1837.

[27] A. J. Johnston, P. Hocking, ACS Symp. Ser. 518 (1993) 106.

[28] K. S. Suslick, Ultrasound: Its Chemical, Physical and Biological Effects (1988) New York: VCH Publ. 336.

[29] V. Parmon, A. V. Emeline, N. Serpone, Intern. J. Photoenergy, 4 (2002) 91.

[30] G. V. Buxton, C. L. Greenstock, W. P. Helman, A. B. Ross, J. Phys. Chem. Ref. Data 17 (1988) 520.

[31] G. R. Helz, R. G. Zepp, D. G. Crosby, Eds. Aquatic and Surface Photochemistry (1994) Lewis Publishers: Boca Raton.

[32] D. F. Ollis, H. Al-Ekabi, Eds. Photocatalytic Purification and Treatment of Water and Air. Trace Metals in the Environment (1993) Elsevier Science Publishers: New York. 820.

[33] N. Serpone, E. Pelizzetti, Eds. Photocatalysis: Fundamentals and Applications (1989) John Wiley & Sons: New York.

[34] D. Bahnemann, Photocatalytic detoxification of polluted waters, in Handbook of Environmental Chemistry, P. Boule, Editor (1999) Springer: Berlin, Germany. 285.

[35] A. Fujishima, K. Hashimoto, T. Watanabe, TiO_2 Photocatalysis Fundamentals and Applications (1999) Tokyo: BKC, Inc.

[36] A. Mills, R. Davies, D. Worsley, Chem. Soc. Rev. 22 (1993) 417.

[37] M. Barbeni, E. Pramauro, E. Pelizzetti, E. Borgarello, N. Serpone, Chemosphere 14 (1985)195.

[38] A. Mills, S. Le Hunte, J. Photochem. Photobiol. A 108 (1997) 1.

[39] K. Rajeshwar, J. Appl. Electrochem. 25 (1995) 1067.

[40] S. T. Martin, H. Herrmann, W. Choi, M. R. Hoffmann, J. Chem. Soc., Faraday Trans. 90 (1994) 3315.

[41] O. I. Micic, Y. Zhang, K. R. Cromack, A. D. Trifunac, M. S. Thurnauer, J. Phys. Chem, 97 (1993) 13288.

[42] O. I. Micic, Y. Zhang, K. R. Cromack, A. D. Trifunac, M. S. Thurnauer, J. Phys. Chem. 97 (1993) 7277.

[43] R. F. Howe, M. Grätzel, J. Phys. Chem. 91 (1987) 3906.

[44] R. B. Draper, M. A. Fox, Langmuir 6 (1990) 1396.

[45] R.B. Draper, M.A. Fox, J. Phys. Chem. 94 (1990) 4628.

[46] M. A. Fox, Photocatalytic Purification and Treatment of Water and Air, D.F. Ollis and H. Al-Ekabi, Eds. (1993) Elsevier. 163.

[47] D., Lawless, N. Serpone, D. Meisel, J. Phys. Chem, 95 (1991)5166-5170.

[48] N. Serpone,E. Pelizzetti, H. Hidaka, Photocatalytic Purification and Treatment of Water and Air, D.F. Ollis and H. Al-Ekabi, Eds. (1993) Elsevier. 225.

[49] N. Serpone, Res. Chem. Intermed. 20 (1994) 953.

[50] M. A. Fox, M.T. Dulay, Chem. Rev. 93 (1993) 341.

[51] X. Li, W. S. Jenks, J. Am. Chem. Soc. 122 (2000)11864.

[52] H. Noda, K. Oikawa, H. Kamada, Bull. Chem. Soc. Jpn. 66 (1993) 455.

[53] C. S. Truchi, D.F. Ollis, J. Catal. 122 (1990) 178.

[54] X. Li, J. W. Cubbage, T. A. Tetzlaf ,W.S. Jenks, J. Org. Chem. 64 (1999) 8509.

[55] Li, X., J.W. Cubbage, and W.S. Jenks, J. Org. Chem. 64 (1999). 8525.

[56] Y. Mao, C. Schoneich, K. D. Asmus, J. Phys. Chem. 95 (1991) 80.

[57] E. R. Carraway, A. J. Hoffmann, M. R. Hoffmann, Environ. Sci. Technol. 28 (1994) 786.

[58] C. Richard, J. Photochem. Photobiol. A 72 (1993) 179.

[59] A. V. Emeline, V. Ryabchuk, N. Serpone, J. Photochem. Photobiol. A 133 (2000) 89.

[60] P. Pichat, J. M. Herrmann, Photocatalysis: Fundamentals and Applications, ed. N. Serpone and E. Pelizzetti (1989) New York: John Wiley & Sons. 218.

[61] H. Al-Ekabi, N. Serpone, E. Pelizzetti, C. Minero, M. A, Fox, R. B. Draper, Langmuir 5 (1989) 250.

[62] R. W. Matthews, J. Catal. 113 (1988) 549.

[63] U. Stafford, K. A. Gray, P. V. Kamat, Chem. Phys. Lett. 205 (1993) 55.

[64] S. Tunesi, M. Anderson, J. Phys. Chem. 95 (1991) 3399.

[65] T. Awatani, K. D. Dobson, A. J. McQuilan, B. Ohtani, K. Uosaki, Chem. Lett. (1998) 849.

[66] Y.-C. Oh, Y. Bao, W. S. Jenks, J. Photochem. Photobiol. A 161 (2003) 69.

[67] X. Li, J. W. Cubbage, W. S. Jenks, J. Photochem. Photobiol. A 143 (2001) 69.

[68] J. Augustynski, Structure and Bonding 69 (1988) 1.

[69] R. Terzian, N. Serpone, C. Minero, E. Pelizzetti, J. Catal. 128 (1991) 352.

[70] K. Okamoto, Y. Yamamoto, H. Tanaka, M. Tanaka, A. Itaya, Bull. Chem. Soc. Jpn. 58 (1985) 2015.

[71] K. Okamoto, Y. Yamamoto, H. Tanaka, M. Tanaka, A. Itaya, Bull. Chem. Soc. Jpn. 58 (1985) 2023.

[72] J. C. D'Oliveira, C. Guillard, C. Maillard, P. Pichat, J. Environ. Sci. Health A 28 (1993) 941.

[73] N. Serpone, A. Salinaro, Pure Appl. Chem. 71 (1999) 303.

[74] A. Salinaro, A. V. Emeline, J. Zhao, H. Hidaka, V. K. Ryabchuk, N. Serpone, Pure Appl. Chem. 71 (1999) 321.

[75] A. Aguila, K. E. O'Shea, T. Tobien, K. -D. Asmus, J. Phys. Chem. A 105 (2001) 7834.

[76] N. San, A. Hatipoglu, G. Kocturk, Z. Cinar, J. Photochem. Photobiol. A 146 (2002) 189.

[77] N. J. Turro, Modern Molecular Photochemistry (1978) Menlo Park: Benjamin/Cummings Publishing Co. 628.

[78] M. A. Fox, Photocatalysis: Fundamentals and Applications, N. Serpone, E. Pellizzetti, Editors (1989) John Wiley & Sons: New York. 421.

[79] H. Al-Ekabi, N. Serpone, J. Phys. Chem. 92 (1988) 5726.

[80] A. Balcioglu, Y. Inel, J. Chem. 17 (1993) 125.

[81] U. Stafford, K. A. Gray, and P. V. Kamat, Res. Chem. Intermed. 23 (1997) 355.

[82] U. Stafford, K. A. Gray, P. V. Kamat, J. Catal. 167 (1997) 25.

[83] U. Stafford, K. A. Gray, P. V. Kamat, Heterog. Chem. Rev. 3 (1996) 7.

[84] U. Stafford, K. A. Gray, P. V. Kamat, J. Phys. Chem. 98 (1994) 6343.

[85] A. Mills, J. Wang, J. Photochem. Photobiol. A 118 (199) 53.

[86] A. Mills, R. Davies, J. Photochem. Photobiol. A 85 (1995) 173.

[87] A. Mills, S. Morris, R. Davies, J. Photochem. Photobiol. A 70 (1993) 183.

[88] M. Lidner, J. Theurich, D. W. Bahnemann, Water Sci. Technol. 35 (1997) 79.

[89] G. Ruppert, R. Bauer, G. Heisler, Chemosphere 28 (1994) 1447.

[90] J. Cunningham, P. Sedlak, J. Photochem. Photobiol. A 77 (1994) 255.

[91] S. Schmid, P. Krajnik, R. M. Quint, S. Solar, Radiat. Phys. Chem. 50 (1997) 493.

[92] J. Theurich, M. Lindner, D. W. Bahnemann, Langmuir 12 (1996) 6368.

[93] J. -M. Hermann, J. Matos, J. Disdier, C. Guillard, J. Laine, S. Malato, J. Blanco, Catalysis Today 54 (1999) 255.

[94] A. -K. Axelsson, L. J. Dunne, J. Photochem. Photobiol. A 144 (2001) 205.

[95] X. Z. Li, J. W. Cubbage, W. S. Jenks,, J. Photochem. Photobiol. A 141 (2001) 209.

[96] Y. R. Do, W. Lee, K. Dwight, A. Wold, J. Solid State Chem. 108 (1994) 198.

[97] G. Ramis, G. Busca, C. Cristiani, L. Lietti, P. Forzatti, F. Bregani, Langmuir 8 (1992) 1744.

[98] P. V. Kamat,, J. Phys. Chem. B 106 (2002) 7729.

[99] D. Liu, P. V. Kamat, J. Phys. Chem. 97(1993) 10769.

[100] C. Nasr, P. V. Kamat, S. Hotchandani, J. Electroanal. Chem. 420 (1997) 201.

[101] C. Nasr, S. Hotchandani, and P. V. Kamat, Proceedings - Electrochemical Society 97-20 (1997) 130.

[102] S. Hotchandani P. V. Kamat, Chem. Phys. Lett. 191 (1992) 320.

Chapter 2

Mechanisms of Catalyst Action in the TiO_2-mediated Photocatalytic Degradation of Maleic and Fumaric Acid

A paper submitted to *Applied Catalysis B: Environmental*

Youn-Chul Oh, Xiaojing Li, Jerry W. Cubbage, and William S. Jenks*

Abstract

The partial photocatalytic degradation of maleic acid has been investigated with the purpose of elucidating the mechanism of catalyst action for some of the early transformations. In particular, it is proposed that the photocatalytically induced *cis-trans* isomerization of maleic acid and fumaric acid is initiated by adsorption-dependent reductive electron transfer. An investigation into the involvement of superoxide in the oxygenation reactions observed near neutral and higher pH clearly demonstrates that superoxide does not initiate the chemistry.

2. 1. Introduction

Semiconductor-mediated photocatalytic degradation of organic pollutants in water is a well-documented phenomenon that has found extreme generality with regard to substrate, particularly with TiO_2 photocatalysts [1-9]. Among the most important classes of compounds from a chemical perspective is the group containing aromatic rings, which includes various phenolic pollutants, PCBs, and many herbicides and pesticides. Over the last few years, an area that has received much greater attention in the study of these pollutants is the array of chemical pathways by which compounds are degraded, and the related issue of the mechanisms by which the chemical transformations take place.

It is widely understood that the great majority of chemical steps are oxidative in nature, usually involving hydroxyl radical-like chemistry or oxidative electron transfer. In other instances, overall or transient reductive steps are observed, for example in the reduction of azo dyes [10-15], electron poor aromatics [16-18], or quinones [19-25]. Such reductions are counterintuitive, since photocatalytic reduction is widely perceived as oxidative. In fact, in many mechanistic discussions of degradations of large organic molecules, a key issue is the competition between processes represented in equations 2, 3, and 4, i.e., whether oxidation occurs by way of hydroxyl type chemistry or direct oxidative electron transfer. However, electron transfer to an organic substrate (eq 8) can be pictured as competing with the usual reductive electron transfer to molecular oxygen (eq 5).

$$TiO_2 + h\nu \rightarrow h^+_{vb} + e^-_{cb} \quad (1)$$

$$H_2O_{ads} + h^+_{vb} \rightarrow \cdot OH_{ads} + H^+ \quad (2)$$

$$OH^-_{ads} + h^+ \rightarrow \cdot OH_{ads} + H^+ \quad (3)$$

$$M + h^+_{vb} \rightarrow M^{+}\cdot \quad (4)$$

$$O_2 + e^-_{cb} \rightarrow O_2^{-}\cdot \quad (5)$$

$$O_2^{-}\bullet + H^+ \rightarrow HO_2\bullet \quad (6)$$

$$2HO_2\bullet \rightarrow H_2O_2 + O_2 \quad (7)$$

$$M + h^+_{vb} \rightarrow M^{-}\bullet \quad (8)$$

In this paper, we examine the early transformations related to the degradation of maleic and fumaric acid under conditions of TiO_2-mediated photocatalytic degradation. These compounds are ubiquitous in the degradation of aromatic compounds [24-32]. Among the earliest studies of carboxylic acids is Bard's report on the degradation of benzoic acid in aqueous media using platinized TiO_2 [33]. Hydroxylation of the aromatic ring to give salicylic acid and decarboxylation with oxidation to give phenol (presumably after subsequent reaction of Ph• with O_2) were the observed primary transformations. Subsequent studies focused on the regiochemistry of hydroxylation of benzoic acid and various halogenated derivatives [34,35]. Some evidence for loss of CO_2 by *ipso* attack was reported, and it was found that hydroxylation was not competitive with decarboxylation of CO_2 in chlorobenzoic acids. With aromatic polycarboxylic acids, both hydroxylation and decarboxylation are reported as primary reaction pathways [36].

There are also several publications reporting the degradation of various simple alkyl carboxylic acids. Again following early work by the Bard group, subsequent workers reported that there is a significant pH dependence on the balance between H_2 and CH_4 evolution from acetic acid and that longer chain acids (e.g., butyric acid) gave evidence for non-Kolbe pathways apparently initiated by hydrogen abstraction from the alkyl groups [37,38]. Production of chloride was also noted for chloroacetic acid derivatives [38]. Several relevant facts emerge from a recent study of the degradation of butyric acid [39]. The equilibrium concentration of butyric acid in aqueous solution is higher at pH values above the acid dissociation constant, implying that adsorption is

stronger for the protonated acid. Nonetheless, the observed rate of degradation was higher at pH 6.9 than that at pH 3.6. Observed product distributions varied, but this was attributed mainly to the different distributions of species available to react after radical formation. Again, the interpretation was based on a competition between hole oxidation to give the decarboxylation and chemistry initiated by hydrogen abstraction done by hydroxyl radicals. Similar competitive chemistry was observed for the more functionalized hydroxybutanedioic acid (malic acid) [40].

2,4-Dichlorophenoxyacetic acid (also known as the herbicide 2,4-D) and closely related compounds have received special attention because of their direct environmental relevance [41-45]. Following the pattern outlined above, the main initial product detected (2,4-dichlorophenol) derives from decarboxylation, but some studies also report competitive formation of arene-hydroxylated species under some conditions. The most detailed mechanistic work of these was interpreted in terms of a competition between direct hole oxidation and hydroxyl radical chemistry [41]. At low pH (where we may infer that the adsorption binding constant is higher), it is asserted that direct oxidation by holes predominates, whereas hydroxyl-type chemistry predominates in neutral and basic solution. A purely radical mechanism based on competition between surface-bound and bulk solution chemistry was rejected on the basis of experiments using solution-phase hydroxyl radical scavengers.

The most relevant study to the present work is a paper by Franch *et al.* in which the degradation of oxalic, fumaric, and maleic acids is reported [46]. Adsorption isotherms indicate that approximately three times more maleic or fumaric acid is bound to TiO_2 at pH 3 than at pH 9. Like the butyric acid case, the initial degradation rate is modestly higher at the higher pH, despite the poorer adsorption. On this basis, they conclude that degradation occurs in the homogeneous phase at high pH by means of solvated hydroxyl radicals. Franch *et al.* also report a change in product distribution with

pH. At pH 3, intermediate build-up is reported. The fastest process is *cis-trans* isomerization, which is attributed to interaction between the acids and photogenerated holes. Aside from this, the major product is reported to be acrylic acid (CH_2=CH-CO_2H), attributed to photo-Kolbe chemistry. A small amount of photohydration to malic acid is reported as well. Downstream intermediates include acetic, oxalic, and formic acids. This is summarized in Scheme 1. At pH 9, very little intermediate build-up is reported aside from oxalic acid, implying that the first chemical step is slower than subsequent oxidations. In a related study of the degradation of malic acid [40], maleic and fumaric acid are reported as observed intermediates, implying that photoinduced *de*hydration may occur, as well as photoinduced hydration. However, this study did not single out maleic/fumaric acid as a starting point for further degradations, and pathways beginning from there are thus speculative.

Scheme 1. Summary of pathways proposed by Franch et al. for photocatalytic degradation of maleic or fumaric acid at pH 3 in TiO_2 slurries [46].

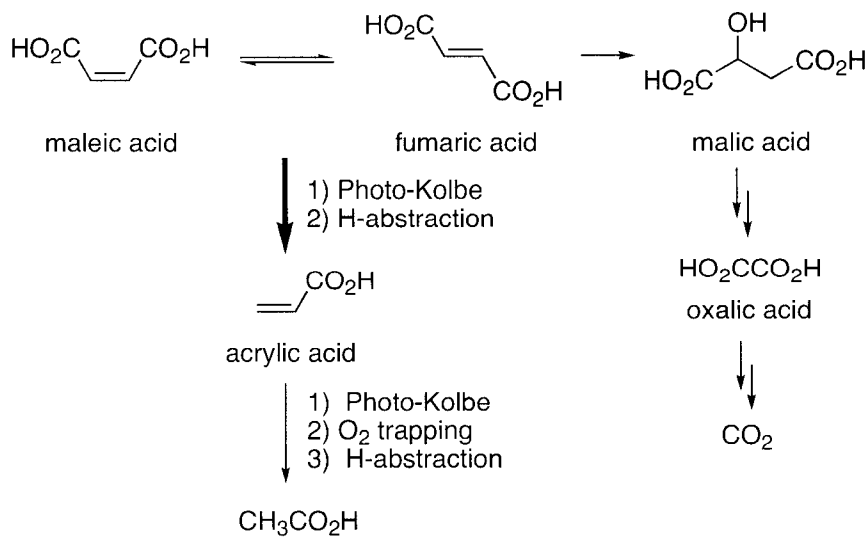

In this paper, we report an investigation of the degradation of maleic and fumaric acids that begins in a manner parallel to the work of Franch. Many, but not all, of our product observations are in agreement with the previous work. We report a series of experiments designed to elucidate more clearly the mode of molecule-catalyst interaction that leads to various processes, including especially tartaric acid formation and the *cis-trans* isomerization.

2. 2 Experimental Section

Materials.

All reagents were purchased from Aldrich and used without further purification unless otherwise indicated. Tartronic acid and Superoxide dismutase (SOD, from bovine erythrocytes, 3000 units in 0.8 mg) were purchased from Sigma. The water employed was purified by Milli-Q UV plus system (Millipore) resulting in a resistivity more than 18 MΩ cm^{-1}. TiO_2 was Degussa P-25. The epoxides of sodium fumarate and sodium maleate were prepared by stereospecific epoxidation by the method of Payne [47]. ^1H NMR (D_2O) d 3.61 (*cis*); 3.32 (*trans*). Dihydroxyfumaric acid dimethyl ester was prepared by a reported method [48].

Standard degradation conditions

Except as noted, degradations followed these standard conditions. A 100 mL aqueous solution containing 2.0 mM starting material (usually maleic acid) and 50 mg suspended TiO_2 was prepared. The pH of solution was adjusted by HCl (pH 2), phosphate buffer (10 mM, pH 7.0), or NaOH (pH 12). The mixture was treated in an ultrasonic bath for 5 minutes to disperse larger aggregates and purged with O_2 for 20 minutes in the dark before the irradiation was started. The mixture was continuously

purged with O_2 throughout the experiment. Irradiations were carried out with stirring and a fan that kept the temperature at ambient levels in a Rayonet mini-photochemical reactor equipped with eight 4 W "black light" which have a broad emission spectrum centered at 360 nm. After reaction, the mixtures were acidified, centrifuged, and filtered to remove TiO_2. Water was removed by freeze-drying. Adipic acid as an internal standard was added after photoreaction as necessary.

General analytical methods

Following the removal of water, the intermediate degradation products were identified and quantified as their trimethylsilyl (TMS) derivatives, using GC-MS procedures reported in our earlier work [24]. Some analyses were carried out after reduction of the reaction mixture with $NaBH_4$ or $NaBD_4$ [24]. The instrument was a Varian 3400CX GC equipped with a 30 m DB-5 column, coupled to a Finnigan Magnum ion trap mass spectrometer. The temperature program was 120 °C for four min, followed by a ramp to 200 °C at 5 °C/min, then ramp at 15 °C/min to 280 °C. An HP 5890 gas chromatograph with FID detection was also used for routine quantification. Some analyses, were carried out after reduction of the reaction mixture with $NaBH_4$ or $NaBD_4$ [24], as noted in the text.

Miscellaneous experimental conditions

Superoxide experiments. Potassium superoxide (KO_2) is slightly soluble in dry dimethyl sulfoxide (DMSO). Using the method of Valentine [49], 0.15 M solutions of KO_2 were prepared in the presence of 0.30 M 18-crown-6 [50]. Maintenance of the characteristic pale yellow color of these solutions was taken as evidence that the superoxide remained. Reactions using either pyridine or DMSO as the solvent for maleic acid were carried out with KO_2:maleic acid ratios of 1:1, 5:1, 5:1 in the presence of

1% water added, and 1000:1. The following example is representative of the reaction conditions. To a solution of maleic acid (100 mL, 2 mM in DMSO), the KO_2 solution (50 mL) was added dropwise over the course of 1 h. The solvent was evaporated under vacuum and the residual material was silylated as usual and analyzed by GC-MS. No degradation of maleic acid nor any new organic compounds were observed.

Superoxide Dismutase (SOD) Experiments. The method of Pichat [27,51-53] was closely followed, and some of his experiments were duplicated as positive controls, as our results were universally negative, i.e., there was little or no effect of adding SOD. In the relevant experiments, maleic acid (39 mmol) and TiO_2 (25 mg) were dispersed in 50 mL water buffered at pH 7 with the buffer supplied with the enzyme by Sigma. After ultrasonic treatment and O_2 purging as usual, 1500 units of SOD was introduced. The mixture was irradiated in the usual fashion for 40 min, followed by the usual workup and analysis.

Fluoride experiments. These degradation reactions, workup, and analyses were carried out in the standard fashion, with the following exceptions: Sufficient NaF was added to raise the concentration of the solution to 20 mM before addition of the TiO_2. The pH of the slurry was adjusted to 3 to maximize surface coverage by fluoride ions [54,55].

2. 3. Results and Discussion

Product mixtures and exploratory degradations

Photocatalytic degradations of maleic acid (**1**) were carried out at pH 2, 7, and 12 using the light from broadly emitting fluorescent tubes centered at 360 nm. The solutions initially contained 2.0 mM maleic acid and 50 mg TiO_2 in 100 mL O_2-saturated water. Control experiments showed that no degradation occurred in the absence of TiO_2 or irradiation. Experiments carried out in the absence of O_2 are described in more

detail below, but oxidative transformations were curtailed, compared to the ordinary conditions. We did not repeat the more extensive kinetic experiments of Franch, *et al.* but qualitatively observed that the degradations were faster at high pH, in line with their observations [46].

We observed many of the same degradation intermediates as Franch, and a few more. This is probably reasonable, given that we used GC-MS detection, and they used HPLC with UV detection. However, we did not observe any acrylic acid, nor did Herrmann *et al.* in their study of malic acid, which generated fumaric/maleic acid [40]. The 4-carbon intermediates observed included fumaric acid, malic acid, tartronic acid, tartaric acid, dihydroxyfumaric acid, and succinic acid. The 3-carbon intermediates included 3-oxopriopionic acid, malonic acid, tartronic acid and 2-hydroxy-3-oxopropionic acid. The only identified 2-carbon product was oxalic acid. We did not assay for either acetic or formic acid. Control experiments showed that all observed compounds were stable on the time-scale of our experiments in the dark throughout the pH range used.

As previously noted [46], there is a distinct dependence of the product mixtures on pH. The observed mixtures obtained after a fixed irradiation period of one hour and silylative workup are shown in Figure 1 and Scheme 2. A representative time-trace of intermediates of partial degradation at pH 12 is given as Figure 2. The standard initial concentration of maleic acid was 2.0 mM. Small quantities of very high molecular weight compounds (i.e., long GC retention times) were sometimes observed. The presence of dihydroxyfumaric acid (**11**) was deduced in the degradations at neutral pH from reductive workups using $NaBD_4$, which yield deuterated tartaric acid before silylation. The ratio of mass intensities showed that slightly more than half of the tartaric acid peak represented **11**.

Control experiments consisting of partial degradations using 30 mM H_2O_2 and irradiation centered at 300 nm in lieu of TiO_2 were carried out. These reactions produce

free hydroxyl and hydroperoxyl radicals. A very similar group of compounds was observed as we report for the pH 7 TiO_2 experiments, regardless of the pH of the solutions with H_2O_2. Tartaric acid was the largest component of the product mixture, but fumaric acid was not observed. This is a good indication that the product distribution in the TiO_2 experiments is a result of differential product *formation*, as opposed to rapid and selective dark degradation of some products at the high or low pH. Further controls showed that the product mixtures obtained from TiO_2 were stable over at least several hours, longer than the timescale of the usual workup and analysis.

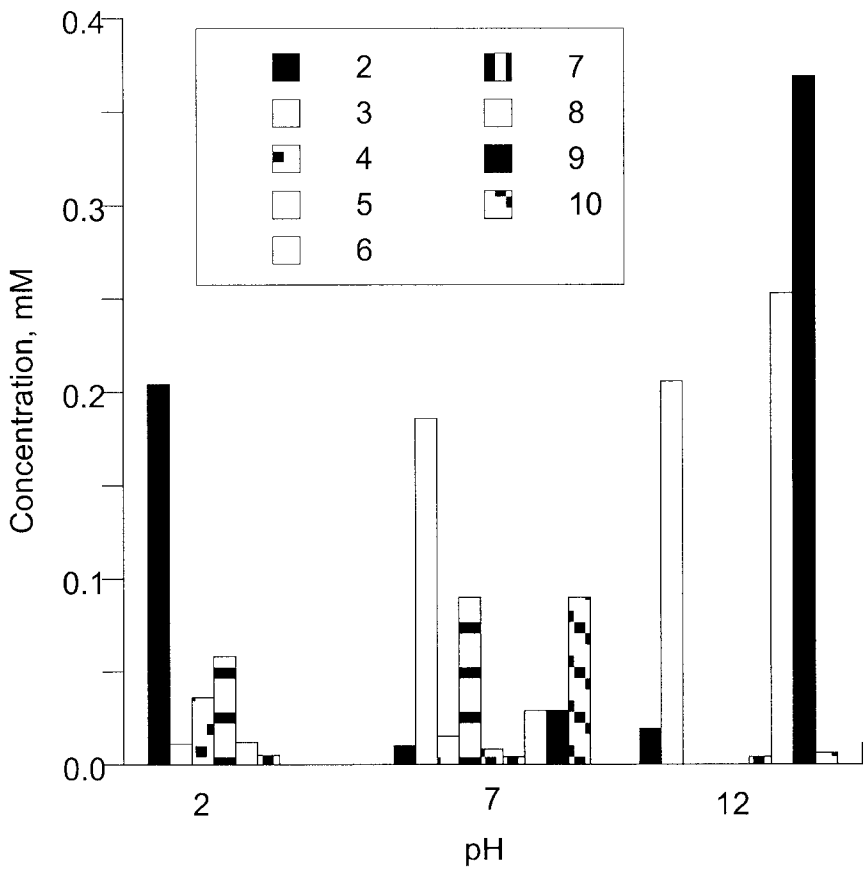

Figure 1. Product distributions after 1 h irradiation for degradations of 2.0 mM maleic acid at pH 2, 7, and 12. The residual maleic acid concentration was 1.4 mM, 1.2 mM, and 0.7 mM, respectively. See Scheme 1 for compound identification.

Scheme 2.

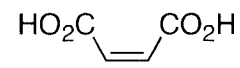

maleic acid, **1**

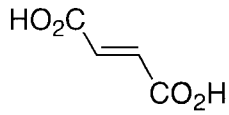

fumaric acid, **2**

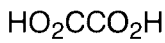

oxalic acid, **3**

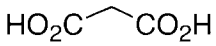

malonic acid, **4**

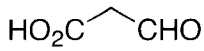

3-oxopropionic acid, **5**

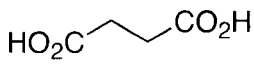

succinic acid, **6**

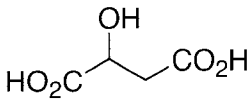

malic acid, **7**

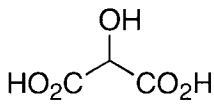

tartronic acid, **8**

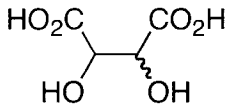

tartaric acid, **9**

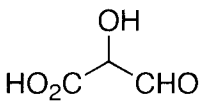

2-hydroxy-3-oxo-
priopionic acid, **10**

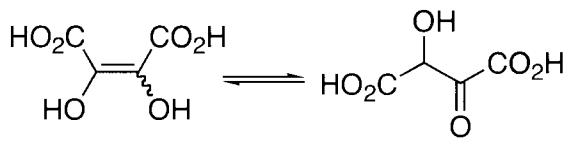

dihydroxyfumaric acid, **11**

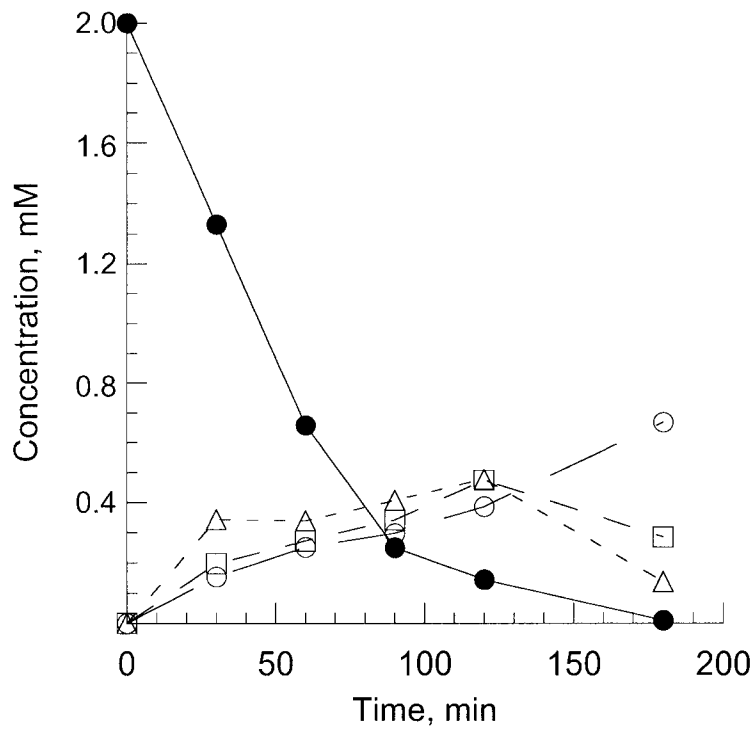

Figure 2. The variation of the relative concentration of maleic acid (●) and oxalic acid (○), tartronic acid (□) and tartaric acid (△) at pH 12. The original concentration of maleic acid was 2.0 mM.

Isomerization mechanisms and the question of homogeneous versus surface-bound mechanisms.

One of the most important questions, from a fundamental perspective, regarding the nature of the substrate-catalyst interaction in photocatalytic degradation is whether reactions occur in the homogeneous bulk phase or at the surface of the catalyst. It is not a question that can be easily settled with steady-state kinetics experiments because every plausible kinetic model based on surface-bound or homogeneous reactive

intermediates reacting with substrate yields kinetic information of the same form [56]. Thus, this is still a question of some dispute, though the more conventional position at this point may be that most reactions occur at the surface [57]. Nonetheless, previous workers on this system argued that degradation at higher initial pH occurs in the bulk water [46]. This conclusion was based on the observation that the rate of the reaction rises, despite a lowering of the binding affinity of maleic and fumaric acid. Furthermore, methanol, a known scavenger of HO• was able to drop the rate of degradation by a factor of 2 at pH 9, but not at all at pH 3.

We have suggested that hydroxyl-like chemistry may occur at or near the surface of the catalyst, but may have less rigorous requirements for specific adsorption modes or sites of adsorption than direct electron transfer reactions between the substrate and the photoactivated TiO_2 particle [24,29]. For example, surface-bound hydroxyl radicals may be formed and remain stable until diffusion either from bulk or through multilayer adsorption brings an appropriate substrate in contact with the reactive species. On the other hand, it is unlikely that a valence-band hole will "wait around" for an organic substrate, rather than finding a surface trap to make a surface-bound hydroxyl radical.

The formation of fumaric acid from maleic acid struck us as a reasonable case to test for surface-bound vs. bulk mechanisms and for the possibility of electron transfer as a mechanism that did not lead to Kolbe chemistry in a carboxylic acid. In principle, several mechanisms may be initially considered.

- Direct photolysis might cause conventional photochemical *cis-trans* isomerization. This mechanism is eliminated by control experiments in which the TiO_2 is not included that do not produce isomerization.
- Acid- or base-catalyzed dark reactions might cause isomerization. Dark control experiments eliminate this pathway.
- Superoxide and/or HOO• might reversibly add to the olefin, transiently

eliminating the double bond and allowing isomerization. Experiments described in section 3.3 eliminate this as a likely explanation.

- Maleic acid may serve as an electron *donor* to activated TiO_2, transiently causing formation of the maleic acid radical cation, which would have a considerably lower barrier to rotation. This is the most conventional explanation [46,58,59]. One problem with this explanation is that it is the same initial step invoked for the Kolbe-type decarboxylation, though it is possible that the same radical cation could lead to both reactions.
- Maleic acid may serve as an electron *acceptor* from photoactivated TiO_2, transiently causing formation of the maleic acid radical anion, which would have a considerably lower barrier to rotation, particularly if C2 is protonated.

Of these possibilities, and related reactions in homogeneous solution, we favor the reversible reductive electron transfer of maleic acid as will be justified below. A plausible mechanism is illustrated in Scheme 3. First, however, we offer an interpretive framework for the observed chemistry that varies slightly from that of Franch *et al.* The essential distinction is that while both they and we postulate two types of reactivity (of which one is electron transfer at the surface), we believe that there is no requirement for their assertion that the second type is reaction in the bulk phase of the water. Below the pKa of the acid, the fraction of adsorbed maleic acid, typical of carboxylic acids, is greater. This could result in the population of a qualitatively different binding mode or a particular type of binding site, both of which could favor the electron-transfer type chemistry. The distinction between this chemistry and HO• chemistry is shown by the results of photolysis of H_2O_2. At higher pH, the predominant chemistry is clearly different, but it need not be in the homogeneous aqueous phase simply because the apparent binding constant is moderately lower. We have reported similar changes in

chemistry from oxidative electron transfer chemistry to hydroxyl-like chemistry with the change of phenolic OH-groups to methoxy groups [29]. Here, adsorption is modified by the capping of the phenols and its resulting prevention of C-O-Ti type adsorption, rather than by changing pH. We argued that the hydroxyl type chemistry could be due to non-specific binding with the titania surface and/or reactions very near the surface. Alcohol additives were more effective in slowing down the hydroxyl-type chemistry than the electron transfer chemistry, but they were also shown to displace the poorly binding substrates; these were also the same ones that suffer the great proportion of hydroxyl-type chemistry.

With this framework in mind, and having established that HO• from H_2O_2 photolysis does not cause substantial *cis-trans* isomerization of maleic acid, we investigate whether maleic acid acts an the electron acceptor or donor with activated TiO_2. Experiments were carried out in the absence of O_2, using Ar purging rather than O_2 purging in otherwise "standard" conditions. This technique generally[60] results in the almost complete shutdown of degradative processes [24,25,29,61]; this is universally attributed to rapid and efficient e^-/h^+ recombination because there is no O_2 available to act an electron sink. Inhibition occurs even when reactions are postulated to occur by oxidative electron transfer. However, if an alternative efficient electron acceptor is available, then reactivity can continue.

Standard maleic acid degradation suspensions, adjusted to pH 2, were prepared such that half were O_2-purged as usual, and half were Ar-purged. After 1 h of photolysis, the O_2-purged solutions had a total conversion of 24%. This could be fully accounted for by the appearance of fumaric acid (19%), malonic acid (1.4%), succinic acid (2.7%), and malic acid (0.9%). After an identical 1 h of photolysis, the Ar-purged solutions had a remarkable 83% conversion, of which 82.5% was fumaric acid, with the observable remainder being succinic acid. This experiment clearly demonstrates that

O_2 in fact *inhibits* the cis-trans isomerization of maleic acid. This is strong evidence that fumaric acid is acting as the electron acceptor. The simplest explanation for the increased efficiency is straightforward: under oxygenated conditions, O_2 acts as a competitor with maleic acid for accepting electrons from activated TiO_2. This interpretation requires that superoxide not be an effective catalyst for *cis-trans* isomerization (see below), that the radical anion isomerize by some unspecified mechanism, and that the radical anion be able to return the electron to TiO_2 or another species [62]. An outline of a reasonable mechanism is given in Scheme 3.

Scheme 3. A plausible schematic mechanism for *cis-trans* isomerization that begins with reductive electron transfer. The position of protonation is purely speculative.

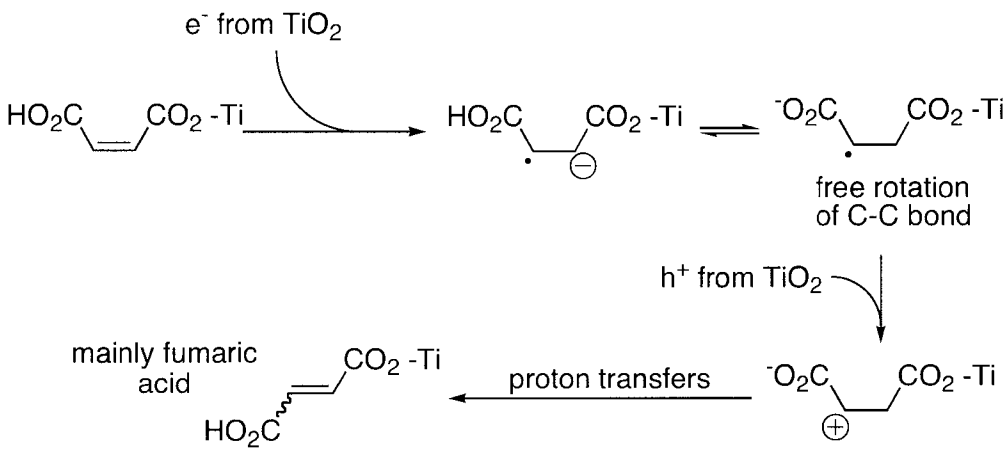

This led us to attempt to obtain a photocatalyzed photostationary state of the maleic/fumaric acid mixture at pH 2. These experiments were carried out under standard pH 2 conditions, save that they were Ar-purged, and in one case fumaric acid was used instead of maleic acid. The results (Figure 3) show that this was achieved and that, as expected, fumaric acid is predominant. The final product mixture was very close to 92%

fumaric acid, 7% maleic acid and 1% succinic acid, relative to the initial 2.0 mM concentration. It is interesting to note that the sole new product observed is a reductive product from maleic/fumaric acid, consistent with reductive electron transfer. What remains a surprise is that there is no oxidative chemistry from $HO\bullet_{ads}$ or other species.

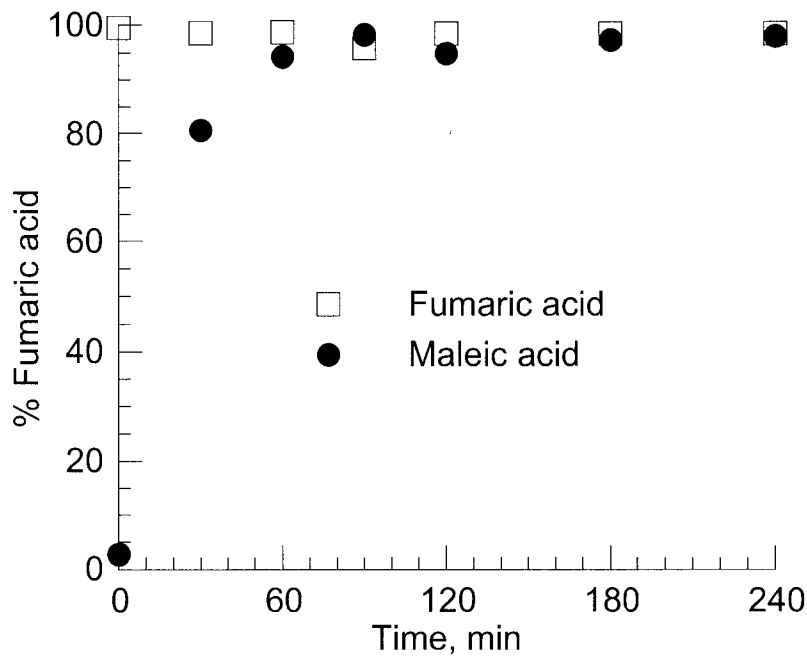

Figure 3. A photostationary state arrived at by photocatalytic treatment of either maleic or fumaric acid in the absence of O_2 at pH 2. The final proportion of Fumaric acid is approximately 94%.

The O_2 vs. Ar experiment was repeated at pH 12, where the acids are completely dissociated when in the bulk phase. Under these conditions, after an hour, the oxygen-saturated sample had lost 85% of its initial maleic acid. Of that, only 2.5% was fumaric acid, with oxalic acid making the bulk of the remainder (78%) along with small

quantities of the other usual materials, in agreement with Franch's reports. This latter result, along with the high conversion obviously implies considerable downstream degradation. With Ar-purging, the total conversion was only 32%, of which only 2.2% was fumaric acid. (Of the rest, 29.5% was malic acid.) The most important result here is that Ar purging does not completely shut down the reaction. A reasonable interpretation is that maleic acid can act as an electron acceptor even at this high pH, but that in its deprotonated state it is not as reactive to isomerization, perhaps because it cannot undergo the necessary protonation for easy bond rotation before back electron transfer or other chemistry occurs (e.g., Scheme 3). The binding isotherms of Franch, *et al.* [46] clearly demonstrate that there is still adsorption between maleic or fumaric acid and TiO_2 even at high pH, which is at least consistent with this speculation.

Another set of experiments were carried out in the presence of fluoride anion. The addition of fluoride anion to TiO_2 suspensions at low pH has been shown to produce homogenous hydroxyl radicals and dramatically reduce the surface-bound chemistry of phenol, a poorly adsorbing substrate [54,55]. Qualitatively speaking, this effect is attributed to displacement of the surface hydroxyls by fluoride and the concomitant change in surface properties. Water can be oxidized to form hydroxyl radicals that are not bound to the titania surface. For example, cyanuric acid, a compound that does not adsorb to TiO_2 in solution and is ordinarily completely resistive to photocatalytic degradation by TiO_2 slurries, is degraded by the TiO_2/F system [63]. Minero also showed that TiO_2/F was able to degrade phenol in the absence of O_2 much more rapidly than does "naked" TiO_2, though more slowly than in the presence of O_2. Presumably, this derives from diffusing HO• effectively leading to more efficient charge separation than is possible with naked TiO_2.

Degradations of maleic acid and fumaric acid were carried out at pH 3 in the absence of O_2 with fluoride added, and without fluoride as a control. Over the course of

an hour of simultaneous photolysis of the four samples, *cis-trans* isomerization was severely curtailed for the fluoride-containing samples. In one hour of photolysis of maleic acid in the absence of fluoride, the product distribution was fumaric acid 6.0%, succinic acid 1.0%, malic acid 2.0%, with a total conversion of 9.0%. In the presence of fluoride, isomerization is dramatically reduced. There was fumaric acid at only 1.8% and malic acid 4.7% for a total conversion of 6.5%. The obvious implication here is that the isomerization requires surface adsorption, and thus electron transfer chemistry is again supported.

When degradations were carried out in the presence of fluoride anion at pH 3 with O_2 purging, the mass balance was poor, even at moderate conversion. Thus, degradation of the early intermediates to CO_2 was probably faster than the initial step. While TOC experiments were not run to check this, the result is consistent with Minero's report of much greater mineralization with O_2 than without [54,55]. At 31% conversion of maleic acid, 0.3% oxalic acid, 1.6% fumaric acid, 0.6% tartronic acid and 2.2% tartaric acid were detected. A similar result showing very little isomerization was observed using fumaric acid as the starting material. Again, the implication is that solution phase chemistry is not responsible for the isomerization reaction.

As a final control, the substrate was modified by using the methyl ester (i.e., dimethyl maleate), rather than the carboxylic acid. This would prevent a binding mode in which C-O-Ti linkages were made. Using otherwise standard degradation conditions, at neutral pH, the major observed products were the dimethyl ester analogs of tartaric acid, dihydroxymaleic acid, and the monomethyl ester of oxalic acid. At pH 2, however, the major product was dihyroxymaleic acid diester, with almost no dimethyl fumarate observed. We thus conclude that there is a quality about the carboxylic acid functionality itself that is required for efficient *cis-trans* isomerization, and we postulate that it is related to a C-O-Ti binding mode analogous to that which was proposed (for example) by

Moser *et al.* for aromatic acid derivatives [64], or characterized by Martin *et al.* for 4-chlorocatechol [65]. The relevant bond lengths make it seem most likely that a single Ti atom is involved, but we cannot rule out a second one, nor can we be sure whether one or both of the carboxylic acids is adsorbed in this way. One might speculate that only a single carboxylic group is chemisorbed in order to account for the favoring of the *trans*-configured fumaric acid over maleic acid, but this is certainly not a requirement.

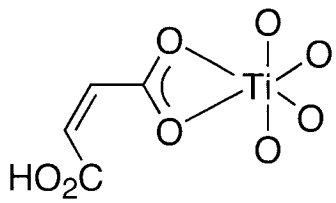

Mechanisms of oxygenation reactions

Given our interpretation that the *cis-trans* isomerization is best explained by reversible reductive electron transfer chemistry, we wished to explore the possibility that some of the oxidation (or, perhaps more properly, oxygenation) products might begin with a step that itself was formally reductive in nature. The most obvious candidate was reaction between maleic acid and superoxide near neutral pH, where the latter is largely deprotonated and nucleophilic. While the acids are also largely deprotonated in homogeneous solution, they might still be associated with the titania in such a way as to make them behave like the ester, rather than the anion or dianion. Though the adsorption coefficient is not as high at high pH as it is acidic solution [46], we were intrigued with the possibility that a surface-bound tartaric acid might suffer from attack by nucleophilic hydroperoxyl/superoxide species, rather than electrophilic hydroxyl species, as outlined in Scheme 4, which is simplified for easier viewing. Maleic and fumaric esters are well known as good acceptors of nucleophilic attack (the

Michael addition).

Scheme 4. Possible mechanisms for formation of **9** and **11**. For simplicity, free, rather than surface-bound compounds are shown. It is understood that protonation states will vary, though protons also stand in for potential Ti atoms in various potential bound states in the Scheme.

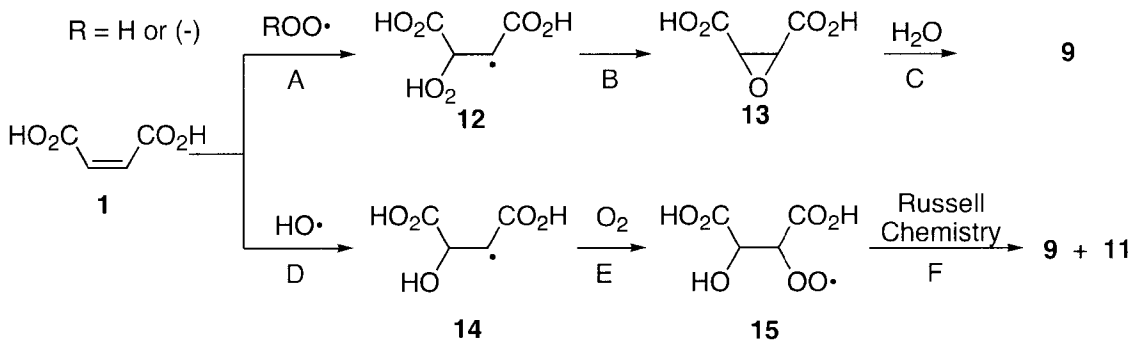

At pH 7 and 12, where the products are observed most readily, the HOO•/O_2^{-}• equilibrium lies far to the side of superoxide. It is obviously more nucleophilic than the conjugate acid, making step A more reasonable. Further, we hypothesize that the substrate is surface-bound to maintain its effectively "protonated" state with regard to Michael-type attack at the b-position, relative to the adsorbing acid group. Step B is thermodynamically downhill and related reactions are well known in the organic literature [66-72]. In aqueous solution, **13** is an obvious precursor to **9** by either acid or base catalyzed ring opening. The path shown by steps D-F is the more conventional mechanism for oxidative chemistry under these and similar conditions [73,74], though it assumes termination by another low concentration intermediate, i.e., another peroxyl species in step F. We thus sought tests to explore plausibility of the path beginning with step A. The first was to test for the intermediacy of **13**.

Compound **13**, the epoxide of maleic acid, was prepared as its sodium salt. It was hypothesized that a competition between hydrolysis and oxidation might lead to **9** and **11**. However, photocatalytic treatment of **13** did not produce detectable amounts of **11** when degradations were carried out to low conversion at pH 2, 7, or 12. The major product at pH 2 was oxalacetic acid (**16**), with some tartaric acid formed. At pH 7, these were observed in reverse order of importance. At pH 12, even at low conversion, more products were observed: **16** > **3** > **9** > **8** > **4**.

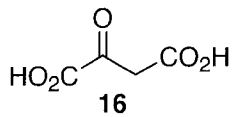

16

A hypothesis that might have accounted for the lack of observation of **16** in the degradations of maleic acid is that **16** is particularly rapidly degraded. In fact, degradations beginning with **16** at 2 mM did produce intermediates that were observed in maleic acid degradations. At pH 2, tartaric acid and dihydroxyfumaric acid were the most predominant products. At pH 7, tartaric acid was predominant. At pH 12, compounds **4**, **8**, **3**, and **9** were observed, in that order of abundance, indicating that decarboxylation reactions had become competitive with initial hydroxylations. However, degradations of **16** were not significantly more rapid than those of any other substrate, and the very fact that it was so easily observed in the degradations of **13** cast doubt on the idea.

It was also plausible that superoxide was involved in the reaction (e.g., step A followed by other chemistry), but that other details of the pathway in Scheme 3 were incorrect. Any mechanism that avoided the epoxide **13** would have been missed by the above experiments. Thus, we sought more direct evidence regarding superoxide itself.

Following the precedent of Pichat and coworkers [27,51-53], degradations were carried out in the presence of commercial samples of superoxide dismutase (SOD), an enzyme that catalyzes the disproportionation of superoxide to hydrogen peroxide and O_2. At near-neutral pH (using the commercial buffer), the presence of SOD did not qualitatively affect the rate of degradation of maleic acid. Neither did it suppress tartaric acid formation, which was still the major 4-carbon intermediate. (Small quantities of fumaric acid were also observed, consistent with ordinary degradations at this pH.) This suggests that superoxide is not the primary reactant in formation of tartaric acid.

Finally, maleic acid was treated with superoxide solutions formed by dissolving commercially available KO_2 in dry DMSO containing 18-crown-6. Reactions were carried out in pyridine, anhydrous DMSO, and wet DMSO with superoxide:maleic acid ratios of 1:1, 5:1, and 1000:1. No maleic acid-derived products were observed at the lower ratios of KO_2:**1**. A trace quantity of fumaric acid (and oxalic acid) was observed after an hour of treatment at the 1000:1 ratio. These conditions are at orders of magnitude higher concentrations of superoxide than is plausible under normal photocatalytic conditions, though the solvent differs and the TiO_2 surface does not serve to pre-organize the mixture. Nonetheless, we conclude that these experiments strongly argue against superoxide being the primary reagent reacting with maleic acid in ordinary photocatalytic conditions. No tartaric acid, oxalacetic acid or any 3-carbon compounds were observed in any of these experiments.

We thus conclude that superoxide is not an important reactant in the formation of any of the four-carbon intermediates, including the *cis-trans* isomerization products. In the absence of evidence to the contrary, we thus favor the conventional hydroxyl addition steps as the primary reaction mode to get to the oxygenated products.

The observed chemistry in neutral to basic oxygenated solution is, as Franch notes, very hydroxyl-like. This does not require that the chemistry be in the

homogeneous phase, though the current results do not require that it be at the surface. They only require the electron transfer chemistry in low pH be reductive. However, though our experiments are not compelling for surface-mediated chemistry other than for the isomerization reaction, we remain compelled by the experiments of Minero and others (e.g., Refs [54,55,57]), and feel that this should be the assumption in the absence of convincing evidence for homogeneous-phase chemistry.

2. 4. Conclusions

Partial photocatalytic degradation of maleic acid gives rise to most of the plausible oxygenated compounds with four carbons or fewer. Our observations are generally in line with the recent report of Franch [46], save that we do not observe by GC-MS acrylic acid, which they report with HPLC and UV detection. The *cis-trans* isomerism of maleic acid under acidic conditions is proposed to occur by way of reductive electron transfer to the adsorbed acid. The bases for this conclusion include the acid's superior adsorption at low pH [46], the near exclusivity of this process in the absence of O_2 (which usually acts as an electron acceptor), the increase in observed isomerization rate in the absence of O_2 (contrary to almost any other known photocatalytic degradation process), and the suppression of isomerization with the addition of fluoride to the system. An investigation into the possibility that other reactions begin with the reaction of maleic acid with superoxide in a similar electron/nucleophile-accepting mode produced results in clear contradiction with this idea. It is presumed that the formation of tartaric acid and dihydroxyfumaric acid – along with other smaller intermediates – occurs by conventional mechanisms beginning with hydroxyl attack on the substrate.

Acknowledgement

The support of this research by the IPRT Center for Catalysis and, in part, the National Science Foundation is gratefully acknowledged. We gratefully acknowledge helpful conversations with Prof. James Espenson and Gabor Lente.

2. 5. References

[1] *Photocatalytic Purification and Treatment of Water and Air*, D.F. Ollis, H. Al-Ekabi, Eds.; Elsevier Science Publishers: New York, 1993, pp 820.

[2] *Aquatic and Surface Photochemistry*, G .R. Helz, R. G. Zepp, D. G. Crosby, Eds.; Lewis Publishers: Boca Raton, 1994.

[3] D.S. Bhatkhande, V.G. Pangarkar, A.A.C.M. Beenackers, J. Chem. Technol. Biotechnol. 77 (2002) 102.

[4] U. Stafford, K.A. Gray, P.V. Kamat, Heterog. Chem. Rev. 3 (1996) 77.

[5] P. V. Kamat, K. Vinodgopal, in: V. Ramamurthy, Schanze, K., Molecular and Supramolecular Photochemistry: Organic and Inorganic Photochemistry, Marcel Dekker, New York, 1998, pp. 307.

[6] M. R. Hoffmann, S. T. Martin, W. Choi, D.W. Bahnemann, Chem. Rev. 95 (1995) 69.

[7] D. Bahnemann, in: P. Boule, Handbook of Environmental Chemistry, Springer, Berlin, Germany, 1999, pp. 285.

[8] A. Mills, S. Le Hunte, J. Photochem. Photobiol. A: Chem. 108 (1997) 1.

[9] N. Serpone, Res. Chem. Intermed. 20 (1994) 953.

[10] C. Hu, J. C. Yu, Z. Hao, P. K. Wong, Applied Catalysis, B: Environmental 42 (2003) 47.

[11] H. Tada, M. Kubo, Y.-i. Inubushi, S. Ito, Chem. Commun. (2000) 977.

[12] G.T. Brown, J.R. Darwent, Journal of the Chemical Society, Faraday

Transactions 1: Physical Chemistry in Condensed Phases 80 (1984) 1631.

[13] K. Kunitou, S. Maeda, S. Hongyou, K. Mishima, Canadian Journal of Chemical Engineering 80 (2002) 208.

[14] K. Tanaka, K. Padermpole, T. Hisanaga, Water Research 34 (1999) 327.

[15] D. You, H. Xie, S. Dai, Journal of Environmental Sciences (China) 4 (1992) 97.

[16] M. Muneer, D. Bahnemann, Water Science and Technology 44 (2001) 331.

[17] M. Muneer, D. Bahnemann, Applied Catalysis, B: Environmental 36 (2002) 95.

[18] M. Muneer, J. Theurich, D. Bahnemann, J. Photochem. Photobiol. A 143 (2001) 213.

[19] D. Bahnemann, Handbook of Environmental Chemistry 2 (1999) 285.

[20] C. Richard, New J. Chem. 18 (1994) 443.

[21] C. Richard, P. Boule, New J. Chem. 18 (1994) 547.

[22] C. Richard, P. Boule, Sol. Energy Mater. Sol. Cells 38 (1995) 431.

[23] J. Theurich, M. Lindner, D.W. Bahnemann, Langmuir 12 (1996) 6368.

[24] X. Li, J.W. Cubbage, T.A. Tetzlaff, W.S. Jenks, J. Org. Chem. 64 (1999) 8509.

[25] X. Li, J.W. Cubbage, W.S. Jenks, J. Org. Chem. 64 (1999) 8525.

[26] C. Bouquet-Somrani, A. Finiels, P. Graffin, J.-L. Olivé, Appl. Catal. B 8 (1996) 101.

[27] L. Amalric, C. Guillard, P. Pichat, Res. Chem. Intermed. 21 (1995) 33.

[28] P. Pichat, Water Sci. Technol. 35 (1997) 73.

[29] X. Li, J.W. Cubbage, W.S. Jenks, J. Photochem. Photobiol. A 143 (2001) 69.

[30] J. M. Tseng, C. P. Huang, Water Sci. Technol. 23 (1991) 377.

[31] E. Vulliet, C. Emmelin, J.-M. Chovelon, C. Guillard, J.-M. Herrmann, Applied Catalysis, B: Environmental 38 (2002) 127.

[32] M. Stylidi, D.I. Kondarides, X.E. Verykios, Appl. Cat. B 40 (2003) 271.

[33] I. Izumi, F. -R. F. Fan, A. J. Bard, J. Phys. Chem. 85 (1981) 218.

[34] R. W. Matthews, J. Chem. Soc. Faraday Trans. 1 80 (1984) 457.

[35] H. Tahiri, Y. Ait Ichou, J. -M. Herrmann, J. Photochem. Photobiol. A 114 (1998) 219.

[36] A. Assabbane, A. Boussaoud, A. Albourine, Y. Aitichou, M. Petit-Ramel, Ann. Chim. (Paris) 22 (1997) 301.

[37] T. Sakata, T. Kawai, K. Hashimoto, J. Phys. Chem. 88 (1984) 2344.

[38] A. Chemseddine, H. P. Boehm, J. Mol. Catal . 60 (1990) 295.

[39] C. Guillard, J. Photochem. Photobiol. A 135 (2000) 65.

[40] J. -M. Herrmann, H. Tahiri, C. Guillard, P. Pichat, Catal. Today 54 (1999) 131.

[41] Y. Sun, J. J. Pignatello, Environ. Sci. Technol. 29 (1995) 2065.

[42] A. Topalov, B. Abramovic, D. Molnár-Gábor, J. Csanádi, O. Arcson, J. Photochem. Photobiol. A 140 (2001) 249.

[43] S. Horikoshi, H. Hidaka, N. Serpone, J. Photochem. Photobiol. A 159 (2003) 289.

[44] K. Tanaka, K. S. N. Reddy, Appl. Catal. B 39 (2002) 305.

[45] M. Trillas, J. Peral, X. Domenech, Appl. Catal. B 5 (1995) 377.

[46] M. I. Franch, J. A. Ayllon, J. Peral, X. Domenech, Catalysis Today 76 (2002) 221.

[47] G. B. Payne, P.H. Williams, J. Org. Chem. 24 (1959) 54.

[48] E. F. Hartree, J. Am. Chem. Soc. 75 (1953) 6244.

[49] J. S. Valentine, A. B. Curtis, J. Am. Chem. Soc. 97 (1975) 224.

[50] C. J. Pedersen, H . K. Frensdorff, Angewandte Chemie, International Edition in English 11 (1972) 16.

[51] L. Amalric, C. Guillard, P. Pichat, Res. Chem. I nt. 20 (1994) 579.

[52] L. Cermenati, A. Albini, P. Pichat, C. Guillard, Res. Chem. Intermed. 26 (2000)

221.

[53] L. Cermenati, P. Pichat, C. Guillard, A. Albini, J. Phys. Chem. B 101 (1997) 2650.

[54] C. Minero, G. Mariella, V. Maurino, D. Vione, E. Pelizzetti, Langmuir 16 (2000) 8964.

[55] C. Minero, G. Mariella, V. Maurino, E. Pelizzetti, Langmuir 16 (2000) 2632.

[56] C. S. Turchi, D. F. Ollis, J. Catal. 122 (1990) 178.

[57] C. Minero, F. Catozzo, E. Pelizzetti, Langmuir 8 (1992) 481.

[58] M. A. Fox, C. C. Chen, J. Am. Chem. Soc. 103 (1981) 6757.

[59] J. Araña, O. Gonzalez Diaz, M. Miranda Saracho, J. M. Dona Rodriguez, J. A. Herrera Melian, J. Perez Pena, Appl. Catal. B 36 (2002) 113.

[60] We cite our own work here not out of vanity or because others have not done it, but because we wish to stress that the conditions we are speaking of are identical to those used with other compounds, i.e., done in our hands with our exact procedures.

[61] Y. -C. Oh, Y. Bao, W.S. Jenks, J. Photochem. Photobiol. A 160 (2003) in press.

[62] This interpretation is also consistent with our lack of observation of acrylic acid, a product that would likely result from oxidative electron transfer.

[63] Y.-C. Oh, W. S. Jenks, J. Photochem. Photobiol. A in press (2003).

[64] J. Moser, S. Punchihewa, P.P. Infelta, M. Grätzel, Langmuir 7 (1991) 3012.

[65] S. T. Martin, J. M. Kesselman, D. S. Park, N. S. Lewis, M. R. Hoffmann, Environ. Sci. Technol 30 (1996) 2535.

[66] J. C. Rienstra-Kracofe, W. D. Allen, H. F. I. Schaefer, J. Phys. Chem. A 104 (2000) 9823.

[67] M. S. Stark, J. Am. Chem. Soc. 122 (2000) 4162.

[68] R. R. Baldwin, D. R. Stout, R. W. Walker, J. Chem. Soc. Faraday Trans. 87 (1991) 2147.

[69] R. R. Baker, R. R. Baldwin, A. R. Fuller, R. W. Waker, J. Chem. Soc. Faraday Trans. 1 71 (1975) 736.

[70] R. Ruiz Diaz, K. Selby, D. J. Waddington, J. Chem. Soc. Perkin Trans. 2 (1975) 758.

[71] N. D. Stothard, R. W. Walker, J. Chem. Soc. Faraday Trans. 86 (1990) 2115.

[72] P. Koelewijn, Recueil 91 (1972) 759.

[73] C. von Sonntag, H.-P. Schuchmann, Angew. Chem. Int. Ed. Engl. 30 (1991) 1229.

[74] G. A. Russell, J. Am. Chem. Soc. 79 (1957) 3871.

Chapter 3

Photocatalytic Degradation of a Cyanuric Acid, a Recalcitrant Species

A paper accepted by *The Journal of Photochemistry and Photobiology: A: Chemistry*

Youn-Chul Oh and William S. Jenks*

Abstract

Degradation of cyanuric acid in aqueous suspensions of DeGussa P25 TiO_2 has been achieved by the addition of fluoride ion at low pH. Consistent with the work of Minero and Pelizzetti, it is suggested that this is due to the formation of homogeneous phase hydroxyl radicals. Support for this hypothesis is brought from successful degradations using other hydroxyl-generating conditions and the successful degradation of 4-*t*-butylpyridine, another organic compound previously shown to be resistant to TiO_2-mediated photocatalytic degradation.

3. 1. Introduction

Nearly every organic molecule ever tested is degraded to CO_2, H_2O, and appropriate inorganic ions when exposed to TiO_2-mediated photocatalytic degradation conditions in oxygenated water. This mineralization process is the basis upon which the use of TiO_2 and other semiconductors for water purification is built.

One of the very few organic molecules known to survive such treatment is cyanuric acid, **1**. This is of both fundamental and practical interest. The latter is true because of the large family of triazine herbicides in popular usage, most notably atrazine. Several studies have all shown that atrazine and other triazine herbicides are all degraded to cyanuric acid in the presence of irradiated TiO_2 suspensions, but that no further degradation takes place [1-7]. While it is known that cyanuric acid is generally difficult to chemically hydrolyze or oxidize [8], this result is still remarkable given the extreme generality of the TiO_2 photocatalytic degradation method. In contrast, biologically based degradations using *Pseudomonas* sp. bacteria have been successful. These degradations proceed through biuret and urea, both of which are intermediates that are formally products of hydrolysis reactions [9-12]. Similarly, hydrolysis can be catalyzed by alumina in the range of 300 °C [13] or in supercritical water at even higher temperature and pressure [14].

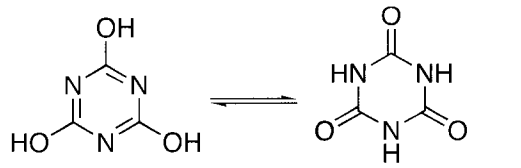

Cyanuric Acid, **1** Isocyanuric acid

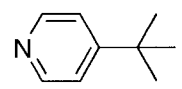

4-*t*-Butylpyridine, **2**

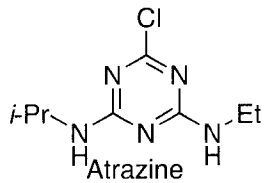

Atrazine

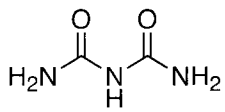

Biuret

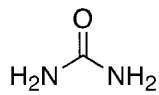

Urea

In neutral to acidic solution, **1** exists predominantly in the tautomeric form known as isocyanuric acid[8], which is related to cyanuric acid by a series of keto-enol equilibria. (For convenience, we will consistently refer to the mixture of tautomers as cyanuric acid.) The pKa values are 6.9, 11.4, and 13.5, and most evidence suggests that the anion that is formed is that of the cyanuric acid tautomer. This suggests that cyanuric acid, were it adsorbed to TiO_2, would probably be in the enolic form, but there is no direct evidence on this point.

A few reasonable hypotheses might be proposed to account for the stability of **1** to TiO_2-mediated photocatalytic degradation, which generally occurs by electron transfer reactions and the action of adsorbed hydroxyl radicals. First, it might be argued that the principle reaction might simply be removal of one of the phenolic hydrogen atoms, either directly or by sequential electron and proton loss. The resulting phenolic-type radical might be sufficiently stable to survive until it can pick

up an electron to return to starting material or its conjugate base. Although it is well known that a great many aromatic compounds (including many phenols) are hydroxylated by irradiated TiO_2 suspensions, we know of no specific evidence to contradict this assertion. A second hypothesis is that that hydroxyl radical addition does occur, but is reversible because loss of water or HO• results in a species that ends up returning to cyanuric acid under the conditions. We refuted this hypothesis a few years ago, showing that ^{18}O in **1** is retained, at least on timescales that are relevant to the usual degradation chemistry [4]. It might also be argued that the carbon atoms in cyanuric acid are already fully oxidized and are simply not reactive with the usual species formed in photocatalytic conditions. However, as we have also previously shown [4], urea is sensitive to TiO_2-mediated degradation, even though its carbon atom is also formally at the CO_2 oxidation state. In this paper, we will present circumstantial evidence for what might be the simplest hypothesis of all, that **1** does not adsorb significantly to TiO_2, and – given that the great majority of TiO_2-mediated degradation chemistry occurs on the catalyst surface – cyanuric acid is not present where the active oxidizing species are formed.

The factor that suggested this idea to us was the recent report from Nedoloujko that 4-*t*-butylpyridine (**2**) also withstood TiO_2 conditions, but was degraded by Fenton chemistry [15]. This was important in that the degradations of pyridine derivatives have been reported a number of times[16-22] without any evidence that pyridines are particularly hardy species. It thus seemed at least plausible that something similar – presumably a lack of contact between the reactive

intermediates and the substrate – was occurring with cyanuric acid. Perhaps it was only the reputation of cyanuric acid as a particularly persistent molecule that made one propose that there would be special chemical explanations.

Here we report the degradation of cyanuric acid, both using Fenton chemistry and the TiO_2-fluoride system introduced by Minero and Pelizzetti [23,24]. These authors, on the basis of elegant kinetic studies, proposed that addition of fluoride ion to TiO_2 suspensions under acidic conditions causes the surface coating of the particles with fluoride and the production of homogeneous hydroxyl radicals. For simplicity, we will refer to conditions in which NaF has been added to TiO_2 suspensions as TiO_2/F. The results simultaneously support two hypotheses: (1) that cyanuric acid is not pathologically resistant in principle to this type of degradation, but is not degraded by TiO_2 because it does not bind at or near catalytically active sites, and (2) the Minero-Pelizzetti proposal that the TiO_2/fluoride system is capable of producing mobile – and presumably homogeneous – hydroxyl radicals.

3.2. Experimental

Materials.

All chemicals were obtained from Aldrich in the highest purity available and used as received, except as noted. The water employed was purified with a Milli-Q UV plus system resulting in a resistivity ≥ 18 MΩ cm^{-1}. TiO_2 was DeGussa P-25.

Degradation and analysis procedures.

Photocatalytic Degradation. All suspensions were prepared at 100 mg TiO_2 per 100 mL water. The pH was regulated by addition of HCl (pH 2), phosphate buffer (10 mM, pH 7) or NaOH (pH 12). NaF, if used, was added at a concentration of 40 mM. After an hour of stirring and equilibration in the dark, the desired organic (**1** or **2**) was introduced at a concentration of 300 μM. The mixture was dispersed in an ultrasonic bath for 5 minutes to disperse larger aggregates and then purged with O_2 and stirred for 20 minutes in the dark before the irradiation was started. The mixture was continuously purged by O_2 throughout the irradiation except as noted. Irradiations were carried out with stirring at ambient temperature using a modified Rayonet mini-reactor equipped with a fan and 8 4-watt broadly emitting 365 nm fluorescent tubes. After the reactions, samples were acidified, centrifuged, and filtered to remove the TiO_2. Water was removed by freeze-drying. Anthracene was added after photolysis as an external standard for GC analysis.

H_2O_2 photodegradation. Solutions were prepared as above, leaving out TiO_2. Immediately before photolysis, 1.0 mL of H_2O_2 (30% in water) was added. Photolysis and analysis were carried out in the ordinary way, save that broadly emitting 300 nm fluorescent tubes were used instead.

Fenton reaction. Reactions were conducted at room temperature. Normal conditions were 300 μM of the organic substrate, 8 mM $FeSO_4$ and 80 mM H_2O_2. The pH of solution was regulated as usual. After desired reaction time, the resultant mixture was filtered through 0.2 μm Whatman filters without otherwise quenching the

reaction and the water was removed by freeze drying. Ordinary analyses were then used.

Analysis. The dried samples were exhaustively silylated by treatment with 1 mL of anhydrous pyridine, 0.2 mL of hexamethyldisilazane, and 0.1 mL chlorotrimethylsilane. The reactions were carried out in 1.5 mL plastic-stoppered vials. The resulting mixtures were shaken vigorously for about 60 seconds and then allowed to stand for 5 minutes at room temperature. Some precipitate was separated by centrifugation prior to chromatographic analysis. The intermediate products were analyzed as their TMS derivatives using GC-MS on a Varian star 3400CX Gas Chromatograph using 25 m DB-5 column, coupled with a Magnum ion trap detector mass spectrometer (Finnigan MAT, San Jose, CA). The temperature program of column was as follows: at 150 ˚C, hold time = 2 min; from 150 to 200 ˚C, rate = 10 ˚C/min; then raise the rate to 40 ˚C/min until 280 ˚C. A HP 5890 series II Gas Chromatograph with a 25 m ZB-5 column and an FID detector was also used for routine analysis.

Adsorption of Cyanuric acid to TiO_2/F and TiO_2. Equilibrium extents of adsorption onto TiO_2/F and TiO_2 were evaluated after equilibration for fixed periods with vigorous magnetic stirring. The adsorption was evaluated at three different pHs: pH 2, 7, and 11 were held by HCl, and 30mM phosphate buffer, and NaOH, respectively. Suspensions were prepared containing 50 mg of TiO_2 in 20 mL water and a variable amount of cyanuric acid. For TiO_2/F 84 mg of NaF was added to each sample. After at least 9 h for equilibration, an aliquot was removed, and

syringe filtered twice through Millipore 0.22 μm and Poll 0.20 μm filters to remove TiO_2. The residual concentration of **1** was determined by UV-VIS spectroscopy using a Shimadzu UV-2101 spectrometer.

3. 3. Results

The experiments of Nedoloujko and Kiwi[15] were qualitatively reproduced. It was found that 4*t*-butylpyridine (**2**) was degraded only very, very slowly under typical TiO_2 conditions, regardless of pH. However, at pH 2, using TiO_2/F, **2** was degraded over the course of several hours. We do not dwell on the products formed under these conditions, as this compound was not of our primary interest. However, early in the degradation, in addition to the usual trace products, a few major products were partially identified on the basis of mass spectral data. A very small amount of dimer was formed. What appeared to be a single isomer of a hydroxylated product (mass = M + OTMS) was the largest new peak at modest degradation conversion. We assume this is the 3-hydroxylated material. An apparently single isomer of a bishydroxylated species (mass = M + 2 OTMS) was also observed. A second dioxygenated species was formed (mass = M + 2 O) that was not silylated, indicating that this was probably a ring-opened product.

Additionally, samples of cyanuric acid (300 μM) were exposed to the standard photocatalytic degradation conditions (100 mg TiO_2 in 100 mL H_2O, broad 365 nm irradiation, O_2-saturated solutions) at pH 2, 7, and 12. Under no conditions was

measurable degradation observed, consistent with literature reports.

Treatment of **1** at the same concentrations, but with the addition of NaF (i.e., TiO_2/F conditions) were also carried out. At pH 12, no degradation was observed. At pH 7, some degradation was observed over the course of several hours, but degradation was 3-4 times faster at pH 2. A qualitative indication of the relative rates can be seen in Figure 1, which illustrates the remaining cyanuric acid after a fixed degradation period of 6 hours. Degradation kinetics were approximately first order for two half-lives, as is often observed for photocatalytic degradations.

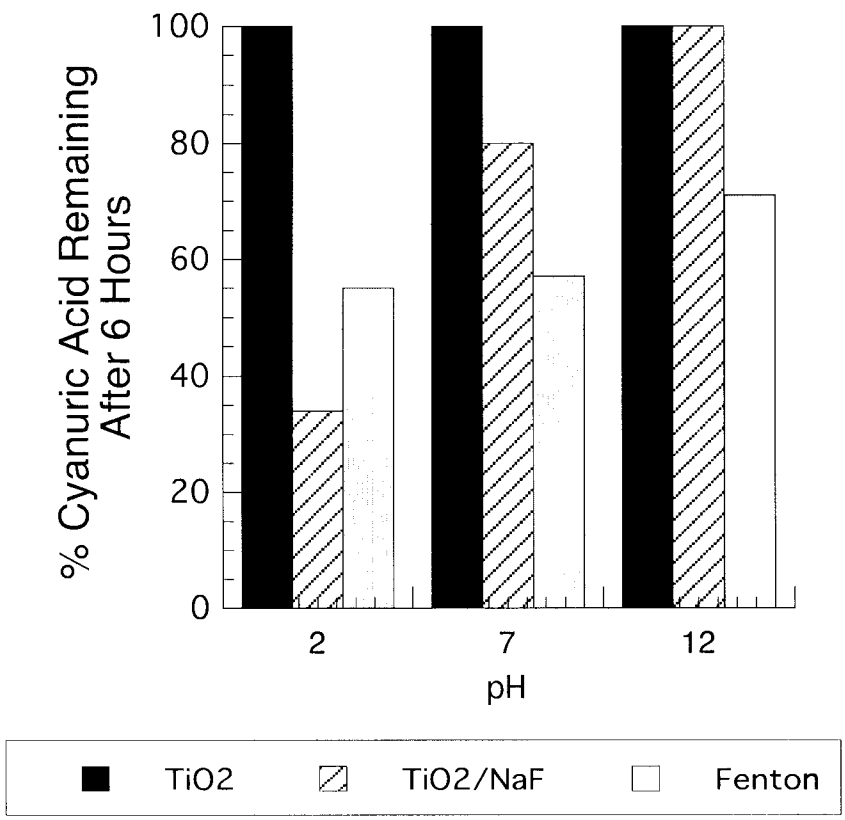

Figure 1. Cyanuric acid remaining after a fixed period of irradiation under several conditions. The initial concentration was 300 μM for all experiments.

Control experiments using extended irradiation in the absence of NaF indicated that the rate of degradation in the presence of fluoride ion at pH 2 was a minimum of 1000 times faster than in its absence. If either the TiO_2 was left out of the suspension or the sample was flushed with Ar to remove all O_2 and kept anaerobic, no degradation of **1** was observed on photolysis.

At appropriate intervals during the degradations using Na/F conditions, samples were removed from the slurry. The TiO_2 was removed from the slurry, and the residual material remaining after the water was removed was exhaustively silylated and subjected to standard GC-MS analysis. In no case were any intermediates in the degradation observed. Control experiments using potential intermediates urea and biuret ($NH_2CONHCONH_2$) showed that these compounds would have been observed had they been in the mixture.

These results were compared to degradations held under other conditions. Photolysis of oxygen-saturated solutions initially containing 300 μM **1** and 8.8 mM H_2O_2 at pH 2 using broadly emitting fluorescent bulbs centered at 300 nm resulted in successful degradation of cyanuric acid on a timescale similar to the TiO_2/F experiments. An exact rate comparison is meaningless because the output of the lamps (though of the same order of magnitude) was not measured, and the absorption of light in the homogeneous sample is much different than in the highly scattering TiO_2 suspensions. However, as expected, the degradations showed zero-order kinetics, as appropriate for a homogeneous photochemical reaction limited by photon absorption. As before, no intermediates were detected.

Fenton chemistry using an excess of $Fe(SO_4)$ and H_2O_2 in the dark was also applied to 300 μM solutions of cyanuric acid. As shown in Figure 1, these degradations were successful at every pH and showed less variation in rate. Again, the comparison of the absolute rates to the TiO_2/F conditions is not particularly meaningful, but what is important is that degradations occur at all pH values tested, indicating that the lack of TiO_2/F-mediated degradation at high pH is not a special feature ot the chemistry of **1**, *per se*. As usual, no degradation intermediates were observed.

The extent of adsorption of cyanuric acid to TiO_2 was determined by UV/Vis spectroscopy. Samples were prepared using 50 mg TiO_2 in 20 mL water and various concentrations of **1**. Figure 2 shows the residual absorptions at 213 nm for three sets of samples: no TiO_2, TiO_2, and TiO_2/F, all at pH 2 after removal of TiO_2 by centrifugation and filtration. The data clearly indicate that there is no more than a few percent of the cyanuric acid adsorbed, even at the highest concentrations. Very similar data were obtained at pH 7 and 12, though the extinction coefficients (and thus the absolute absorptions) vary because of the protonation state of the cyanuric acid.

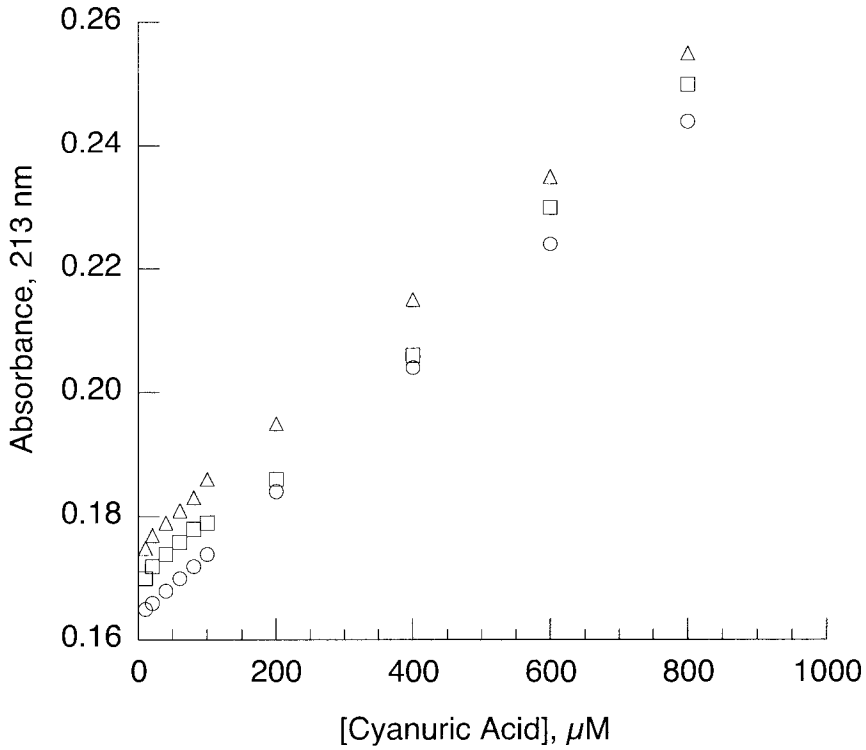

Figure 2. Residual absorption at 213 nm after removal of TiO_2. Circles: no TiO_2; Squares: TiO_2; Triangles: TiO_2/F.

3. 4. Discussion

Minero, Pelizzetti, and coworkers carried out an elegant set of experiments, based largely on kinetic analyses of the degradation of phenol, using TiO_2 suspensions at various pH values in the presence and absence of fluoride ion [23,24]. At low pH, fluoride displaces OH from the surface of the TiO_2 particles, with a maximum fluoride coverage calculated in the range of approximately pH 2.5 to 4.5, based on reasonable assumptions for the TiOH acid-base equilibria, the fluoride exchange equilibrium constant, and a fixed concentration of TiO_2 and fluoride. For

phenol, they determined that at pH 3.6 with 10 mM F^-, virtually all of the reactivity of phenol is with homogeneous hydroxyl radicals formed by oxidation of water. They report a change in the ratio of *ortho* and *para* hydroxylation that occurs when NaF is present, though also note this can be sensitive to many parameters.

We hypothesize here that this formation of freely diffusing hydroxyl radicals caused by addition of fluoride at low pH facilitates the photocatalytic degradation of cyanuric acid. Consistent with the data in Figure 2, we suggest that, more than its general resistance to hydrolysis and oxidation, the reason cyanuric acid is not degraded in the presence of "naked" TiO_2 is that it does not adsorb to the surface of TiO_2 to any measurable extent. Therefore, when surface-bound hydroxyl radicals or trapped valence bond holes are formed, it is effectively inert simply because it is virtually never in the immediate vicinity of the reactive species. In contrast to naked TiO_2 conditions, cyanuric acid *is* degraded on photolysis of hydrogen peroxide or by Fenton chemistry. These results clearly show that it is not solely the inherent unreactivity of cyanuric acid that causes its stability to normal photocatalytic conditions by showing that it is degraded by homogeneously dispersed hydroxyl radicals (or in the case of the Fenton reaction, hydroxyl-like species).

We further infer from the results of the Fenton and hydrogen peroxide photolysis results that the relative unreactivity of **1** does play a role in the current results, however. That comes from the result that no intermediates such as biuret or urea are observed. If the rate constants for "productive" reactivity between HO• and cyanuric acid are well below the near-diffusion controlled limit that is typical for

reactivity between HO• and organic substrates, then any putative stable intermediates may simply be much more reactive with HO• than cyanuric acid. In such a case, it is plausible that the intermediates never build up a reasonable steady state concentration because they are degraded faster than they are formed [25].

When cyanuric acid is subjected to TiO_2/F photolysis conditions, formation of freely diffusing hydroxyl radicals is consistent both with the hypothesis of Minero and Pelizzetti regarding hydroxyl radical formation and with our own regarding cyanuric acid adsorption as the root cause for its inertness. Because this logic may be considered somewhat circular, it is important to note that TiO_2-mediated degradation of 4-*t*-butylpyridine is also allowed by the addition of fluoride. There is no reason to believe that **2** possesses any special chemical resistance to hydroxyl-like species or valence bond holes, nor that it is reactive with fluoride ion. Indeed, Nedoloujko showed that it too is subject to oxidation by homogeneously dispersed reagents [15]. Thus, these paired results provide strong supporting evidence for the Minero hypothesis, this time using a very simple observable: removal of cyanuric acid from solution at least 3 orders of magnitude more rapidly than without the fluoride.

Moreover, the observation of "ordinary" hydroxylation intermediates in the TiO_2/F-mediated degradation of **2** is consistent with our explanation for the lack of observable intermediates in the degradation of **1**. There is no reason to believe that compound **2** is considerably less reactive than any of its obvious derivatives towards HO•. Thus, the rate of intermediate formation is not grossly lower than that of intermediate degradation early in the course of the reaction, and the steady state

concentration initially builds up. In contrast, as in the homogeneous oxidations, the intermediates from degradation of **1** are consumed more rapidly than they are formed and are thus not detected. An unfortunate corollary of this is that, although the expected reactivity of hydroxyl radicals with **1** would presumably be by addition to the carbon atoms, any further mechanistic discussion is too speculative to be fruitful.

The pH sensitivity of the degradation of **1** under TiO_2/F conditions is also consistent with Minero. By working at pH 2, it is reasonable to suggest that we have not maximized the amount of surface fluoride coverage (which peaks at slightly higher pH according to them), though we used a higher [NaF] than Minero. However, the considerably lower rate at pH 7 is consistent with their prediction of still lower surface coverage by fluoride, and the complete lack of degradation at pH 12 is further consistent with their prediction of negligible fluoride coverage. An important secondary conclusion to draw from this work is that the formation of free hydroxyl radicals apparently does not depend on complete fluoride coverage. While undoubtedly more homogeneous HO• is formed with higher fluoride coverage, some appears to remain even at pH values where coverage is incomplete. The exact form of the pH dependence is beyond the modest scope of this paper, but it is clear that an accurate assessment of the level of fluoride coverage would be required [26]. Finally, it should be noted that we have not optimized the rate of cyanuric acid degradation with respect to lamp output, pH, TiO_2 concentration, [NaF], etc., and it is possible that relative rates could be significantly improved with sufficient effort.

Previous to this, we are aware of only a single report of degradation of cyanuric acid by any TiO_2-mediated system [27]. In contrast to the consistently reported result that cyanuric acid is inert to photocatalytic degradation when using TiO_2 in suspension [1-7], these workers report that cyanuric acid could be degraded by use of their proprietary PHOTOPERM membranes. These membranes contain significant quantities of TiO_2 immobilized in a polyester support formed by polymerization around pre-formed TiO_2 particles. The reasons for this apparently anomalous result are not clear. However, it would be consistent with the current results if their immobilization procedure provides for binding sites that are more attractive to cyanuric acid in addition to immobilizing the TiO_2 particles. Reactions between the TiO_2 and cyanuric acid might then take place. However, this interpretation is purely speculative.

3. 5. Conclusions

The addition of fluoride to aqueous suspensions of titania has proved to be an important mechanistic tool in unraveling a long-standing conundrum in photocatalytic degradation. By using this method in parallel with other methods for producing homogeneous hydroxyl-type reagents, it is shown that cyanuric acid is susceptible to degradation under easily accessible conditions. The comparatively unrelated, but not as generally unreactive, 4-*t*-butylpyridine (which is also almost untouched by ordinary TiO_2 photolysis conditions) is also degraded by TiO_2/F. It gives predictable

hydroxylated intermediates, and thus supports the hypothesis that the induced reactivity is due to the formation of homogeneous HO•. The reason that cyanuric acid is ordinarily inert to TiO_2-mediated photocatalytic degradation appears to be that it simply is not bound to the reactive portions of the TiO_2 surface to any measurable extent, perhaps in combination with its lower reactivity evident from other reactions. Its inherent chemical resistance to degradation is still exhibited in the inability to observe intermediate degradation products, regardless of degradation method, because the intermediates are consumed more rapidly than they are formed.

Acknowledgement

The support of this research by the IPRT Center for Catalysis and, in part, the National Science Foundation is gratefully acknowledged.

3. 6. References

[1] C. M. Maurino, E. Pelizzetti, Res. Chem. Intermed. 23 (1997) 291.

[2] C. Minero, V. Maurino, E. Pelizzetti, Res. Chem. Int. 23 (1997) 291.

[3] E. Pelizzetti, V. Maurino, C. Minero, V. Carlin, E. Pramauro, O. Zerbinati, M.L. Tosato, Environ. Sci. Technol. 24 (1990) 1559.

[4] T. Tetzlaff, W.S. Jenks, Org. Lett. 1 (1999) 463.

[5] V. Héquet, P. Le Cloirec, C. Gonzalez, B. Meunier, Chemosphere 41 (2000) 379.

[6] V. Hequet, C. Gonzalez, P. Le Cloirec, Wat. Res. 35 (2001) 4253.

[7] G. Goutailler, J.C. Valette, C. Guillard, O. Paisse, R. Faure, J. Photochem. Photobiol. A 141 (2001) 79.

[8] J. A. Wojtowicz, in: J. I. Kroschwitz, Kirk-Othmer Encyclopedia of Chemical Technology, Wiley, New York, 1991, pp. 835.

[9] A. M. Cook, FEMS Microbiology Rev. 46 (1987) 93.

[10] M.-S. Lai, A.S. Weber, J.N. Jensen, Water Environ. Res. 67 (1995) 347.

[11] C. Ernst, H.-J. Rehm, Appl. Microbiol. Biotechnol. 43 (1995) 150.

[12] A. M. Cook, P. Beilstein, H. Grossenbacher, R. Hütter, Biochem. J. 231 (1985) 25.

[13] Z. Zhan, M. Müllner, J.A. Lercher, Catal. Today 27 (1996) 167.

[14] S. Horikoshi, H. Hidaka, Chemosphere 51 (2003) 139.

[15] A. Nedoloujko, J. Kiwi, Water Res. 34 (2000) 3277.

[16] I. A. Balcioglu, Y. Inel, J. Environ. Sci. Health, Part A: Environ. Sci. Eng. Toxic Hazard. Subst. Control A31 (1996) 123.

[17] C. Maillard-Dupuy, C. Guillard, H. Courbon, P. Pichat, Environ. Sci. Technol. 28 (1994) 2176.

[18] J. Prousek, A. Klcova, Chem. Listy 91 (1997) 575.

[19] S. Sampath, H. Uchida, H. Yoneyama, J. Catal. 149 (1994) 189.

[20] P. Pichat, L. Cermenati, A. Albini, D. Mas, H. Delprat, C. Guillard, Res. Chem. Int. 26 (2000) 161.

[21] L. Cermenati, A. Albini, P. Pichat, C. Guillard, Res. Chem. Intermed. 26

(2000) 221.

[22] P. Pichat, Water Sci. Technol. 35 (1997) 73.

[23] C. Minero, G. Mariella, V. Maurino, E. Pelizzetti, Langmuir 16 (2000) 2632.

[24] C. Minero, G. Mariella, V. Maurino, D. Vione, E. Pelizzetti, Langmuir 16 (2000) 8964.

[25] We cannot eliminate the possibility of strongly adsorbed intermediates that we cannot detect, though our previous experience makes this seem unlikely.

[26] To the extent that cyanuric acid represents a compound that gives very easily distinguished reactivity, its initial rate of degradation might serve as a useful probe to determine the relative HO• production efficiencies as a function of solution parameters.

[27] B.M. Gawlik, A. Moroni, I.R. Bellobono, H.W. Muntau, Global Nest: the Int. J. 1 (1999) 23.

Chapter 4

Isotope Studies of Photocatalysis. TiO_2-Mediated Degradation of Dimethyl Phenylphosphonate

A paper published by *The Journal of Photochemistry and Photobiology: A: Chemistry*

Youn-Chul Oh, Yun Bao, and William S. Jenks*

Abstract: The initial step of TiO_2 mediated photocatalytic degradation of dimethyl phenyl phosphonate, labeled with ^{18}O or deuteria in the methoxy group, results in products due to ring hydroxylation and demethylation. The ^{18}O laveling experiments clearly demonstrate that the methyl group is lost, resulting in a phosphonic mono-acid, rather than substituting a hydroxy group for methoxy.

4. 1. Introduction

The oxidative degradation of phosphates and phosphonates has received significant attention in recent years because of their inclusion in chemical warfare agents and pesticides[1-12]. Among the relevant compounds are sarin, soman, VX, and malathion. Because of the hazards associated with these compounds, most study has been done with model compounds, such as dimethyl methylphosphonate (DMMP). Our own interest is in TiO_2-mediated photocatalytic degradation and indeed detailed lists of compounds observed in the degradation of DMMP are now available[1,2,6].

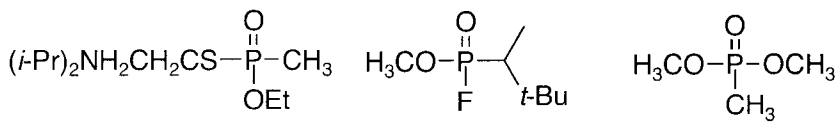

VX **soman** **DMMP**

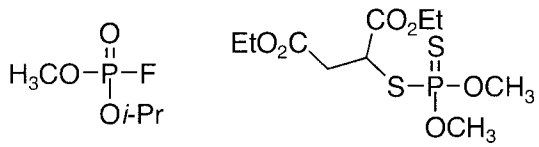

sarin **malathion**

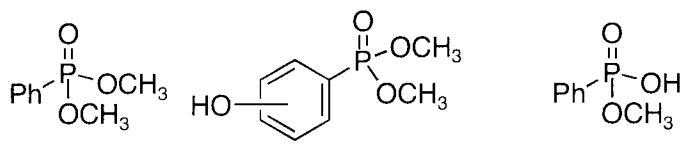

DMPP **OHD, MHD, PHD** **MMPP**

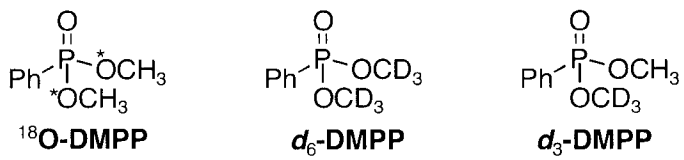

^{18}O-DMPP **d_6-DMPP** **d_3-DMPP**

Exposure of DMMP and related simple phosphonates to TiO_2-mediated photocatalytic conditions results first in the loss of one of the methyl esters. An important unsettled mechanistic point is the mechanism by which the methyl is removed. The question is whether attack occurs at the methyl or at the phosphorus or both.

As originally pointed out by O'Shea, one potential mechanism for the dealkylation of a phosphonate diester to the monoester is by an addition-elimination mechanism in which a hydroxyl radical adds to the phosphorus center to yield a transient 9-electron radical, as illustrated in Scheme 1. (Although illustrated as an oxygen-centered radical, it must be understood that the axial X-P-X system is a 3-centered-4-electron bond, or, in this hypothetical case, a 3-centered-3-electron bond.) Subsequent loss of HO or CH_3O should be approximately equally favorable, especially if the phosphorus center has sufficient lifetime to undergo Berry pseudorotation to place the alkoxyl group in the axial position. This mechanism is of particular interest because of the very well known chemistry in which hydroxyl radicals add to dimethyl sulfoxide at the sulfur center, causing expulsion of a methyl radical[13]. Furthermore, there is fundamental interest because of the question of the relationship between conventional free hydroxyl radicals and the adsorbed hydroxyl radical species presumed to be involved in photocatalysis. An alternative mechanism occasionally invoked in discussions of photocatalysis, but not discussed by O'Shea, is that local generation of a proton as a result of water oxidation leads to acid catalyzed hydrolysis of the phosphonate, again by attack at phosphorus. Either

of these mechanisms might be characterized by the observation of methanol production early in the degradation, as reported by Satyapal[7] under moist gas phase conditions.

Scheme 1. Potential phosphonate dealkylation mechanisms

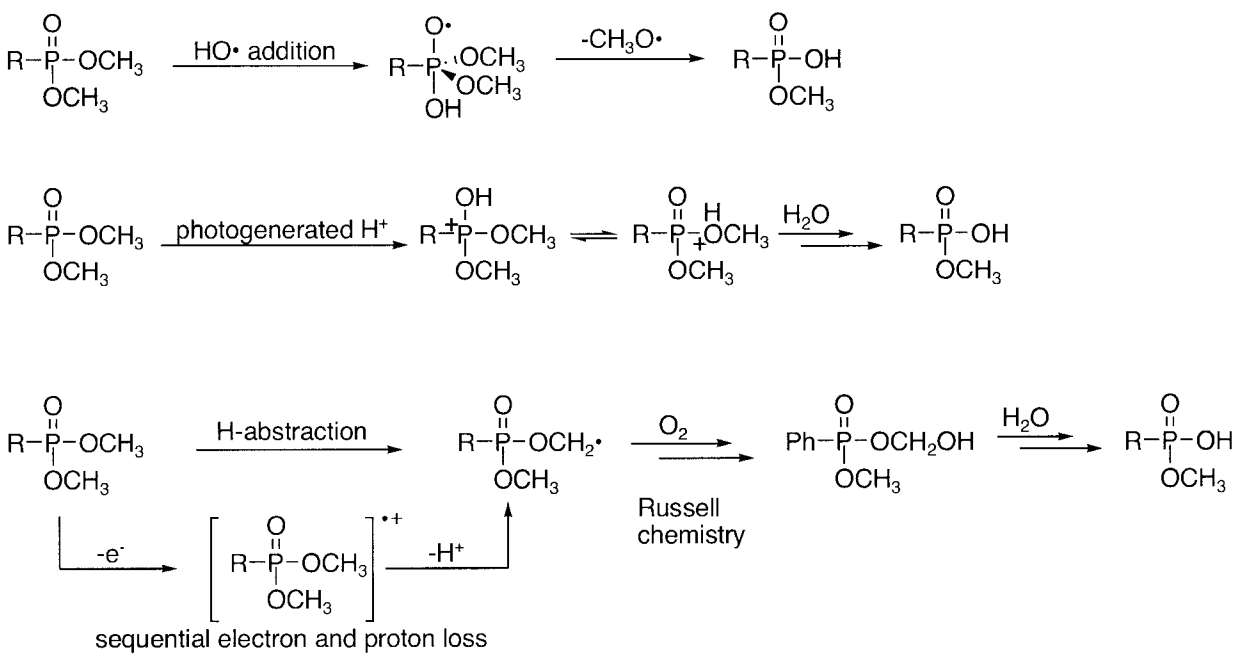

Alternatively, a very conventional mechanism can be written in which hydrogen abstraction occurs at the alkyl hydrogens, followed by O_2 trapping. Russell chemistry[14] then leads to an easily hydrolyzable group. Formaldehyde and formic acid have both been detected as products[1,6]. A recent study using radiolysis to generate hydroxyl radicals[8] supports this pathway, in that (indirect)

spectroscopic product studies indicated that carbon-centered radicals were formed. The same carbon-centered intermediate, can at least in principle, be obtained by sequential loss of an electron and a proton[6], a reaction considerably more likely with TiO_2 than under radiolysis conditions. Finally, there is also no reason not to believe that mechanisms of both types (attack at P or at CH) cannot be occurring simultaneously. This circumstance might explain some confusion among reports in the literature.

To address these issues, especially regarding the mechanism under conditions of TiO_2-mediated photocatalytic degradation, we report a study on the initial steps of degradation of a closely related compound dimethyl phenylphosphonate (DMMP). We use the phenyl group to clearly distinguish reactivity on the alkoxyl groups form that on the phosphonic acid side of the functionality. As expected, this introduces a new set of hydroxylated products: dimethyl *o*-, *m*-, and *p*-hydroxyphenylphosphonates (OHP, MHP, and PHP, respectively), but we are less concerned with these than the product of demethylation: monomethyl phenylphosphonate (MMPP). To definitively and directly answer whether a substitution reaction or an alkyl degradation occurs either alone or in combination with other mechanisms, MMPP was prepared with ^{18}O labels in the alkoxyl positions (^{18}O-DMPP), and to probe for kinetic isotope effects, the degradation of d_6-DMPP and d_3-DMPP was also studied.

4. 2. Experimental Section

General instrumentation

^{1}H and ^{13}C NMR (internal standard TMS), ^{31}P NMR (external standard 85% phosphoric acid) spectral data were obtained on a Varian DRX-400 MHz spectrometer. ^{31}P and ^{13}C NMR spectral data were obtained with ^{1}H decoupling, but ^{31}P coupling remains in the ^{13}C and ^{1}H NMR spectral data. HPLC data were collected with an HP 1050 liquid chromatograph with diode array UV/VIS absorption detector. LC/MS data were collected on Shimadzu LC/MS-2010 by electrospray ionization (ESI) or atmospheric pressure chemical ionization (APCI). An ODS Hypersil reverse phase column (5 μm, 200 X 2.1 mm, Hewlett Packard) was used. The eluent consisted of a 50/50 mixture of acetonitrile and water. GC data were obtained on HP 5890 gas chromatograph with a 30 m (0.25 mm ID x 0.25 μm) DB-5 column and an FID detector. Mesitylene was used as the internal standard when necessary. The GC/MS data were obtained on a VG Magnum ion trap, a Finnegan TSQ700 triple quadruple mass spectrometer, or a Micromass GCT time-of-flight (TOF) mass spectrometer, as indicated. Centrifugation was accomplished using an Eppendorf 5415 C Microcentrifuge. UV data were obtained on a Shimadzu UV-2101 PC.

Degradation and analysis procedures

Standard degradation procedure. Suspensions were prepared containing 5 mM DMPP and 50 mg TiO_2 in 100 mL water. When $^{18}O_2$-DMPP was used, this scale

was dropped ten-fold. When regulated, the initial pH of the solution was controlled by using HCl (pH = 3), 10 mM phosphate buffer (pH = 7) or 10 mM carbonate buffer (pH = 10). The resultant mixtures were treated in an ultrasonic bath for 5 min to disperse large TiO_2 aggregates immediately prior to photolysis. The photodegradation was performed in a Rayonet photochemical reactor with 8 x 4 W "black light" bulbs whose emission is centered at 350 nm. Solutions were purged with O_2 for several minutes in advance of and during photolysis. Samples for analysis were taken out at desired time intervals. The TiO_2 was separated by centrifugation with an Eppendorf Netheler Hinz 5415 C, followed by filtration through a syringe-mounted 0.2 μm Whatman filter to obtain 5 mL aliquots. This solution was analyzed directly when HPLC was used. For GC analysis, additional treatment was necessary. The water was removed *in vacuo* from the 5 mL aliquots. The samples were then silylated by dissolving in 0.5 mL pyridine, followed by treatment for a few minutes with 0.1 mL 1,1,1,3,3,3-hexamethyldisilazane and 0.05 mL chlorotrimethylsilane. After the pyridinium salts were separated by centrifugation, the samples were analyzed by GC/MS.

H_2O_2 photodegradations. Solutions were prepared as above, leaving out the TiO_2. Immediately before photolysis, 1.0 mL of H_2O_2 (30% in water) was added. Photolysis and analysis were carried out in the ordinary way.

Fenton reactions. Reactions were conducted at room temperature. Normal conditions were 4 mM DMPP, 8 mM $FeSO_4$ and 80 mM H_2O_2 in aqueous solution. The pH was controlled at 7 by using 0.1 M phosphate buffer. After 15 min, the

resultant mixture was filtered through 0.2 μm Whatman filters without otherwise quenching the reaction. Ordinary analysis procedures were then used.

Persulfate oxidations. A solution at room temperature containing 10 mM DMPP and 3 mM $K_2S_2O_4$ was purged with Ar to remove O_2. The resulting solution was held at 90 °K under Ar for 14 hours. After cooling, it was extracted with methylene chloride, and the residual material remaining after evaporation was silylated and analyzed as usual.

Photochemical degradations were carried out using persulfate. These solutions contained 10 mM DMPP and 100 mM $K_2S_2O_4$. The concentration of $K_2S_2O_4$ was so high because the extinction coefficient at 254 nm is about one tenth that of DMPP. Photolysis of this mixture caused it to turn dark yellow. Samples were analyzed as usual. Control experiments, in which the persulfate was left out, showed that direct photolysis caused degradation on a much slower timescale than in the presence of persulfate. It was thus assumed that the photochemical degradation was due entirely to persulfate chemistry.

Competition experiments. Competition experiments between DMPP and d_6-DMPP were carried out like all other degradations, save that mixtures of the two isotopologs were used. The same total concentrations were used. MS analysis of the resultant mixtures allowed quantification of the MMPP and d_3-MMPP produced. After accounting for the concentration ratios of the starting materials (usually 1:1), selectivities were obtained from these data. Mass spectral integrations were carried out from either GC-TOF data or ion trap data and were well within experimental error

of one another.

Adsorption experiments. Either 5 or 25 mg TiO_2 was added to 10 mL solutions of DMPP or other substrate at various concentrations. The resulting suspensions were stirred for a minimum of four hours. The TiO_2 was removed by centrifugation and filtration as above, and the concentration of the organic compound in the supernatant was determined by quantitative UV spectroscopy. Dimethyl phenyl phosphonate e(264 nm) = 905 $M^{-1}cm^{-1}$; Monomethyl phenyl phosphonate e(263 nm) = 452 $M^{-1}cm^{-1}$; Dimethyl *meta*-hydroxyphosphonate e(283 nm) = 2401 $M^{-1}cm^{-1}$.

Materials

DeGussa P25 TiO_2 was used as received. Water was obtained from an ultrapurification unit from Millipore and had resistivity ≥ 17 MW cm^{-1}. DryTHF was obtained by distillation under argon from THF solution dried by sodium and benzophenone. Dried benzene was obtained by distillation under argon from benzene solution with CaH_2. Phenylphosphonic acid was purified by recrystallization from ethyl acetate. Other solvents and reagents were used as received. Flash SiO_2 column chromatography or preparative TLC with 2 mm thickness of silica gel on a 20 cm x 20 cm glass plate was usually used to purify the products.

Dimethyl phenylphosphonate (DMPP)[15]. To a stirred solution of pyridine (6.57 mL, 0.081 mol) and methanol (3.14 mL, 0.078 mol) in 80 mL of methylene chloride at 0 °C under argon, phenylphosphononyl dichloride (5 mL, 0.035 mol) was

added dropwise. The mixture was stirred for 5 h at room temperature. The resultant solution was washed with cold water, cold 1 M HCl, cold saturated $NaHCO_3$ solution, and again with cold water, in that order. After drying over anhydrous $MgSO_4$ and subsequent removal of the methylene chloride *in vacuo*, crude DMPP (6.05 g, 93% yield) was obtained. DMPP was purified by SiO_2 column chromatography with ethyl acetate solvent to yield a clear viscous liquid. ^1H NMR (400 MHz, $CDCl_3$) δ 7.73 (2H, dd, J= 13.6, 7.5 Hz), 7.50 (1H, t, J= 7.5 Hz), 7.40 (2H, td, J= 7.5, 4.0 Hz), 3.68 (6H, d, J = 11.2 Hz); ^{13}C NMR (400 MHz, $CDCl_3$) δ 132.7 (d, J = 12 Hz), 131.9 (d, J= 39 Hz), 128.6 (d, J = 60 Hz), 126.9 (d, J = 750 Hz) and 52.7 (d, J= 22 Hz); and ^{31}P NMR (161.5 MHz, $CDCl_3$) δ 22.2; MS (EI, 70 eV, with TOF ion detector) M/Z (relative intensity), 187 (5), 186 (64), 185 (100), 155 (27), 141 (57), 91 (54), 77 (38).

d_6-Dimethyl phenylphosphonate (d_6-DMPP). The preparation of d_6-DMPP was the same as that of the DMPP except that methanol-d_4 was used instead of methanol. d_6-DMPP: ^1H NMR (400 MHz, $CDCl_3$) δ 7.76 (2H, dd, J = 13.6, 7.5 Hz), 7.53 (1H, t, J = 7.5 Hz), 7.43 (2H, td, J = 7.5, 4.0 Hz); ^{13}C NMR ($CDCl_3$) δ 132.7 (d, J = 12 Hz), 131.9 (d, J = 39 Hz), 128.6 (d, J = 60 Hz), and 126.9 (d, J = 750 Hz); and ^{31}P NMR (161.5 MHz, $CDCl_3$) δ 22.2; MS (EI, 70 eV, ion trap) M/Z (relative abundance), 193 (9), 192 (100), 191 (91), 162 (40), 142 (40), 94 (78), 94 (78), 77 (10).

^{18}O-Labeled phenylphosphinic acid[16,17]. Dichlorophenylphosphine (0.6 mL, 0.0042 mol) in 5 mL THF was added over 15 min to water (0.3 mL; 10% ^{18}O) in 10 mL of THF under Ar. The mixture was stirred for 5 h, followed by removal of the

solvent *in vacuo* to produce phenylphosphinic acid, which was recrystallized from ethyl acetate to obtain the product (0.599 g, 96%). ^{1}H NMR (400 MHz, $CDCl_3$) δ 7.74 (2H, dd, J = 14, 7.5 Hz), 7.69 (1H, t, J = 7.5 Hz), 7.53 (2H, t, J = 7.5 Hz), 7.52 (1H, d, J = 569.6 Hz); ^{31}P NMR (161.5 MHz, $CDCl_3$) δ 22.8. HPLC/MS (APCI) 144 (20), 143(100), 142 (90), 91(7), 77(6).

^{18}O-Labeled methyl phenylphosphinate[18]. Cold ethereal diazomethane, prepared from the Aldrich diazald kit immediately before using, was added to the above phenylphosphinic acid (0.599 g) until the yellow color persisted in the solution, and further stirred for 0.5 h at 0 °C. Solvent was removed *in vacuo* to generate reasonably methyl phenylphosphinate (0.661 g, 95.8%) that was sufficiently pure to be carried on to the next step. ^{1}H NMR (400 MHz, $CDCl_3$) δ 3.78 (3H, d, J = 12 Hz), 7.70 (2H, t, J = 10 Hz), 7.59 (1H, d, J = 7.2 Hz), 7.51 (2H), 7.54 (1H, d, J = 566 Hz); ^{31}P NMR (161.5 MHz, $CDCl_3$) δ 27.8. GC/MS (EI, 70 eV, with ion trap) M/Z 158 (18), 157 (100), 156 (90), 141 (20), 126 (20), 91 (30), 77 (90), 51 (80).

^{18}O-Labeled Dimethyl phenylphosphonite. This compound was prepared based on the procedure of Quin[19]. To the above crude methyl phenylphosphinate (0.661 g, 0.0042 mol), methyl trifloromethanesulfonate (0.65 mL, 0.0055 mol) was added dropwise. The reaction mixture was stirred for several minutes at room temperature, then cooled down to about –20 °C. Triethylamine (1.38 mL, 0.0099 mol) in 20 mL dry benzene was added. The mixture was warmed up to ambient temperature, whereby two layers were formed. The top layer contained the desired dimethyl phenylphosphonite. ^{1}H NMR (400 MHz, $CDCl_3$) δ 7.64 -7.58 (2H, m), 7.47-

7.38 (3H, m), 3.54 (6H, d, J = 10.4 Hz); ^{31}P NMR (161.5 MHz, $CDCl_3$) δ 161.3; GC/MS (EI, 70 eV, with ion trap) M/Z (relative abundance), 170 (60), 155 (100), 139 (17), 109 (21), 93 (47), 77 (44), 63 (20), 51 (22). After removal of solvent, the resulting product mixture (0.524 g) contained a 2:1:3 mixture of dimethyl phenyl phosphonite, methyl phenylphosphinate and methyl methyl-phenylphosphinate, ^{31}P NMR (161.5 MHz, $CDCl_3$) δ 44.8. Because dimethyl phenylphosphonite is easily hydrolyzed, this mixture was carried forward to the next synthetic step, where purification was more straightforward.

^{18}O-Labeled Dimethyl phenylphosphonates ($^{18}O_2$-DMPP).[15,20] *t*-Butyl hydroperoxide (3.0 M in isooctane,1.02 mL, 3.1 mmol) was added to the above product mixture (0.524 g). The mixture was stirred for 0.5 h. The solvent was removed *in vacuo*, and the residue (0.40 g) was obtained and purified by preparative TLC with ethyl acetate to yield $^{18}O_2$-DMPP (0.159 g, 20% from dichlorophenylphosphine). ^{1}H NMR (400 MHz, $CDCl_3$) δ 7.73 (2H, d, *J* = 7.5 Hz), 7.50 (1H, t, *J* = 7.5 Hz), 7.40 (2H, td, *J* = 7.5, 4.0 Hz), 3.68 (6H, d, *J* = 11.2 Hz); ^{13}C NMR (400 MHz, $CDCl_3$) δ 132.8 (d, *J* = 12 Hz), 131.9 (d, *J*= 40 Hz), 128.7 (d, *J* = 60 Hz), 127.0 (d, *J* = 750 Hz) and 52.7 (d, *J*= 22 Hz); ^{31}P NMR(161.5 MHz, $CDCl_3$) δ 22.37; GC/MS (EI, 70 eV, TOF) M/Z (relative abundance), 188 (15),187 (30), 186 (71), 185 (100), 156 (38), 155 (32), 141 (64), 91 (78), 77 (53).

$^2H_3$-Labeled dimethyl phenylphosphonate (d_3-DMPP). d_3-DMPP was prepared using a sequence of reactions closely related to the preparation of ^{18}O-DMPP. d_3-Methyl phenylphosphonate was prepared from dichlorophenylphosphine

and deuterated methanol in 90% yield using the method of Lei[18]. ^{1}H NMR (400 MHz, $CDCl_3$) δ 7.7-7.8 (2 H, m) 7.45-7.60 (3H, m), 7.51 (d, J = 564 Hz). MS (EI, 70 eV, ion trap), M/Z 160 (100), 142 (27), 94 (38), 77 (98), 51 (73). This material was then methylated and oxidized as described immediately above to yield d_3-DMPP. ^{1}H NMR (400 MHz, $CDCl_3$) δ 7.7-7.8 (m, 2H), 7.45-7.6 (m, 3H), 3.73 (3 H, d, J = 14.8 Hz). IR (neat, cm^{-1}) 3060, 2955, 2852, 2256, 2201, 2137, 2078, 1593, 1439, 1252, 1045. GC/MS (EI, 70 eV, ion trap) M/Z (relative abundance), 191(100), 160(22), 158(20), 142(83), 94(66), 77(63), 51(62).

Monomethyl phenylphosphonate (MMPP)[21]. To a solution of phenyl phosphonic acid (0.326 g, 0.0020 mol) in dry *N,N*-dimethylformamide (10 mL) at -20 °C, thionyl chloride (0.18 mL, 0.0024 mol) was added. The mixture was warmed to 0 °C and kept at that temperature for 20 min. Then methanol (0.123 mL, 0.0030 mol) was added. Afterwards, the mixture was warmed to room temperature and stirred overnight. About 20 mL saturated sodium bicarbonate was added to the resultant solution. The aqueous solution was washed with ether (2 x 15 mL), and acidified with concentrated hydrochloric acid. The product was extracted with ethyl acetate. After drying over anhydrous $MgSO_4$ and subsequent removal of ethyl acetate, crude MMPP (0.24 g, yield 70%) was obtained. ^{1}H NMR (400 MHz, $CDCl_3$) δ 7.79 (2H, dd, J = 13.6, 7.8 Hz), 7.51 (1H, t, J = 7.8 Hz), 7.41(2H, td, J = 7.8, 4.4 Hz), 3.67 (3H, d, J = 11.2 Hz); ^{13}C NMR (400 MHz, $CDCl_3$) δ 132.4 (d, J = 11 Hz), 131.5 (d, J = 40 Hz), 128.5 (d, J = 60 Hz), 128.3 (d, J = 770 Hz) and 52.5 (d, J = 22 Hz); ^{31}P NMR (161.5 MHz, $CDCl_3$) δ 21.5. The purity of MMPP was determined by GCMS, but this

required silylation for the compound to tolerate the GC conditions. MMPP (1 mg) was treated for a few minutes with 0.5 mL pyridine, 0.1 mL 1,1,1,3,3,3-hexamethyldisilazane and 0.05 mL chlorotrimethylsilane, followed by removal of pyridinium salts by centrifugation to yield the TMS derivative of MMPP in a mixture that could be shot directly on a GC column. The purity of the product is about 80% with DMPP (10%) and phenylphosphonic acid (10%) as the other major products. Attempts to further purify with preparative TLC were unsuccessful. The mass spectrum of the TMS derivative of MMPP: (EI, 70 eV, TOF) M/Z (relative abundance), 244 (5), 229 (100), 199 (10), 153 (17), 121 (11), 89 (13), 75 (13).

d_3-Monomethyl phenylphosphonate (d_3-MMPP). Methanol-d_4 was used instead of methanol in the above procedure. ^{1}H NMR (400 MHz, $CDCl_3$) δ 7.80 (2H, dd, *J* = 13.6, 7.8 Hz); 7.53 (1H, t, *J* = 7.8 Hz); 7.43 (2H, td, *J* = 7.8, 4.4 Hz); ^{13}C NMR (400 MHz, $CDCl_3$) δ 132.5 (d, *J* = 12 Hz), 131.6 (d, *J* = 40 Hz), 128.5 (d, *J* = 60 Hz), and 128.2 (d, *J* = 770 Hz); ^{31}P NMR (161.5 MHz, $CDCl_3$) δ 22.0; mass spectrum of the TMS derivative (EI, 70 eV, with TOF ion detector) M/Z (relative intensity) 247 (5), 232 (100), 200 (5), 156 (10), 121 (10).

Dimethyl (*o*-hydroxy)phenyl phosphonate (OHD), dimethyl (*m*-hydroxy)phenyl phosphonate (MHD), and dimethyl (*p*-hydroxy)phenyl phosphonate (PHD). These compounds were prepared as noted in the literature.[22] They were purified by preparative TLC with developing solvents methylene cloride/EtOAc (6:1), EtOAc, and EtOAc/MeOH (4:1), respectively. OHD: ^{1}H NMR (400 MHz, $CDCl_3$) δ 10.1 (1H, s), 7.45 (1H, br t, *J* = 7.8 Hz), 7.34 (1H, ddd,

J = 14.4, 7.6, 1.6 Hz), 6.97 (1H, br t, J = 7.6 Hz), 6.92 (1H, tdd, J = 7.8, 4.2, 1 Hz), 3.75 (6H, d, J = 11.6 Hz); ^{31}P NMR (161.5 MHz, $CDCl_3$) δ 25.9; mass spectrum of its TMS derivative (EI, 70 eV, ion trap) M/Z (relative intensity), 274 (22), 259 (100), 213 (10), 156 (9), 135 (10), 107 (10), 73 (18), 59 (19). MHD: ^{1}H NMR (400 MHz, $CDCl_3$) δ 7.82 (1H, d, J = 15.2 Hz), 7.35 (1H, dd, J = 13.6 Hz), 7.15 (1H, dd, J = 12.8, 7.6 Hz), 7.10 (1H, d, J = 8 Hz), 3.77 (6H, d, J = 11.2 Hz); ^{31}P NMR (161.5 MHz, $CDCl_3$) δ 22.9; mass spectrum of its TMS derivative (EI, 70 eV, ion trap) M/Z (relative intensity), 274 (25), 259 (100), 91 (7), 73 (10), 63 (8). PHD: ^{1}H NMR (400 MHz, $CDCl_3$) δ 10.1 (1H s), 7.61 (2H, dd, J = 12.4, 8.4 Hz), 7.01 (2H, d, J = 4.8 Hz), 3.71 (6H, d, J = 11.2 Hz); ^{31}P NMR (161.5 MHz, $CDCl_3$) δ 24.8; mass spectrum of its TMS derivative (EI, 70 eV, ion trap) M/Z (relative intensity), 275 (30), 259 (100), 109 (10), 91 (8), 73 (15), 63 (8).

4. 3. Results and Discussion

General characteristics of TiO_2-mediated partial degradations of Dimethyl phenyl phosphonate (DMPP).

Standard conditions for degradations were 100 mL aqueous suspensions containing 50 mg DeGussa P25 and 5 mM DMPP. The pH of the solution was either unregulated or set to 3 with HCl, 7 with 10 mM phosphate buffer, or 9-10 with carbonate buffer. All solutions were treated in an ultrasonic bath to disperse aggregates immediately before photolysis and purged with O_2 before and during

photolysis. Irradiation was carried out using broadly emitting 355 nm fluorescent tubes. Samples were removed at appropriate intervals and analyzed after removal of the TiO_2. For HPLC analysis, no further processing was necessary, but for GC analysis, the water was removed and the resulting materials were exhaustively silylated with TMSCl and $(TMS)_2NH$. Control experiments showed that degradation in the absence of any one or more of the key elements (light, TiO_2, and O_2) was negligibly slow. Without regulation of pH, complete loss of DMPP could be achieved in about 22 h and complete mineralization was achieved in about 33 h. A maximum of phenolic products, as observed by an unstructured UV absorption at 285 nm was observed at about 10 h.

At early degradation times (e.g., 30 – 60 min), four primary degradation products were observed (Scheme 2). They result from hydroxylation of the arene ring in the *ortho*, *meta*, and *para* positions and from demethylation of the phosphonate. No phenol was observed. The *meta* hydroxylated product (MHD) was produced in about 3 times the concentration as the other isomers (which were formed in similar amounts), in keeping with the notion that hydroxylation by $HO^{\bullet}_{ad}$ is an electrophilic reaction.

Scheme 2.

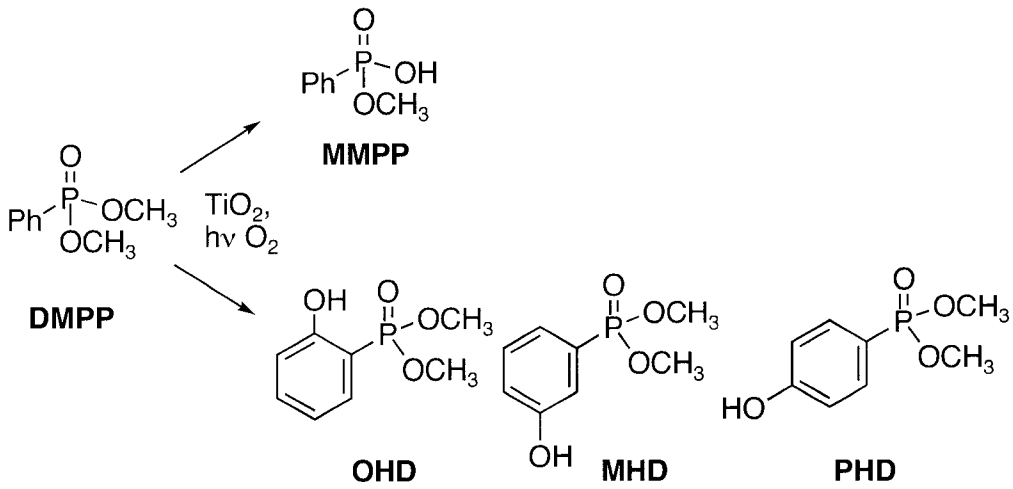

The influence of pH on the initial rate of photocatalytic degradation of DMPP was briefly investigated. Degradations were carried out for 1 h at pH 3, 7, and 10, and the percentage DMPP remaining was assessed. The degradation was fastest at pH 10 (40% consumption), with 22% and 13% consumption at pH 7 and 3, respectively. This is in qualitative agreement with the observations of O'Shea for MMPP[1,2].

The kinetics of the disappearance of DMPP could be fit to first order decays. The apparent rate constants for three concentrations in the mM range at pH 7 are shown in Table 1. The inverse relationship between [DMPP] and k_{app} is analogous to that observed by O'Shea for DMMP[2], though here the relationship is sufficiently strong that even the absolute initial rate of decomposition is slower for the higher concentrations. O'Shea suggested that strong adsorption by intermediate products

may be the cause of this.

Table 1. First order rate constants and initial rates for the oxygen-saturated TiO_2 photoinduced disappearance of DMPP

[DMPP] mM	k_{app} ($x10^{-5}$ s^{-1})	Rate (M/s)
2.3	11.17 ± 0.1	2.7×10^{-7}
4.6	3.6 ± 0.3	1.6×10^{-7}
9.1	1.8 ± 0.1	1.6×10^{-7}

We thus investigated the adsorption of MHD, MMPP, and DMPP at pH 3, 7, and 10. At the high pH, where the phenol is presumably deprotonated, MHD adsorbs much more strongly than the other two in the concentration region investigated, as shown in Figure 1. However, while the adsorption of MHD is marginally stronger at the lower pH values, it does not appear to be sufficiently so as to completely displace DMPP at any pH unless it is the case that only very specific adsorption sites are active. It is, by now, understood that dark adsorption properties do not always correlate with reactivity, and it is not clear in the end what these data imply as to this particular phenomenon.

Figure 1. Adsorption isotherm for DMPP, MMPP, and MHD at pH10 with 25 mg TiO_2 per 10 mL

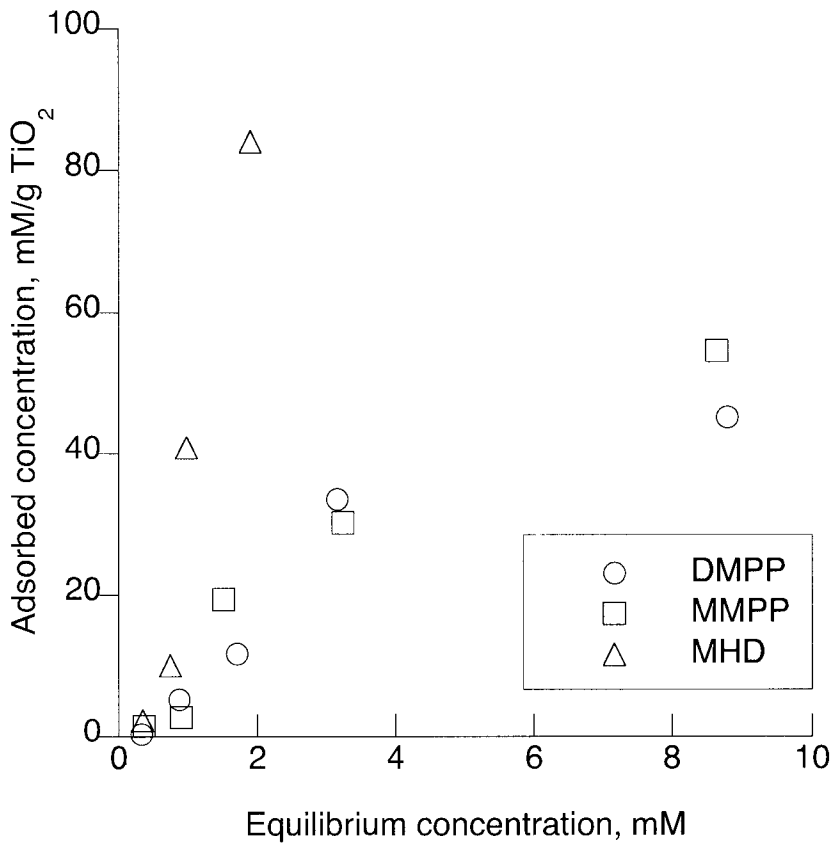

Isotope labeling experiments on the demethylation of DMPP.

In order to test whether substitution of a hydroxyl group for a methoxy group in DMPP goes by a mechanism that involves substitution of OH for CH_3O or by a mechanism in which the methyl group is degraded off, leaving the oxygen behind, experiments were carried out using two different types of isotopologs of DMPP.

The most critical of these is ^{18}O-DMPP. This compound was prepared by a

synthetic route that unambiguously places the ^{18}O labels in the alkoxy positions, rather than at the phosphine oxide position (Scheme 3), so that any loss of ^{18}O label carried into the MMPP product detected by MS is directly attributable to a substitution type mechanism. Using labeled water nominally 10% in ^{18}O, ^{18}O-DMPP was obtained with (9.23 ± 0.06)% enrichment was obtained, such that approximately 18% of the DMPP molecules contained a single ^{18}O label, and only a small fraction were double-labeled.

Scheme 3. Preparation of labeled DMPP.

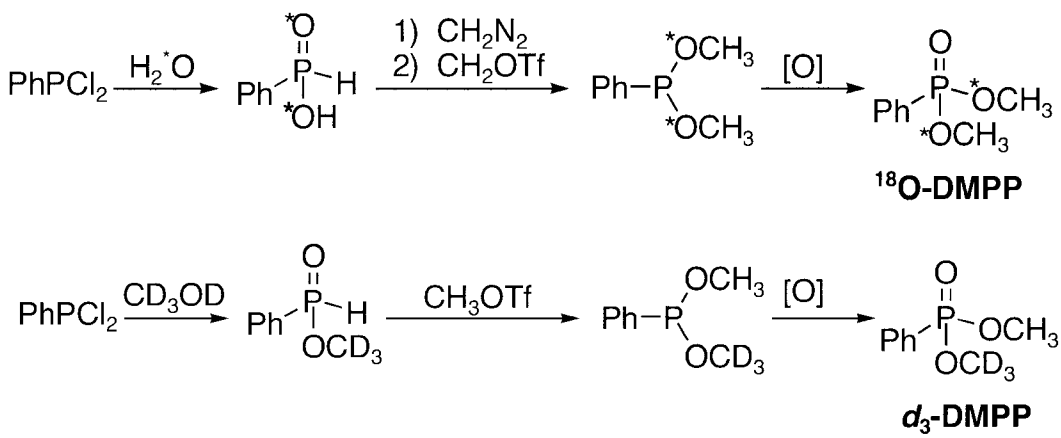

Degradations were carried out in the usual fashion, save for a 10-fold drop in scale, at pH 3, 7, and 10, and also with H_2O_2 in lieu of TiO_2. The results of these experiments, shown in Table 2 are unambiguous: there is no significant loss of ^{18}O, and thus the mechanism of loss of the methyl group cannot involve direct attack by any species at the phosphorus center in such a way that expels $CH_3O\bullet$ or CH_3O^-. Naturally, the ^{18}O is also retained in the hydroxylated products.

Table 2. ^{18}O Enrichment in MMPP after formation by degradation of DMPP

	^{18}O enrichment in MMPP (%)*
Without control of pH	9.2 ± 0.2
pH = 3, TiO_2, hν	9.4 ± 0.3
pH = 7,TiO_2, hν	9.4 ± 0.1
pH =10, TiO_2, hν	9.3 ± 0.1
H_2O_2, hν	9.0 ± 0.2

Errors limits are the standard deviations among triplicate or greater measurements. Enrichment of DMPP is 9.23 ± 0.06%.

We thus sought to confirm that the product/rate determining step in the sequence that leads to MMPP is hydrogen abstraction. In previous reports, we have shown an H/D selectivity[23] of approximately 3 for the demethylation of trimethyl cyanurate and anisole[24,25]. In the spirit of these previous experiments, we prepared d_6-DMPP from phenylphosphonyl dichloride and deuterated methanol. Degradations were then carried out in which both unlabeled DMPP and d_6-DMPP were employed. Usually the ratio of the two isotopologs was kept near 1.0, but several experiments were also run with ratios of 1:3 and 3:1. After compensating for the isotopolog ratios, the ratio of MMPP to *d*3-MMPP is taken as the H/D selectivity for the demethylation reaction. To our surprise, the H/D selectivities were very near 1.0, i.e., essentially no selectivity (Table 3). This implied either that hydrogen

abstraction is not the product/rate determining step or that an unusually small primary isotope effect was being observed.

One alternative mechanism that would remove isotope-selective hydrogen abstraction as the rate determining step is to hypothesize that the initial step is electron transfer from the phosphonate to the TiO_2. This would presumably not have any isotope selectivity. Subsequent loss of one of the methyl protons from the resulting radical cation would in principle be istotope-selective, but if the efficiency of that step is near 1, the selectivity would not be observed. We thus subjected mixtures of d_6-DMPP and DMPP to several other conditions that were thought to produce hydroxyl radicals and/or the possibility of electron transfer reactions, thinking that perhaps a pattern would arise that would be consistent with this hypothesis. Instead, as can be seen in Table 3, the H/D selectivity was near 1.0 for the whole set of conditions. While the numbers were almost all slightly greater than 1.0, we were not convinced that this represented a real, very small selectivity.

Table 3. H/D isotope selectivities of DMPP demethylation under different experimental conditions and general product distributions at low conversion

Degradation conditions	H/D selectivity	MMPP	OHD	MHD	PHD
		Relative Yields			
TiO_2, hn, O_2	1.07 ± 0.04	67	2	24	7
pH unregulated					
TiO_2, hn, O_2, pH 3	1.05 ± 0.08				
TiO_2, hn, O_2, pH 7	1.05 ± 0.08				
TiO_2, hn, O_2, pH 10	1.01 ± 0.04				
H_2O_2, hν	0.99 ± 0.05				
Fenton, pH 7	1.01 ± 0.13	81	6	8	5
$K_2S_2O_8$, 90 °C	0.99 ± 0.03	100[a]			
$K_2S_2O_8$, hn	1.05 ± 0.13	100[a]			
TiO_2, hn, O_2, NaF pH 3	1.02 ± 0.02	70	3	23	4
TiO_2, hn, Ar, NaF pH 3		100[a]			

Error limits are standard deviations from multiple runs. [a] No other primary products were detected at levels above ~3% of MMPP.

Among the chemical methods used, we did not expect an electron transfer mediated mechanism for Fenton chemistry or hydrogen peroxide photolysis, but persulfate chemistry can sometimes lead to direct 1-electron oxidation, along with

oxidation by sulfate radical anion and/or hydroxyl radical. We attempted sub-band gap irradiation of TiO_2 suspensions (broad irradiation with cutoff filter having 50% transmittance at 435 nm) with the idea that successful degradation here would clearly indicate electron transfer via irradiation of a charge transfer complex, but no degradation was observed after extended irradiation. By contrast, irradiation of low pH suspensions of TiO_2 in the presence of NaF are known[26,27] to produce free hydroxyl radicals. In the end, we realized we could not absolutely rule out even that the hydroxyl radicals would react by this stepwise electron/proton transfer, though we thought it unlikely.

Thus, we resolved to explore one last route to probing for such an isotope effect and considered the degradation of d_3-DMPP. Its preparation is shown in Scheme 3. For this compound, the observed ratio of d_3-MMPP to MMPP reflects the H/D selectivity, since it is the other methyl group that has been removed. A key difference between this intramolecular competition compared to the intermolecular competition is that if electron transfer is an irreversible primary step, there still remains the possibility for isotope selectivity in the deprotonation of the radical cation. In contrast, for the bimolecular competition experiments, once the electron loss has occurred, the choice for H^+ or D^+ loss has already been made. The results of this set of experiments are shown in Table 4, along with product distributions taken from very low conversion (<10%) measurements.

Table 4. H/D Selectivities observed for demethylation of d_3-DMPP and relative product distributions at the lowest conversions

Degradation Conditions	H/D Selectivity
TiO_2, O_2, hv	1.38 ± 0.08
H_2O_2, O_2, hv (300nm)	1.21 ± 0.14
Fenton	1.22 ± 0.13

The H/D selectivities in Table 4 appear convincingly to be greater than 1.00, but are still quite small for a primary isotope effect. They are, in fact, what one might expect for a *secondary* isotope effect with attack at the methyl group. However, such a mechanism does not seem physically reasonable. A survey of the literature on the deprotonation of related radical cations (e.g., dimethyl aniline structure types and/or benzyl structure types) suggests that directly measured kinetic isotope effects for radical cation deprotonations, while structure-dependent, are in the normal range for primary KIEs, i.e., 2-7, with a few very large ones that implicate H-atom tunneling[28-33]. We were unable to find any directly measured KIEs for radical cations more closely related to $DMPP^{\bullet+}$ than these. Though we have difficulty in rationalizing this final magnitude of an H/D selectivity (i.e., related to a kinetic isotope effect), the important point remains that the fact that there is any isotope effect to be observed at all further implies that the mechanism of demethylation derives from

attack at the methyl group, rather than attack at phosphorus.

4. 4. Conclusions

The TiO_2-mediated photocatalytic degradation of phosphonates is now well understood to include removal of the alkyl ester portion of the compounds to produce phosphonic acid monoesters among the primary steps. While there is ambiguity in the interpretation of small H/D selectivity in the dealkylation of DMPP by TIO_2 photocatalysis and various other methods, the results of ^{18}O labeling are clear. They do not rely on any kinetic effect, and the retention of ^{18}O in the formation of MMPP clearly demonstrates that the dealkylation mechanism involves degradation of the methyl group exclusively, and neither attack at phosphorus by $HO\bullet_{ads}$ or a related species, nor photoinduced hydrolysis.

Acknowledgements. The authors thank the National Science Foundation and IPRT for their partial support of this work.

4. 5. References

[1] K.E. O'shea, S. Beightol, I. Garcia, M. Aguilar, D.V. Kalen, W.J. Cooper, J. Photochem. Photobiol., A 107 (1997) 221.

[2] K. E. O'shea, I. Garcia, M. Aguilar, Res. Chem. Intermed. 23 (1997) 325.

[3] M. G. Nickelsen, W. J. Cooper, K. E. O'shea, M. Aguilar, D.V. Kalen, C. N. Kurucz, T.D. Waite, J. Adv. Oxid. Technol. 3 (1998) 43.

[4] A. Aguila, K.E. O'shea, P. V. Kamat, J. Adv. Oxid. Technol. 3 (1998) 37.

[5] K. E. O'shea, A. Aguila, L. K. Vinodgopal, P. V. Kamat, Res. Chem. Intermed. 24 (1998) 695.

[6] A. V. Vorontsov, L. Davydov, E. P. Reddy, C. Lion, E. N. Savinov, P.G. Smirniotis, New J. Chem. 26 (2002) 732.

[7] T. N. Obee, S. Satyapal, J. Photochem. Photobiol. A 118 (1998) 45.

[8] A. Aguila, K. E. O'shea, T. Tobien, K.-D. Asmus, J. Phys. Chem. A 105 (2001) 7834.

[9] J. -M. Hermann, C. Guillard, M. Arguello, A. Agüera, A. Tejedor, L. Piedra, A. Fernandez-Alba, Catalysis Today 54 (1999) 353.

[10] C. K. Grätzel, M. Jirousek, M. Grätzel, J. Molec. Catal. 60 (1990) 375.

[11] K. Harada, T. Hisanaga, K. Tanaka, Wat. Res. 24 (1990) 1415.

[12] R. -A. Doong, W.-H. Chang, J. Photochem. Photobiol. A 107 (1997) 239.

[13] W. T. Dixon, R. O. C. Norman, A. L. Buley, J. Chem. Soc. (1964) 3625.

[14] G. A. Russell, J. Am. Chem. Soc. 79 (1957) 3871.

[15] T. H. Siddall, C. A. Prohaska, J. Am. Chem. Soc. 84 (1962) 3467.

[16] P. B. Kay, S. Trippett, J. Chem. Res., Synop. (1985) 292.

[17] T. A. Van Der Knaap, T. C. Klebach, R. Lourens, M. Vos, F. Bickelhaupt, J. Am. Chem. Soc. 105 (1983) 4026.

[18] H. Lei, M.S. Stoakes, A.W. Schwabacher, Synthesis (1992) 1255.

[19] L. D. Quin, K. C. Caster, J. C. Kisalus, K. A. Mesch, J. Am. Chem. Soc. 106 (1984) 7021.

[20] T. H. Siddall, C. A. Prohaska, J. Am. Chem. Soc. 84 (1962) 2502.

[21] M. Hoffmann, Synthesis (1986) 557.

[22] R. Obrycki, C. E. Griffin, J. Org. Chem. 33 (1968) 632.

[23] We hesitate to use the term "kinetic isotope effect" since these are not strictly kinetic experiments, but product isolation studies after several chemical steps.

[24] T. Tetzlaff, W. S. Jenks, Org. Lett. 1 (1999) 463.

[25] X. Li, W.S. Jenks, J. Am. Chem. Soc. 122 (2000) 11864.

[26] C. Minero, G. Mariella, V. Maurino, E. Pelizzetti, Langmuir 16 (2000) 2632.

[27] C. Minero, G. Mariella, V. Maurino, D. Vione, E. Pelizzetti, Langmuir 16 (2000) 8964.

[28] Y. Lu, Y. Zhao, V.D. Parker, J. Am. Chem. Soc. 123 (2001) 5900.

[29] S. B. Karki, J. P. Dinnocenzo, J. P. Jones, K. R. Korzekwa, J. Am. Chem. Soc. 117 (1995) 3657.

[30] X. Zhang, S. -R. Yeh, S. Hong, M. Freccero, A. Albini, D.E. Falvey, P. S. Mariano, J. Am. Chem. Soc. 116 (1994) 4211.

[31] J. P. Dinnocenzo, T. E. Banach, J. Am. Chem. Soc. 111 (1989) 8646.

[32] E. Baciocchi, T. Del Giacco, F. Elisei, J. Am. Chem. Soc. 115 (1993) 12290.

[33] V. D. Parker, M. Tilset, J. Am. Chem. Soc. 113 (1991) 8778.

Chapter 5

Photocatalytic degradation of organics using WO_x-TiO_2

A paper to be submitted to *The Journal of Photochemistry and Photobiology. A: Chemistry*

Youn-Chul Oh and William S. Jenks

Abstract

As an attempt to extend photocatalytic activity of modified TiO_2 photocatalysts with light and to decrease the rapid recombination of photogenerated electrons/holes during photoreaction, WO_x-TiO_2 powder was prepared by a sol-gel method. This method is distinct from the incipient wetness method and grafting method, which can provide a true composite semiconductor catalyst by binding the W to every possible site of TiO_2. The goal to degrade organic contaminants in aqueous solution by using WO_x-TiO_2 with visible light irradiation was achieved. The modification of TiO_2 by W shows its benefit of utilizing visible light for photocatalytic degradation of organic compounds. Differently prepared (incipient wetness method for P25 Degussa and PC 50 Millennium Chemical) WO_x-TiO_2 also shows similar effect of photoactivation with visible light. WO_x-TiO_2 by sol-gel method consistently shows higher degradation efficiency (c.a. 20%).

5. 1. Introduction

TiO_2 has been shown to be an excellent photocatalyst for the degradation of organic contaminants in water and air. Nearly every organic molecule ever tested was degraded to CO_2, H_2O, and appropriate inorganic ions when exposed to TiO_2-mediated photocatalytic degradation conditions in oxygenated water. However, single component semiconductor photocatalyst such as pure TiO_2 has two limitations. Firstly, TiO_2 is a wide band gap (3.2 eV) semiconductor that can be excited by high energy UV irradiation (with a wavelength of 385 nm for anatase and 410 nm for rutile). This allows that no more than 5% of sunlight can be utilized for photocatalytic degradation since the proportion of UV light in the solar spectrum is very low (less than 5%) [1]. Secondly, a low rate of electron transfer to oxygen and a high rate of recombination between excited electron/hole pair results in a limited quantum yield for photocatalytic degradation [2-4].

In principle, a photocatalytic reaction may proceed on the surface of TiO_2 particles in several steps [5, 6], namely;

(a) Production of electron-hole pairs, photogenerated by exciting the semiconductors with light energy greater than band-gap;

(b) Separation of electrons and holes by traps available on the TiO_2 surface;

(c) A redox process induced by the separated electrons and holes with the adsorbed molecules present on the surface; and

(d) desorption of the products and reconstruction of the surface.

Electron-hole recombination, which lead the low quantum yields, is in indirect competition with the trapping process (step b). The efficiency of trapping and the photocatalytic activity of TiO_2 can be enhanced by retarding electron-hole recombination. The most common method for slowing electron-hole recombination is thought to be through the loading of metals onto the surface of the TiO_2 particles. It is thought that the metal dispersed on the TiO_2 particles expedites the transport of electrons produced by the photo-excitation to the outer system[7]. It has been shown that the photocatalytic activity of TiO_2 is influenced by the crystal structure (anatase and/or rutile), surface area, size distribution, porosity, surface hydroxyl group density, etc [6, 8, 9]. These have an influence on the production of electron-hole pairs, the surface adsorption, the desorption process and the redox processes.

Previously, photochemical deposition of metal on semiconductor particles has been used to recover noble metals from waste solution [10]. This technique has been widely employed for the purpose of improving the photocatalytic activity of semiconductors by depositing metals on the catalyst surface. Pt, Pd, Au, Rh, RuO_2, *etc.* have all been utilized [11-15]. However, these metals may not be suitable for industrial applications since they are rare and expensive. In this study, less expensive WO_3 was used for the preparation of efficient modified photocatalysts [2-4].

Modified photocatalysts (composite semiconductors) can extend the photo-response of large band-gap semiconductors. Depend on the topology, they can also rectifies the flow of photo-generated charge carriers [16, 17], and improve the

efficiency of dye sensitization [18, 19], and interfacial charge transfer processes. Composite semiconductors can be classified into two categories, namely, capped-, and coupled-type hetero structures. The capped semiconductors essentially have a core-shell geometry while in a coupled system two semiconductors are in contact with each other. The principle of charge separation in capped and coupled semiconductor system, which was adapted from Kamat's figure, is illustrated in Figure. 1. [16, 20]

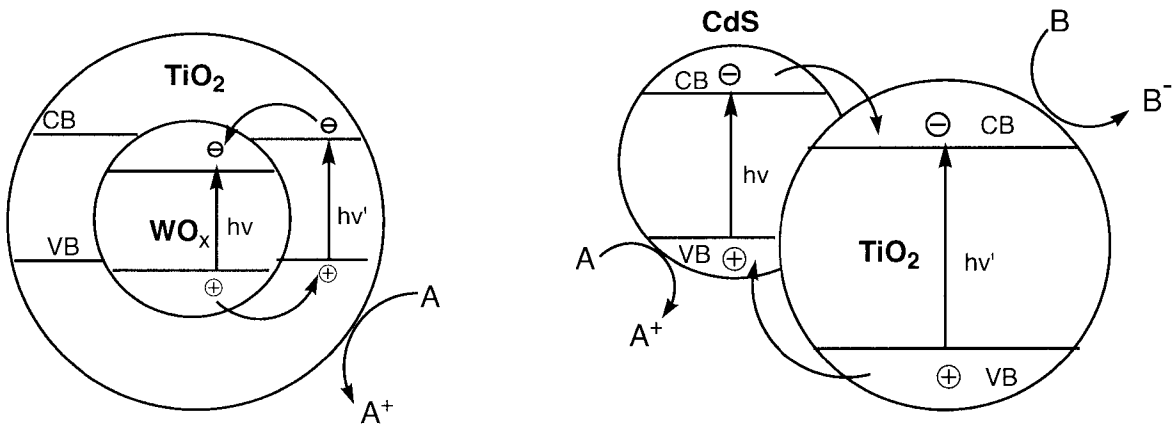

(a) Capped (or Core-Shell) Geometry (b) Coupled Geometry

Figure 1. Principle of charge separation in semiconductor heterostructures: (a) capped (or Core-Shell) geometry and (b) coupled geometry. Electrons accumulate at the conduction band (CB) of WO_x while holes accumulate at the valence band (VB) of TiO_2.

While the mechanism of charge separation in a capped semiconductor system is similar to that in coupled system, the interfacial charge transfer or charge collection in a capped site is significantly different. Only one of the charge carriers is accessible at the surface in a capped semiconductor system, thus making selective charge transfer possible at the semiconductor/electrolyte interface. The other charge carrier (e.g., the electron in example of Fig 1.) gets trapped within the inner semiconductor particle and is not readily accessible [16, 20]. However, the trapped charge carriers would not accumulate within the bulk semiconductor forever; they will eventually escape from the trap after retarding fast e^-_{cb} / h^+_{vb} (electron/hole) recombination. In a coupled semiconductor system both holes and electrons are accessible for selective oxidation and reduction processes on different particle surfaces. Our modified photocatalysts can be belonged to the capped geometry (reductive isomerization of maleic acid or reduction test of quinone will be a probing experiment). However, the cartoon shown above is more proper to explain geometry of band-edge and related oxidation/reduction potential than actual geometry. Actual geometry is looks like evenly dispersed sugar on the surface of sugar cookie.

In this study, WO_x-TiO_2 samples were prepared by a sol-gel process with the aims of extending the light absorption spectrum toward the visible region. We are particularly interested in a recent report by Li *et al.* that describe the preparation and characterization of WO_x-dispersed TiO_2 by the sol-gel method [2]. These catalysts have relatively featureless absorption spectra that extend well into the visible,

potentially making them extremely valuable photocatalysts because they will absorb a greater fraction of sunlight. Their photocatalytic effectiveness were tested by measuring the disappearance of methylene blue. Hence, we tried to prepare some of this material and assess it with more typical substrates, where mechanistic information is more available, to understand if the same general mechanisms apply for organic degradation, despite the narrower band gap. With an attempt to activate the modified TiO_2 photocatalysts by the visible light and decrease the rapid recombination of excited electrons/holes during photoreaction, WO_x-TiO_2 powder was prepared by a sol-gel method. The WO_x-TiO_2 catalysts were characterized by XRD, XPS, and SEM-EDX. The attempt to decompose 4-methoxyresorcinol and 4-chlororesorcinol in aqueous solution by using WO_x-TiO_2 under visible light was tested.

5. 2. Experimental Section

Materials. All reagents were purchased from Aldrich and used without further purification unless otherwise indicated. The water employed was purified by Milli-Q UV plus system (Millipore) resulting in a resistivity more than 18 MΩ cm^{-1}. TiO_2 were Degussa P-25 and DT52, PC 10, PC 50, PC 100, and PC 500 from Millennium Chemical. 4-Methoxyresorcinol was prepared by a reported method [21].

Preparation of WO_x-TiO_2 catalysts. WO_x-TiO_2 was prepared by a sol-gel method modified from Li's method [2]. The WO_x-TiO_2 samples with different WO_x

fraction from different WO_x source were also prepared by sol-gel process. A TiO_2 transparent sol was prepared by using 17.5 g of $Ti(O\text{-}nBu)_4$, 120 ml of ethanol, 15 mL of acetic acid, and 5 mL of de-ionized water, and aged for 1 day (stirring at room temperature). Then, 60 ml of aqueous solution of containing 1.52 g of ammonium paratungstate ($(NH_4)_{10}W_{12}O_{41}$, F.W.= 3042.55) was added drop-wise to the TiO_2 sol under vigorous stirring over 2h until WO_x-TiO_2 (1 mol % of WO_x to TiO_2) gel is formed (similarly 3 and 5 % WO_x-TiO_2 samples were also prepared by using 4.56 g, and 7.61 g of ammonium paratungstate). We also used different source of tungsten , ammonium tungstate, and WO_x-TiO_2 (3 mol % of WO_x to TiO_2) gel prepared as mentioned above. WO_x-TiO_2 gel was aged 2 days with vigorous stirring, 1 day undisturbed and then 1day with vigorous stirring. The WO_x-TiO_2 gel was dried with a rotary evaporator at 358 K until the dried gel was formed. As WO_x-TiO_2 gel was dried, it shrunk and coated the surface of flask, and eventually formed a powder. After drying, WO_x-TiO_2 samples were ground and sintered at 923 K for 2h. Grinding was carried out by SPEX® Mill (ball mill, which grinds samples by placing them in a container along with one grinding elements, and imparting motion to the container. The container is cylindrical agate vial; the grinding element is agate ball. As the container is vibrated, the inertia of the grinding elements causes them to move independently, into each other and against the container wall, grinding the sample) for 8 Min. Hand ground samples were prepared also prepared by using agate mortar and pestle. WO_x-TiO_2 was sintered using the

following procedure. Dried samples were placed in porcelain crucibles, and the crucibles were placed in a furnace at room temperature. The furnace was heated at a moderate rate (10 K/min) to make sure volatiles did not discharge and powder from the crucibles. Once the furnace reached the temperature of 923 K, a timer was set for 2 h. A calibrated thermocouple was placed in the center of the cluster of crucibles to continuously monitor the temperature at the location of the samples. After 2h, the furnace was allowed to cool down slowly for 2h. When the samples and crucibles were down near room temperature they were removed from the furnace and the powders were immediately transferred to vials. Incipient wetness method reported by Do et al. [3] was used to prepare WOx-TiO_2 from commercial TiO_2 such as P 25 DeGussa, and PC 50 Millennium Chemical.

Characterization of photocatalysts. X-ray diffraction (XRD), X-ray photoelectron emission spectroscopy (XPS), scanning electron microscopy (SEM), and SEM-Energy Dispersive X-ray spectrometry (SEM-EDX) examined the chemical composition, particle size, and morphology of WO_x-TiO_2.

Powder X-ray diffraction (XRD) experiment were performed to determine the crystal phase composition of the prepared photocatalysts (WO_x-TiO_2). XRD measurement was carried out at room temperature using a Scintag 2000 diffractometer with Cu Kα radiation. The accelerating voltage of 40 kV and emission current of 30 mA were used.

X-ray photoelectron spectroscopy (XPS) was carried out to study the valance state of the photocatalysts. The XPS measurements were performed with a Perkin Elmer Model 5500 multi-technique spectrometer employing monochromatized Al Kα radiation. The take-off angle was fixed at 45°. The X-ray source was run at 14kV and 250 W. The emitted photoelectrons were sampled from a 1mm^2 area. The XPS energy scale was calibrated against Au $4f_{7/2}$ and Ag $3d_{5/2}$ peaks at 84.0 and 368.27 eV, respectively. The sample was mounted on an Indium foil for XPS analysis, and placed in the XPS chamber. The temperature was measured with a Type K thermocouple. The base pressure of the chamber was about $3x10^{-10}$ Torr. The instrumental Gaussian full-width at half maximum (GFWHM), which characterizes the resolution, was 0.65 eV for the Al source.

WO_x-TiO_2 particle morphology was determined by scanning electron microscopy (SEM) using a Hitatch S-2460N variable pressure scanning electron microscope with 20 kV accelerating voltage and ~0.5 nA of beam current for imaging in 25 mm working distance.

Oxford Instruments Link Isis Model 200 x-ray analyzer was used for SEM-EDX analyses to characterize the WO_x-TiO_2 particles and the location of tungsten atom (mapping). High-purity Ge, light-element X-ray detector was employed and the take-off angle was fixed at 30°.

Standard degradation conditions. Except as noted, degradations followed these standard conditions. A 100 mL aqueous solution containing 2.0 mM starting

material (for example 4-methoxyresorcinol) and 50 mg suspended TiO_2 was prepared. The pH of solution was adjusted by HCl (pH 2), phosphate buffer (10 mM, pH 7.0), or NaOH (pH 12). The mixture was treated in an ultrasonic bath for 5 minutes to disperse larger aggregates and purged with O_2 for 20 minutes in the dark before the irradiation was started. The mixture was continuously purged with O_2 throughout the experiment. Irradiations were carried out with stirring and a fan that kept the temperature near to ambient levels in a Rayonet photochemical reactor equipped with six 8 W fluorescent bulbs (RPR4190, The Southern new England Ultraviolet Co.) which have a broad emission spectrum centered at 419 nm. After reaction, the mixtures were acidified to pH 2, centrifuged, and filtered to remove TiO_2. Water was removed by freeze-drying.

A 150 W Xe-Arc lamp with cut-off filter from Ealing® (50% of transmittance at 435 nm) was also applied for irradiation source for visible range. The concentrations of the samples were the same as with the Rayonet-based experiments, but smaller samples (10 mL) were used.

Dark adsorption. Equilibrium extents of adsorption onto TiO_2 were evaluated after equilibration for fixed periods with vigorous magnetic stirring. The pH of solution was adjusted by HCl (pH 2), phosphate buffer (10 mM, pH 7.0), or NaOH (pH 12). Suspensions were prepared from 10 ml aliquots of solution with 5 mg TiO_2. After allowing the desired contact time, an aliquot was removed, centrifuged, and syringe filtered through Millipore filters to remove TiO_2. The residual concentration of

the compounds was determined by UV-VIS spectroscopy using a Shimadzu UV-2101 spectrometer. Kinetic study showed that the extent of adsorption reached a constant value after no more than 4 h for all compounds [21]. For the quantitative adsorption experiments, at least 12 h equilibration was allowed before measurement.

General analytical methods. Following the removal of water, the intermediate degradation products were identified and quantified as their trimethylsilyl (TMS) derivatives, using GC-MS procedures reported in our earlier work [21]. The instrument was a Varian 3400CX GC equipped with a 30 m DB-5 column, coupled to a Finnigan Magnum ion trap mass spectrometer. The temperature program was 120 °C for four min, followed by a ramp to 200 °C at 5 °C/min, then ramp at 15 °C/min to 280 °C. An HP 5890 gas chromatograph with FID detection was also used for routine quantification.

TOC Analysis. 2.4 mg of 4-methoxyresorcinol (or 4-chlororesorcinol) in 8 mL of DI water with 4 mg of catalyst (initial TOC 183 ppm), was irradiated by 419 nm (6x8W, Rayonet) light for 3 h. After filtering TiO_2 with micro-syringe Millipore filters, the removal of TOC of reaction mixture was analyzed by Shimadzu 5000A TOC analyzer. Experiments for the time profile of TOC removal were also carried out under the same reaction condition with 30 min of sampling interval.

5. 3. Results

Characterization of modified photocatalyst (WO_x-TiO_2)

XRD Analysis: X-ray diffraction patterns were measured on the final sintered photocatalysts using a Scintag 2000 X-ray diffractometer and Cu Kα radiation of wavelength 1.54 Å in the range 20-70 (2θ). XRD data shows the phase transformation of titania. Titania containing 0% W in Figure 2 shows both rutile and anatase peak in the range of 20 to 70 degree (2θ). The tungstated titania shows a distinct hindering of phase transformation from anatase to rutile during sintering process. This XRD result is good agreement with the result from Li et al. [2]. We tried different source of tungsten such as ammonium tungstate and ammonium paratungstate. This change of tungstate source did not affect the composition of crystal phase of WO_x-TiO_2. We applied lower sintering temperature (923 K) rather than Li's 973 K to minimize the phase transformation to rutile at higher sintering temperature.

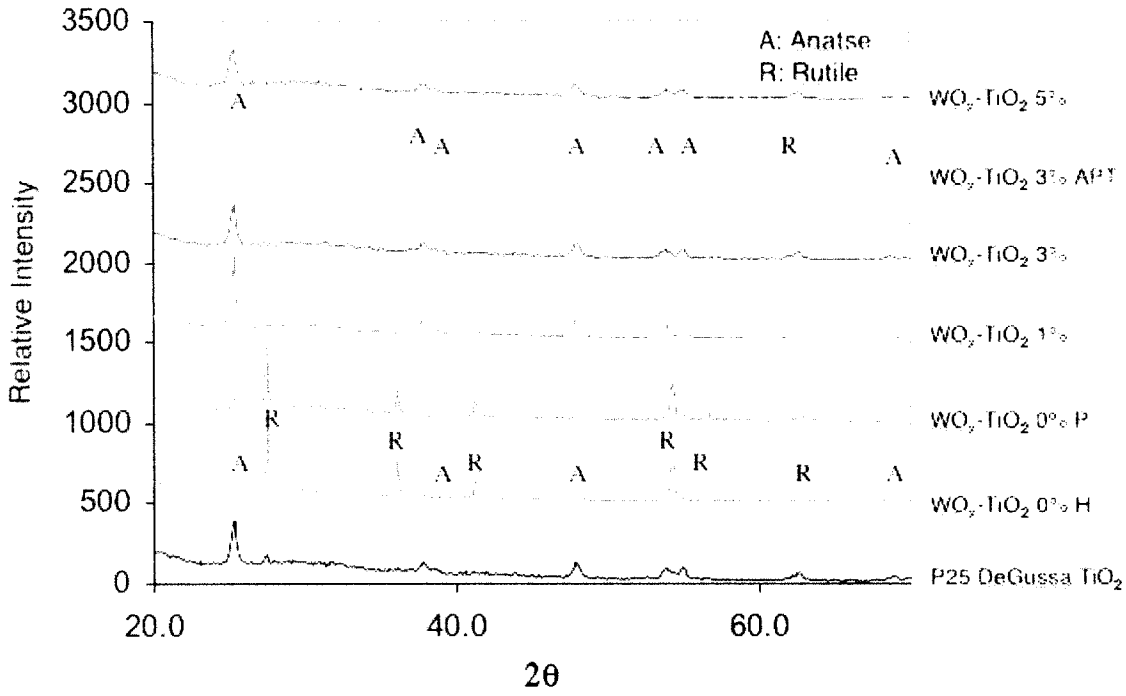

Figure 2. XRD powder diffraction spectra. Anatase phase (A) and rutile phase were assigned by reported XRD data from Li [2] and Andersson [22].

It has been reported by several studies that sol-gel sample of TiO_2 should undergo a phase transformation from anatase to rutile during sintering treatment [4, 23, 24]. In general, higher sintering temperatures lead to greater rutile formation. In this study, all the samples were sintered at 923 K and their diffractograms are described in Figure 2. The XRD results indicated that all the WO_x-TiO_2 samples contained lower fraction of rutile than the pure TiO_2. Obviously from Figure 2, tungsten oxides hindered the phase transformation from anatase to rutile during sintering step [2, 25].

SEM analysis. Scanning electron micrographs of the produced materials were obtained with a Hitachi S-2460N microscope. Samples for SEM analyses were prepared by gold coating. Sample containing no W were analyzed as control experiments. Catalysts containing 1, 3 and 5% of W (mol %) were analyzed. Samples prepared by different milling methods were also analyzed. Hand ground TiO_2 samples by using agate mortar and pestle yielded material with a wide range of particle sizes: 100 nm to a few micrometers. Samples which were prepared by PREX® mill (ball mill, which grinds samples by placing them in a cylindrical agate vial along with agate ball as a grinding element, and imparting motion to the container) showed smaller particle sizes (20 – 100 nm) and less variation in particle sizes. The particle sizes among different mol percentage of W were not significantly different. DeGussa P25 was also checked by the same method. It shows much smaller particle size; such as 10-30 nm, but most of TiO_2 particles are agglomerated (1 μm – 5 μm) in P25. The location of W should be characterized by different experiment like SEM-EDX.

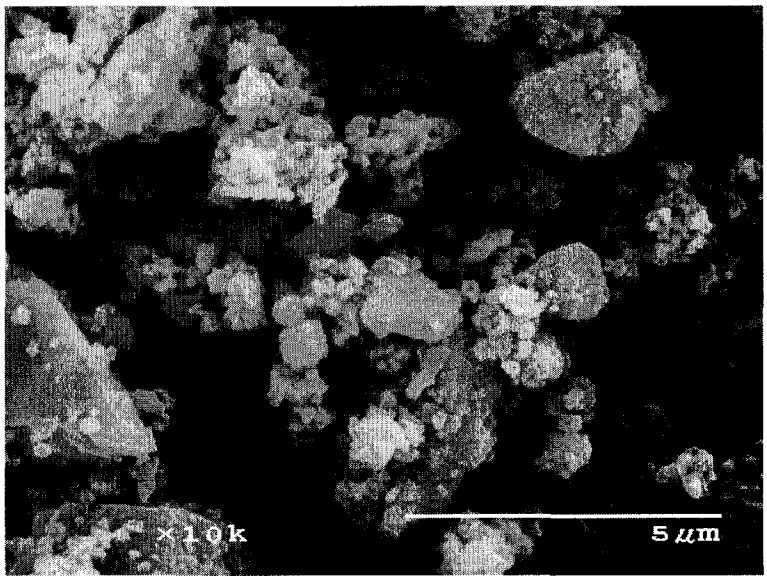

Figure 3. (a) SEM image of TiO_2 (0 % W) hand ground using agate mortar and pestle.

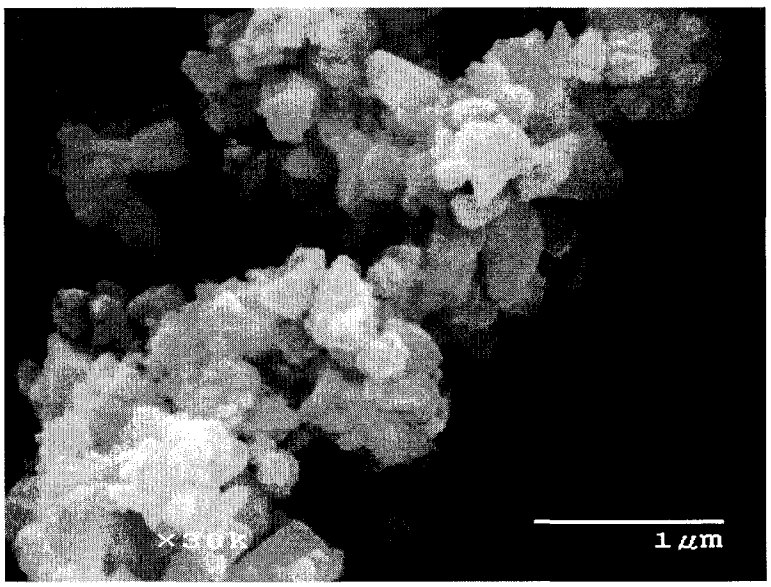

Figure 3. (b) SEM image of TiO_2 (0 % W) ground using PREX® mill (agate ball mill).

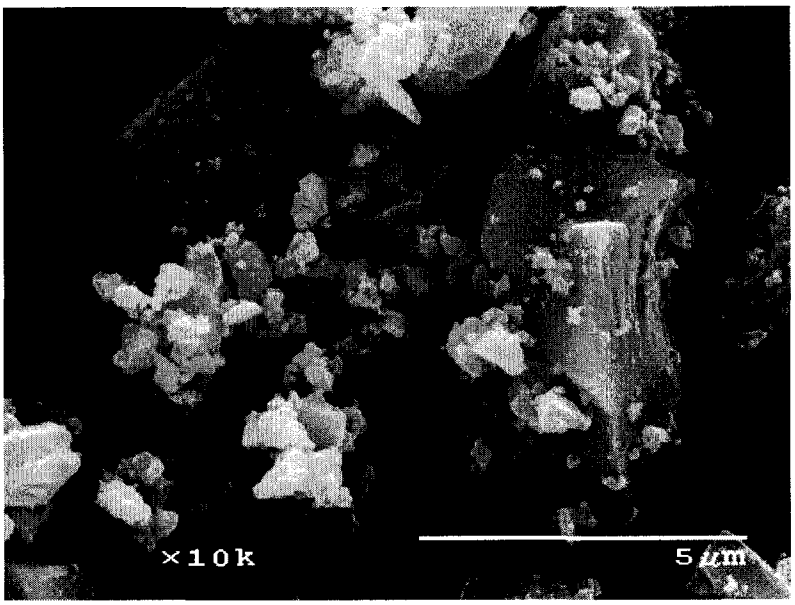

Figure 3. (c) SEM image of WO_x-TiO_2 (1% W) ground using PREX® mill (agate ball mill).

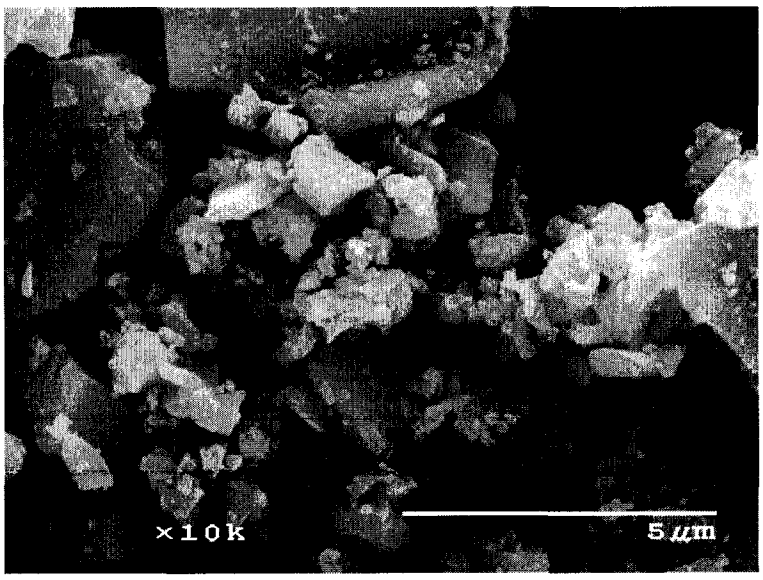

Figure 3. (d) SEM image of WO_x-TiO_2 (3% W) ground using PREX® mill (agate ball mill).

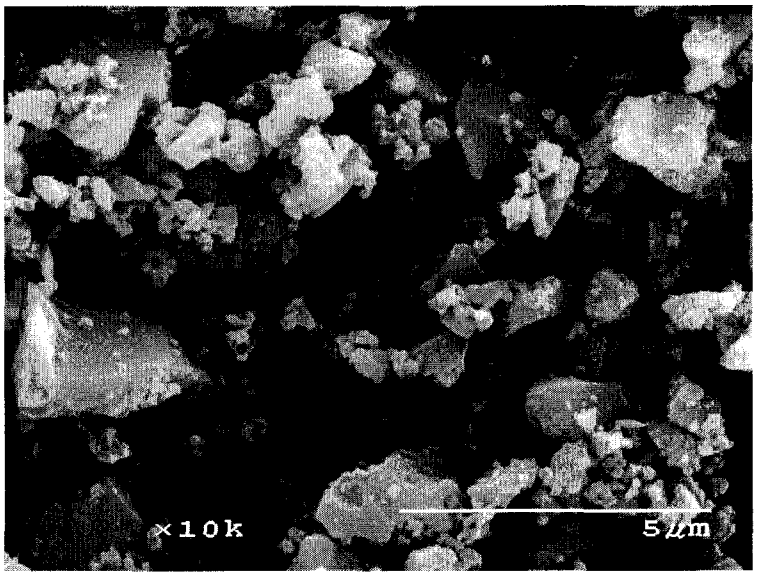

Figure 3. (e) SEM image of WO_x-TiO_2 (5% W) ground using PREX® mill (agate ball mill).

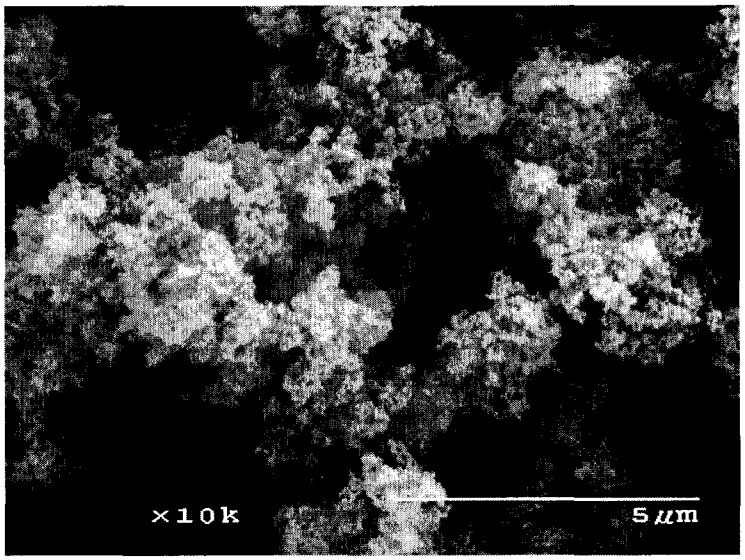

Figure 3. (f) SEM image of TiO_2 P25 DeGussa show small particle size (10-30 nm), but most of TiO_2 particles are agglomerated (1 μm – 5 μm).

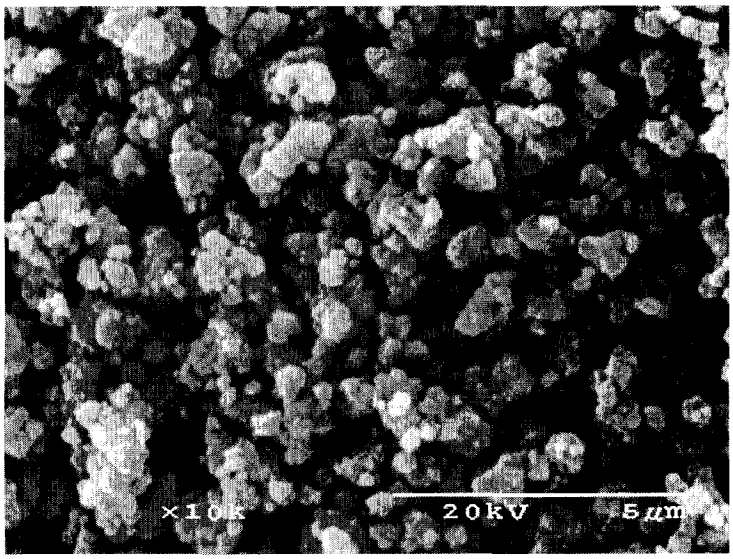

Figure 3. (g) SEM image DT 52; (3% W) WO_x-TiO_2 prepared by incipient wetness method.

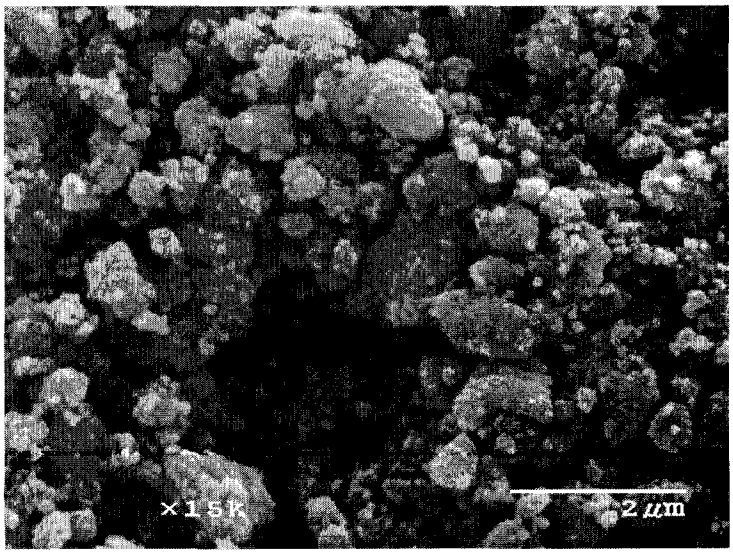

Figure 3. (h) SEM image WO_x-TiO_2 (3% W) prepared by P 25 DeGusa with incipient wetness method.

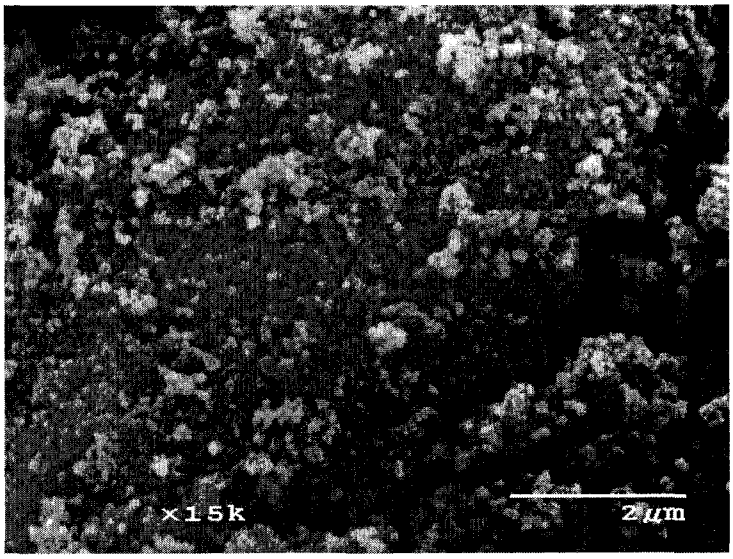

Figure 3. (i) SEM image WO_x-TiO_2 (3% W) prepared by PC 50 Millennium Chemical with incipient wetness method.

TiO_2 prepared by sol-gel method and sintered at 923 K show the same characteristic particle shape of anatase which was reported by Anderson *et al.* [22]. Based on the SEM results, the particle size of homemade WO_x-TiO_2 is larger than that of DeGussa P25. Because photocatalytic activity is increased as the particle size decreases, DeGussa P25 may have advantage in the particle size over homemade WO_x-TiO_2 save defects sites provided by mixture of 70% of anatase and 30% of rutile. However, the effect of particle size on photocatalytic activity is saturated at the particle size below 200 nm [6]. Increased surface area not only enhances active sites but also increases chance of recombination of hole and electron. Homemade WO_x-TiO_2 can take the advantage of enhanced photocatalytic activity due to the WO_x as long as keep the particle size below 200 nm. In addition,

homemade WO_x-TiO_2 has no problem of agglomeration, but DeGussa P25 shows extensive agglomeration due to its small particle size. Differently prepared (incipient wetness method for P25 Degussa and PC 50 Millennium Chemical) WO_x-TiO_2 and commercial DT 52 shows agglomerated shapes under size between 200 nm and 2 μm.

SEM-EDX Analysis. EDX data show the presence of Ti, O, and W atom and mol % of each atom. This is a mapping technique helped to see the location of W (tungsten atom) and it has a spatial resolution between 200 nm and 1 μm. Based on EDX results, tungsten atom is evenly dispersed all through the TiO_2 particles. As a control experiment physical mixture of WO_3 and TiO_2 shows distinctive feature compared to WO_x-TiO_2 samples, which presented evenly dispersed tungsten atom through the whole WO_x-TiO_2 particle. The physical mixture has localized distribution of tungsten atom shown as bright spot on the SEM-EDX map. This result indicates that WO_x-TiO_2 prepared by sol-gel method does not have large-scale segregation of WO_x islands or particles. However, information at atomic resolution, such as the depth profile of WO_x-TiO_2 or tungstate distribution information on small particle (<1 μm) is difficult to collect due to the limitation of the instrument. Other WO_x-TiO_2 prepared by incipient wetness method generally shows similar SEM-EDX images as the sol-gel WOx-TiO_2.

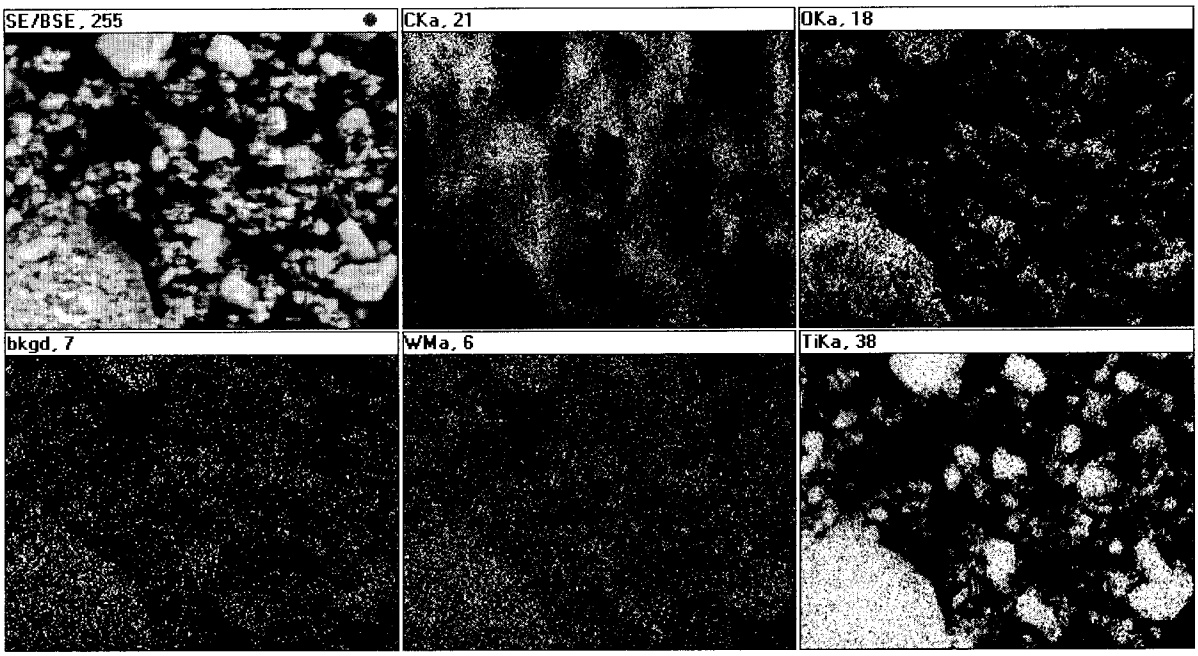

Figure 4. (a) SEM-EDX map of TiO_2 (0% W) hand ground (10 μm across from left to right).

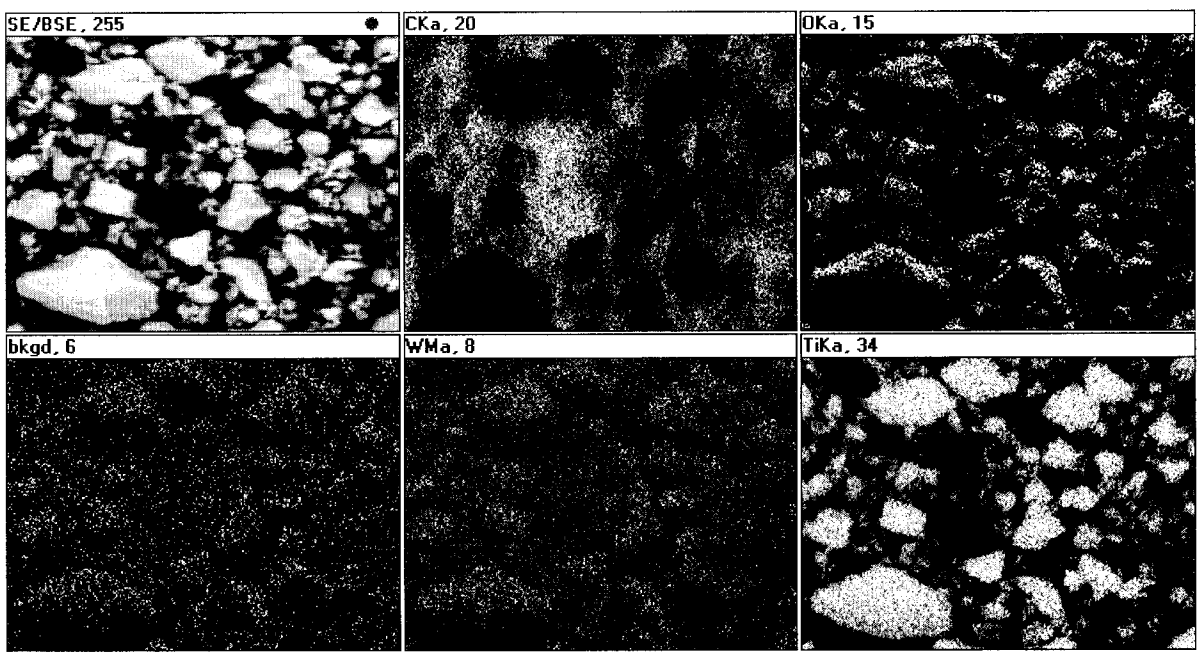

Figure 4. (b) SEM-EDX map of WO_x-TiO_2 (1% W) ground using PREX® mill (10 μm across from left to right).

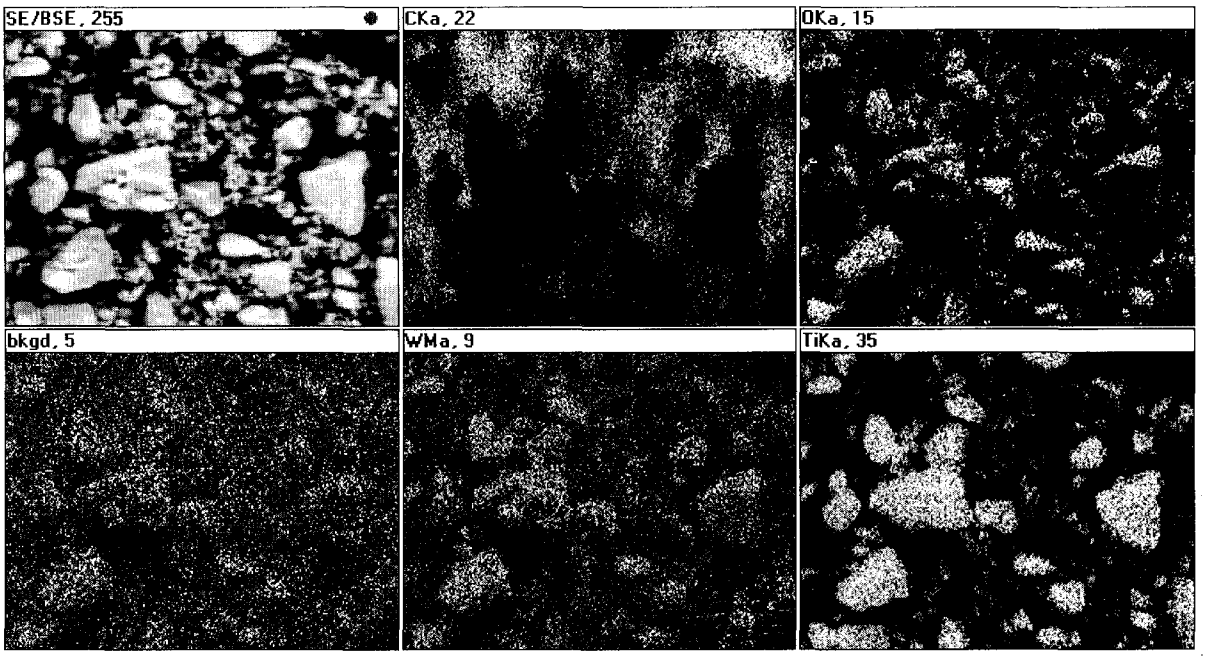

Figure 4. (c) SEM-EDX map of WO_x-TiO_2 (3% W) ground using PREX® mill (10 μm across from left to right).

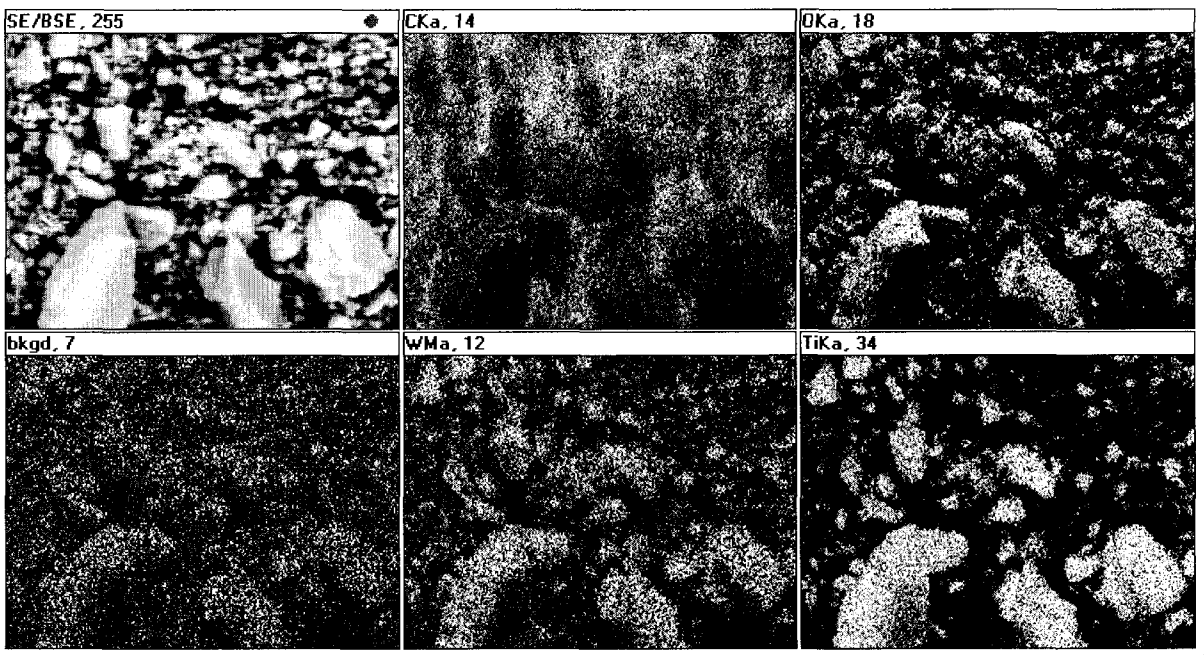

Figure 4. (d) SEM-EDX map of WO_x-TiO_2 (5% W) ground using PREX® mill (10 μm across from left to right).

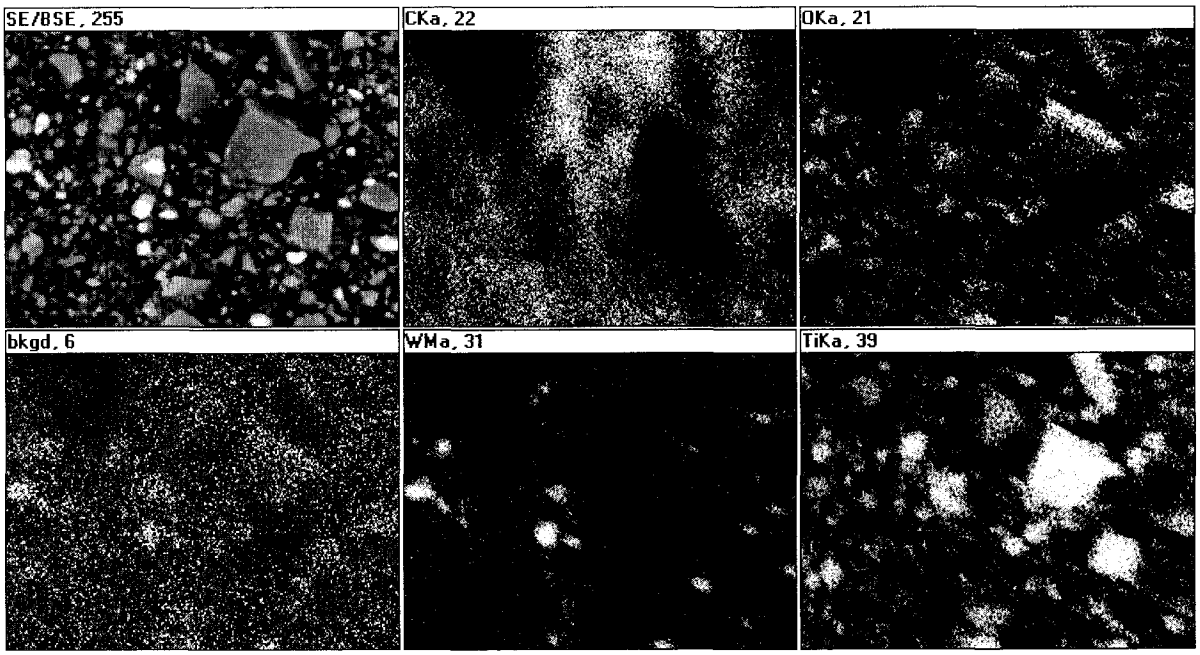

Figure 4. (e) SEM-EDX map of physical mixture of ammonium tungstate (c.a. 3% by mol) and TiO_2 (10 μm across from left to right).

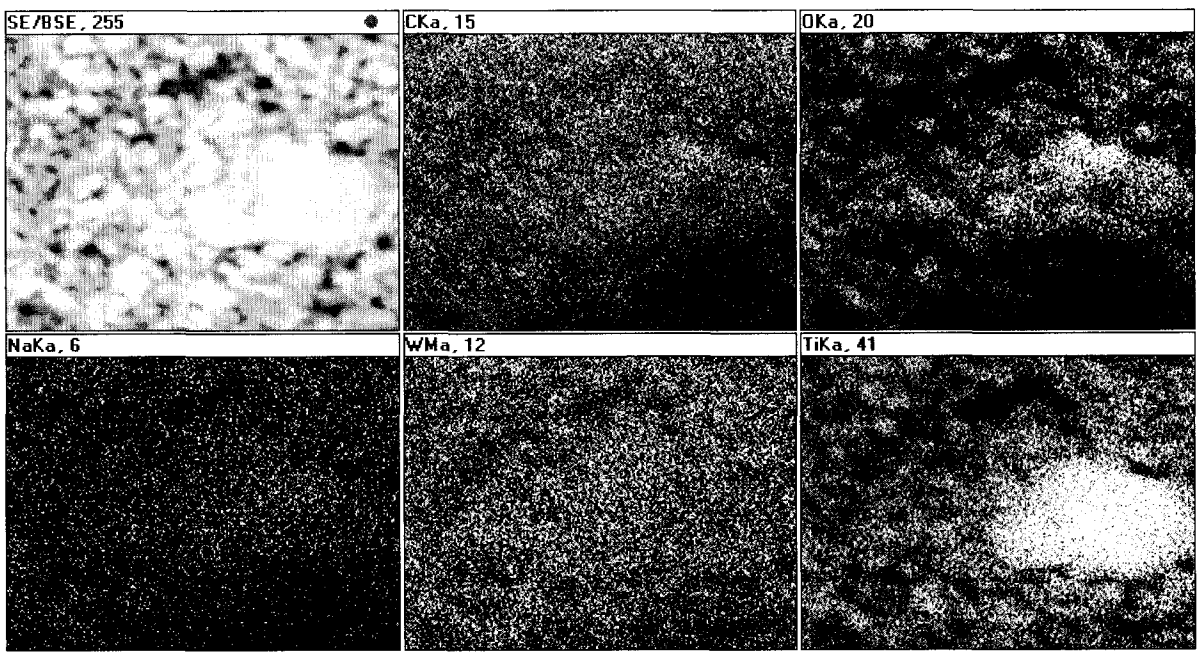

Figure 4. (f) SEM-EDX map of DT 52; (3% W) WO_x-TiO_2 prepared by incipient wetness method (10 μm across from left to right).

XPS analysis. XPS analysis was carried out to determine the chemical composition of the catalysts and the valence states of various species present in Figure 5. For the pure TiO_2, the Ti 2p peaks are narrow with slight asymmetry and have a binding energy of 460.88 eV, attributed to Ti^{4+}. For the 3% WO_x-TiO_2, the spectrum appears in a slightly decreased intensity, perhaps due to the tungsten oxides being doped in the lattice of TiO_2. The binding energy was 0.48 eV higher than that of pure TiO_2 which implies an intimate mixture of W and Ti, at least on coverage near the surface. The peak intensity of O 1s in 3% WOx-TiO_2 was also smaller than that of TiO_2 due to WO_x being doped on the surface of TiO_2. The binding energy was 0.4 eV higher than that of pure TiO_2. Both decreased intensity and increased binding energies of Ti 2p and O 1s in WO_x-TiO_2 consistently reflect the effect of compositing WO_x to TiO_2. A peak at 532.65 eV for the 3% WO_x-TiO_2 agree with the O 1s electron binding energy for WO_x molecule. TiO_2. For the pure TiO_2, the O 1s peak was also narrow with slight asymmetry and had a binding energy of 532.25 eV. These results are in good agreement with previous reports except *ca.* 2 eV differences that may be due to a systematic error [2, 26-29]. The W 4f peak is boarder and deformed by Ti 3p and other possible mixed valence of W^{4+}, $W_xO_y^{n-}$ (W^{5+}), and W^{6+}. Thus, the assignment of the existence of the precise mixtures of WO_2, WO_3, and some non-stoichiometric tungsten oxides is difficult by fitting analysis.

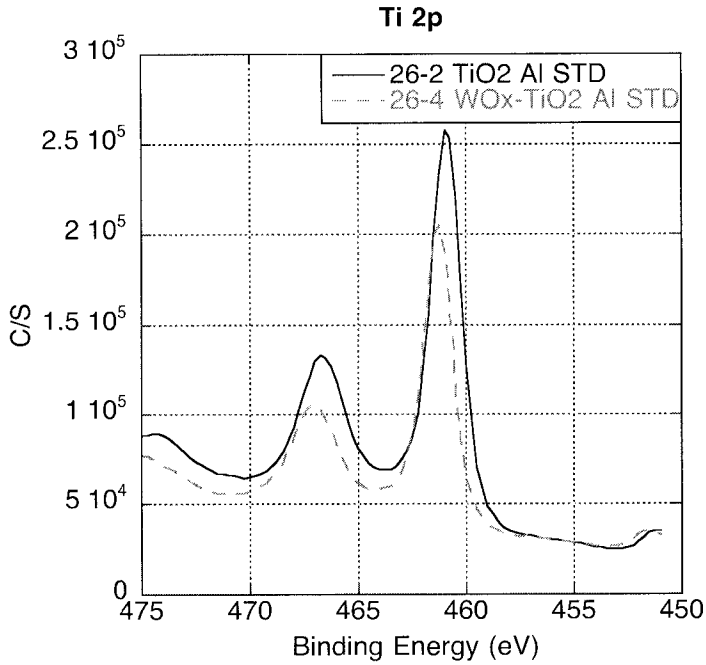

Figure 5. (a) XPS spectra for Ti 2p from pure TiO_2 and the 3% WO_x- TiO_2.

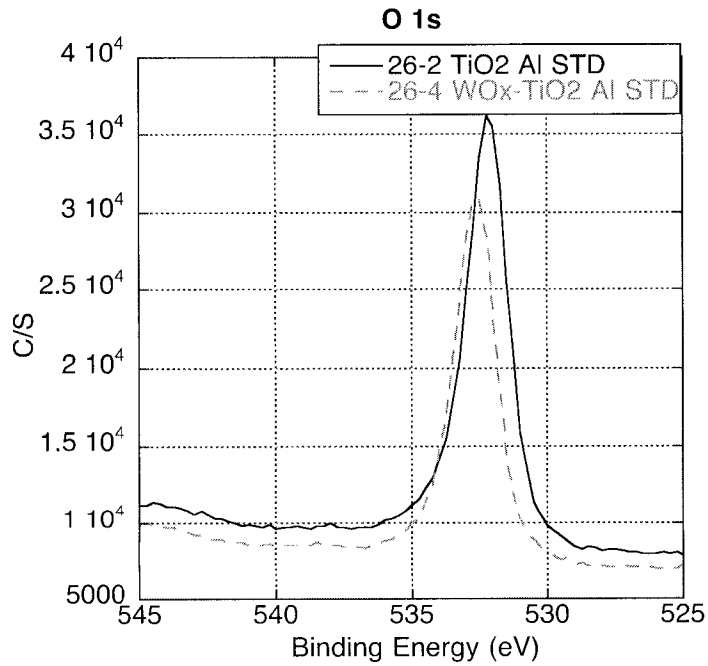

Figure 5. (b) XPS spectra for O 1s peak from pure TiO_2 and the 3% WO_x- TiO_2.

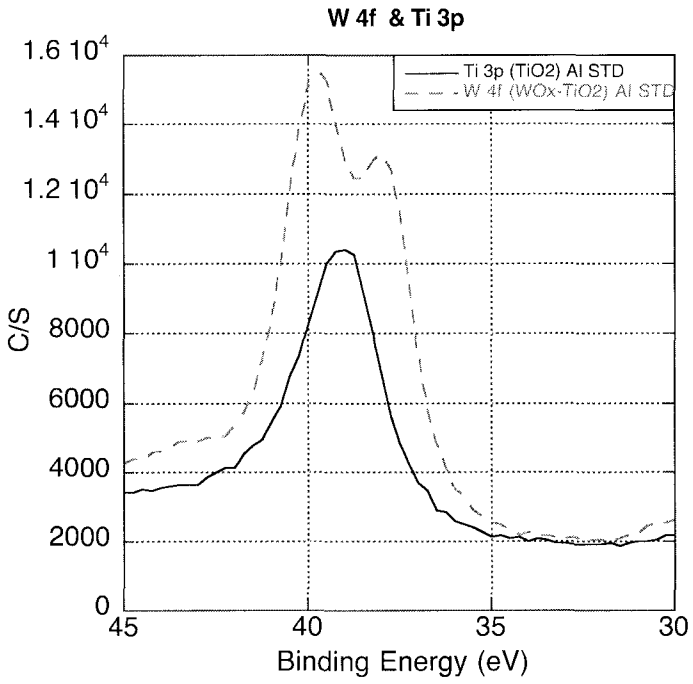

Figure 5. (c) XPS spectra for W 4f peak from pure TiO_2 and the 3% WO_x- TiO_2.

Photocatalytic degradation of 4-methoxyresorcinol and 4-chlororesorcinol with WO_x-TiO_2 under visible light irradiation.

The efficiency and some selectivity of photocatalytic degradation using the WO_x-TiO_2 was evaluated on the basis of the photo-degradation rate of 4-methoxyresorcinol (4MRC, **1**) and 4-chlororesorcinol (4CRC, **6**) in aqueous solution.

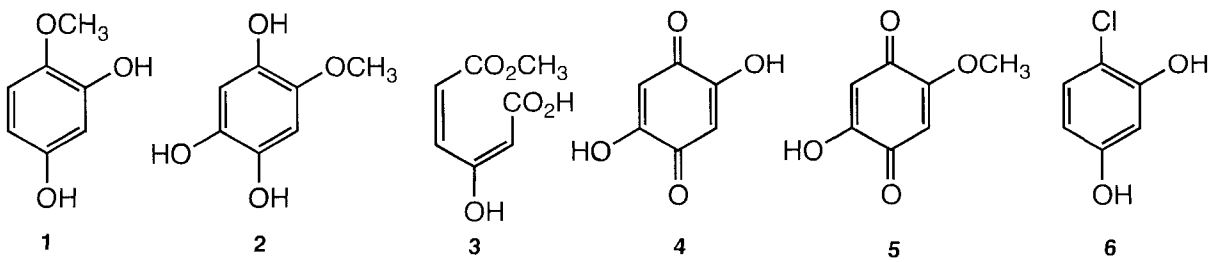

The reaction of 4MRC and 4CRC photo-degradation showed that the WO_x impurity dispersed in TiO_2 could enhance the photocatalytic activity of TiO_2 significantly under visible light irradiation. Because it is not a hydroquinone, 4-methoxyresorcinol (**1**) is considerably more stable than its isomer 2-methoxyhydroquinone in the presence of O_2. No dark degradation was observed. Direct irradiation in the absence of TiO_2 led to its decomposition, but about 10 times slower than that under normal conditions. The products of direct irradiation were different from TiO_2 mediated photocatalytic degradation and the direct irradiation products were not significant under normal photocatalytic degradation conditions [21].

Dark adsorption experiments were carried out to see the effect of adsorption of 4MRC in photocatalytic degradation at three different pHs; 2, 7, and 12. The extent of adsorption of 4MRC was determined by UV-VIS spectroscopy. Samples were prepared using 25 mg of catalyst (WO_x-TiO_2 or P25) in 20 mL water and various concentration of 4MRC. Figure 6 shows the residual adsorption ffor three sets of samples: no TiO_2, WO_x-TiO_2, and P 25. The adsorption pattern of 4MRC at pH 2 and 7 was very similar. There was significant adsorption of 4MRC neither on WO_x-TiO_2 nor on DeGussa P 25. Under the basic condition, UV spectrum of 4MRC was changed due to base promoted decomposition; λ_{max} has changed from 286 nm under pH 2 and 7 to 301 nm. Another absorption at shorter wavelength, 245 nm was observed. These changes in basic condition were due to the degradation (dark reaction) of 4MRC into oxalic acid, fumaric acid, and other degradation

intermediates. Overall adsorption of 4MRC on WO_x-TiO_2 and P 25 was not significant.

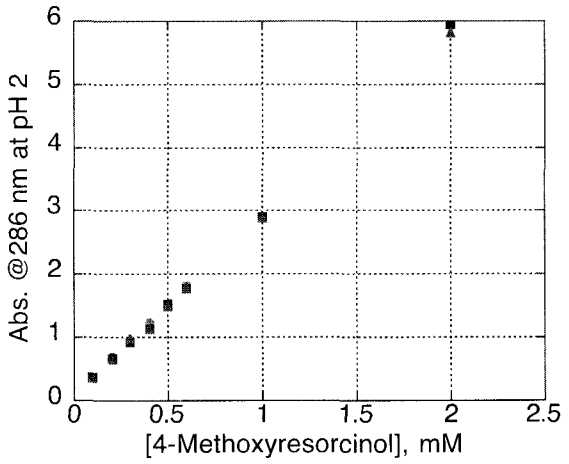

6 (a) 4-MRC adsorption at pH 2

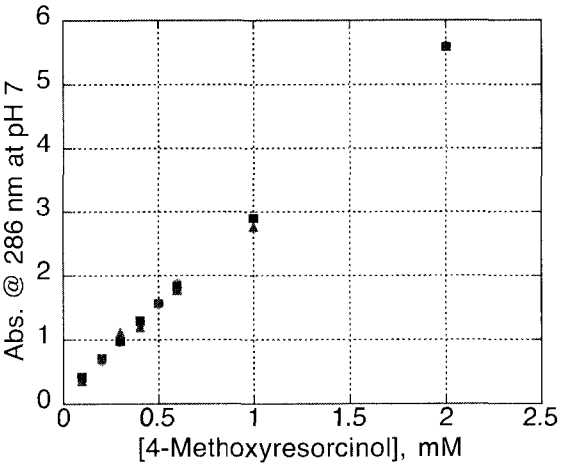

6 (b) 4-MRC adsorption at pH 7

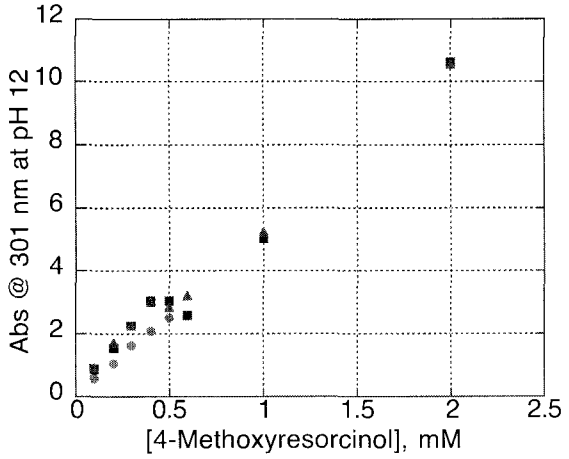

6 (c) 4-MRC adsorption at pH 12

Figure 6. Residual adsorption of 4MRC in three pHs; (a) pH=2, (b) pH=7, and (c) pH=12, ●: no TiO_2; ■ : WO_x-TiO_2 ; ▲: P 25.

Li *et al.* reported that both hydroxylation (2, 2-hydroxy-4-methoxyhydroquinone) and ring-opening (**3**) products appear as major primary products from the TiO_2-mediated photocatalytic degradation by using P25 DeGussa [21]. The other large peak (**4**) is clearly a secondary product derived from hydroxylation and demethylation. The quinone derived from a simple hydroxylation (**5**) and the product derived from both hydroxylation and ring-opening (**6**) are observed as mid-sized peaks. Li *et al.* reported that ring-opening and hydroxylation are competitive processes for this compound [21]. They also reported separate experiment in which degradation of 4MRC was carried out by 300 nm photolysis of solution without TiO_2 in the presence of H_2O_2 as a source of hydroxyl radicals. The major degradation product was (**2**), consistent with the supposition that arene hydroxylation is from the chemistry of the hydroxyl radical. Although some ring-opened products with only a few carbons were observed, (**3**) appeared only as a tiny trace peak [21].

Photocatalytic degradation of 4-methoyresorcinol by Xe-Arc lamp with cut-off filter (< 435 nm).

Standard conditions for degradation were 100 mL aqueous suspensions containing 50 mg of photocatalyst and 0.2 mM of 4MRC. Xe-Arc lamp (150 W) with cut-off filter (Ealing® 50% of transmittance at 435 nm) was used as an irradiation source. The pH of solution was adjusted by HCl (pH 2), phosphate buffer (10 mM, pH 7.0), or NaOH (pH 12). TiO_2 has two major crystal types such as anatase and

rutile. This applied light has longer wavelength than the band gap of both anatase and rutile. Thus photoactivation of the photoctalysts will be through visible light activation due to doping or sub-bandgap activation due to charge transfer complex formation. For the degradation experiment using Xe-Arc lamp, 5 mg of photocatalyst was used in 10 mL of solution using conditions otherwise identical to the standard conditions. Observed intermediates are oxalic acid, fumaric acid, malic acid, 2,5-dihydroxybenzoquinone (secondary product), succinic acid, 1,2,4,5-benzeneteraol, and 4-hydroxy-2-methoxyhydroquinone (primary product) as shown in Figure 7.

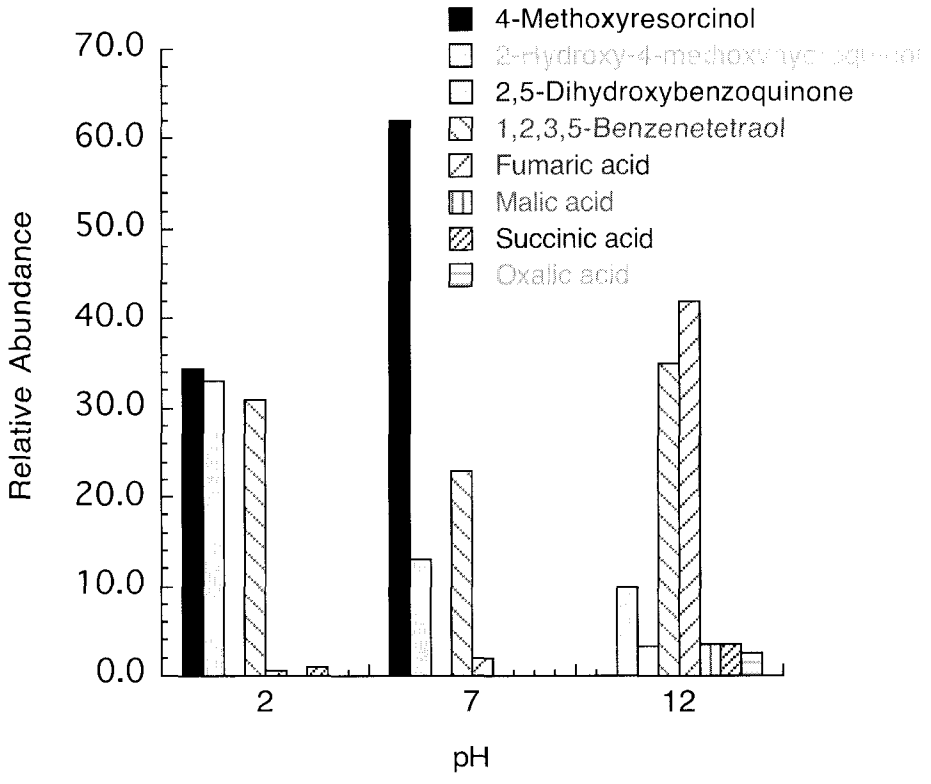

Figure 7. PCD of 4-MRC Xe-Arc w/ 435 cut-off filter; product distribution at 3 different pHs (equal GC response was assumed for degradation products). Those deradation products are from high conversion (greater than 50 % conversion).

Photocatalytic degradation of 4MRC with 3% WOx-TiO_2 of using a Xe-Arc lamp was compared at pH 2, 7 and 12. As the pH increased to basic conditions, the degree of degradation was increased after a fixed interval of photolysis. The amount of hydrxoylated products were increased as pH increased, and furthermore, secondary degradation intermediates such as 2,5-dihydroxybenzoquinone, fumaric acid, and malic acid were observed as major peaks in GC-MS spectra. Based on the observation of degradation intermediate of down stream such as oxalic acid, fumaric acid, and malic acid, the ring-opening product should have been formed. However, the ring-opened product was not observed. It may due to the faster degradation than formation of ring-opened product under strong Xe-Arc irradiation. The oxalic acid, fumaric acid, and malic acid observed as major degradation intermediate at pH12, where the degradation reaction proceeded too far down stream faster than the lower pH under relatively long (3 h) irradiation time with intensive Xe-Arc (150 W) irradiation than normal UV lamp (8 W).

Photocatalytic degradation of 4-methoyresorcinol at 419 nm.

40 mL of 0.2 mM MRC with 20 mg of photocatalysts (0, 1, 3, and 5% WOx-TiO_2) was irradiated by 419 nm UV lamp for 1 h under open air with stirring. The primary ring-opening product was observed as a major intermediate when the 419 nm lamp was used in a 1h, low conversion experiment. Among 1, 3, and 5% WOx-TiO_2, The 1% doped WO_x-TiO_2 shows the higher initial degradation as shown in Figure 8.

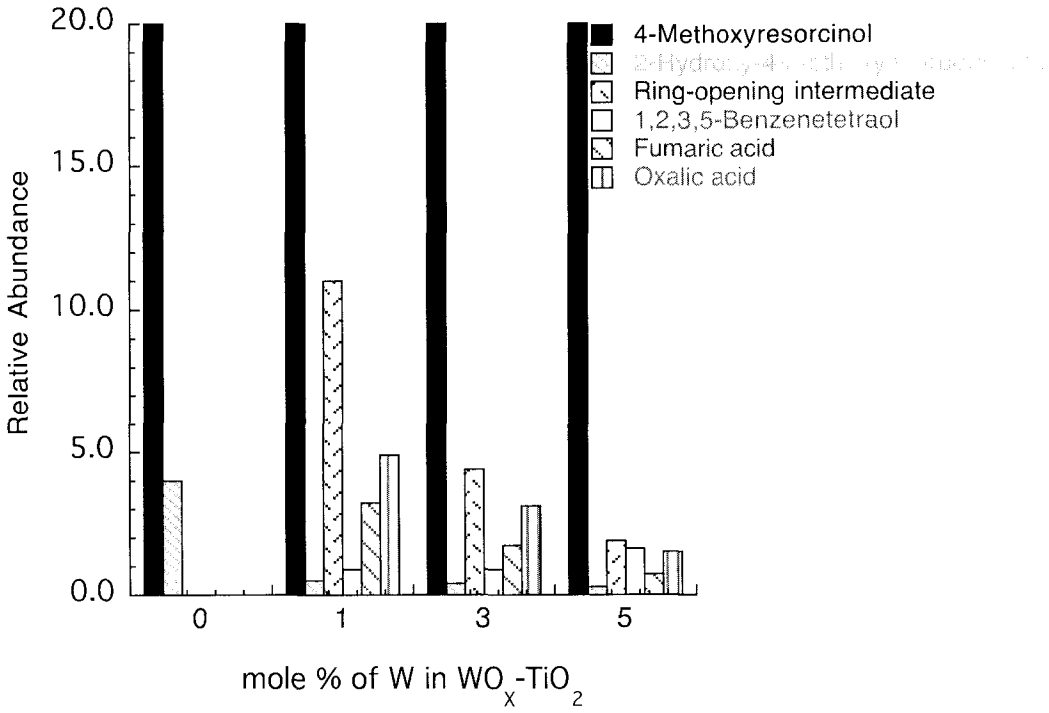

Figure 8. PCD of 4MRC at 419 nm for 1h; 4MRC is off scale from low conversion (less than 20% of degradation).

The relatively shorter reaction time (1 h) and reduced intensity of irradiation source (6 X 8 W) compared to Xe-Arc (150 W, 3h irradiation) reaction gave more information about early degradation intermediates under low conversion state. Under the same photodegradation conditions, the pure TiO_2 only yield small amount (less than 4% of conversion) 2-hdroxy-4-methoxyhydroquinone as shown in Figure 8.

Degradation efficiency comparision. The determination of photo-catalytic degradation efficiency for 4-methoxyresorcinol was carried out with different photo catalysts. 4-methoxyresorcinol (2.4 mg) dissolved in 8 mL suspension of photocatalyst in DI water. The mixture was irradiated by 419 nm lamps (6 x 8W) for 3 hours under open air in a Rayonet equipped with merry-go-round. Photoreaction mixtures were treated with usual filtration and silylation (1 mL pyridine, 0.2 mL HMDS, and 0.1 mL TMSCl) and analyzed by GC and GC-MS. WOx-TiO_2 (containing 3% WO_x) and DT 52 from Millennium Chemical (3% of WO_x was doped by incipient wetness method) showed significant degradation of substrate in 3 hours as shown in Figure 9 (a). DeGussa P25, and pure TiO_2 (0% WO_x-TiO_2 which is containing 0% of WO_x) do not degrade substrate in significant level.

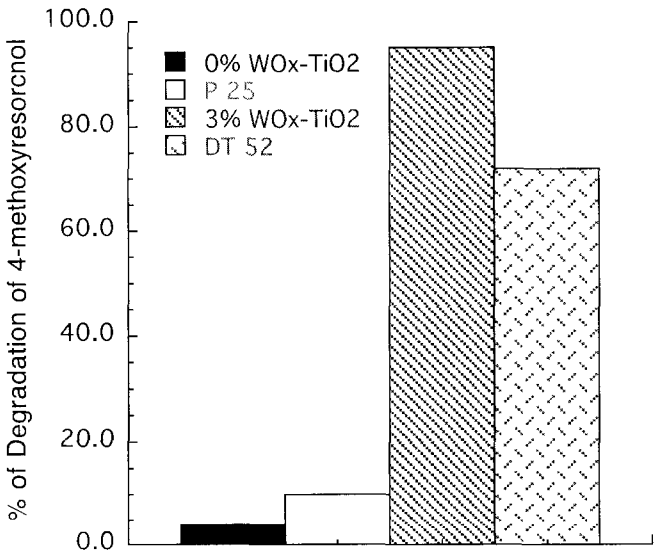

Figure 9. (a) Degradation of 4-methoxyresorcinol comparison among different photocatayst with 419 nm irradiation for 3h.

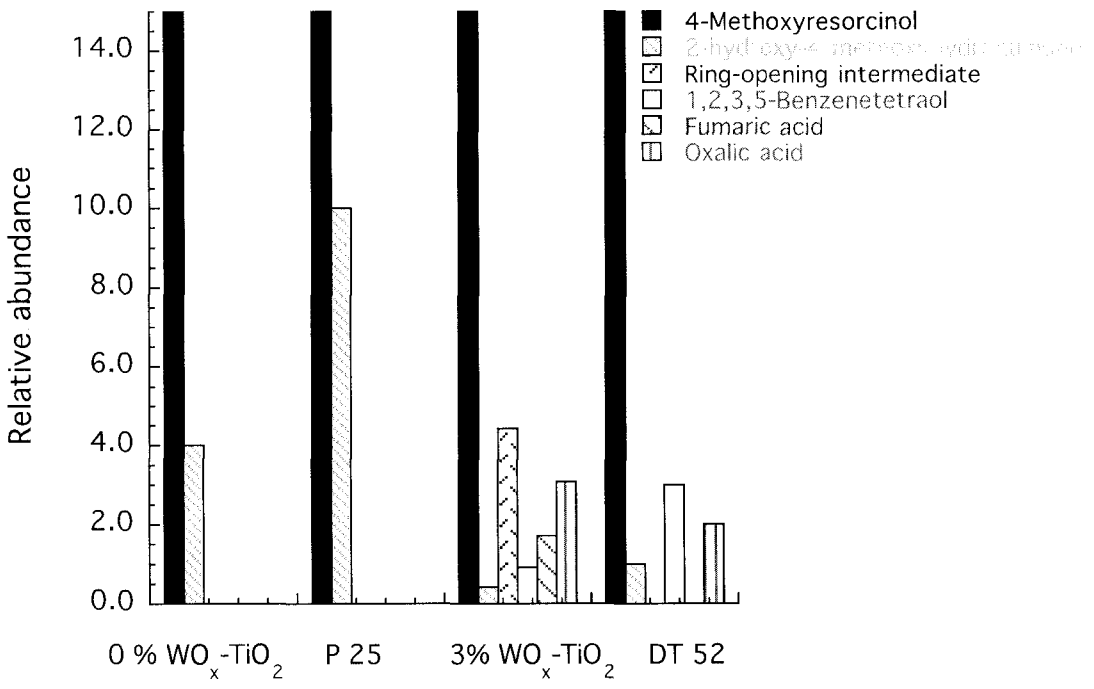

Figure 9. (b) Product distribution of photodegradation of 4-methoxyresorcinol with different photocatayst using 419 nm irradiation. 4MRC is off scale from low conversion (less than 10% of degradation).

Another set of degradation efficiency experiments with a similar molecule to 4MRC, 4-chloromethoxyresorcinol (4MRC), was carried out under the same condition as the previous experiment. 4-chloromethoxyresorcinol (2.5 mg) was dissolved in 8 mL of suspension of photo-catalyst in DI water. The mixture was irradiated at 419 nm lamps (6 x 8W) for 3 hours under open air in a Rayonet equipped with merry-go-round. Photoreaction mixtures were treated as usual with filtration and silylation and analyzed by GC and GC-MS. WOx-TiO_2 (containing 3%

WO_x) and DT 52 show significant degradation of substrate in 3 hours as shown in Figure 10. P25 and pure TiO_2 (containing 0% WO_x) do not degrade substrate in significant level.

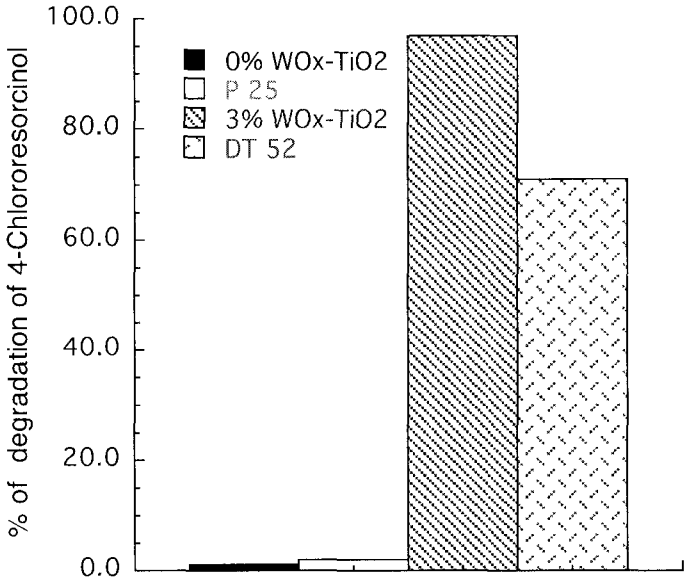

Figure 10. Degradation of 4-chlororesorcinol comparison among different photocatayst with 419 nm irradiation for 3h.

TOC Study from photocatalytic degradation of 4-methoxyresorcinol and of 4-chlororesorcinol.

4-methoxyresorcinol (2.4 mg) dissolved in 8 mL suspension of photocatalyst in DI water. The mixture was irradiated by 419 nm lamps (6 x 8W) for 3 hours under open air in a Rayonet equipped with merry-go-round. Photoreaction mixtures were treated with usual filtration. Then, the removal of TOC was analyzed by Shimadzu 5000A TOC analyzer. The initial TOC measured from the standard solution (2.4 mg

of 4-chlororesorcinol in 8 mL of DI water) was183 ppm. TOC removal was not as high as disappearance of starting material (4-methoxyresorcinol). This implies that initial reaction intermediates are hydroxylation products and mineralization of these would take further degradation time.

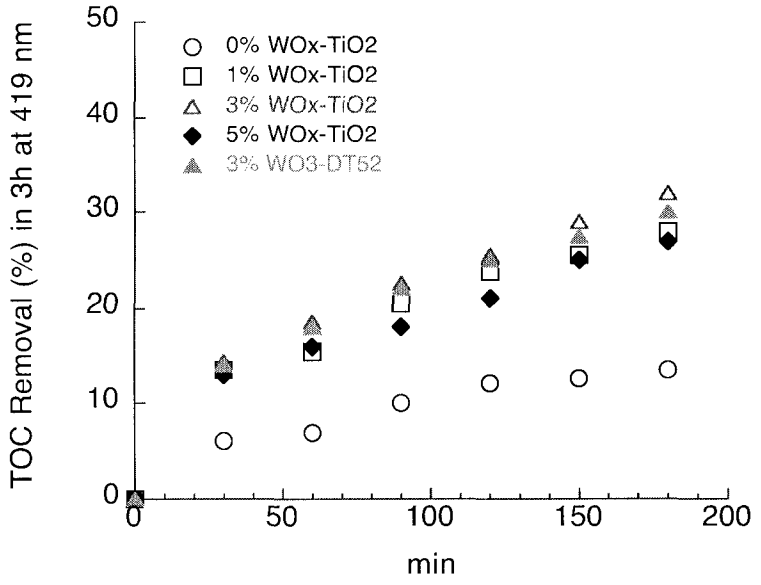

Figure 11. TOC Study from photocatalytic degradation of 4-methoxysorcinol.

Another set of TOC removal experiments with 4-chloromethoxyresorcinol (4CRC) was carried out under the same condition as the previous experiment. 4-CRC (2.5 mg) was dissolved in 8 mL of suspension of photo-catalyst in DI water. The initial TOC measured from the standard solution (2.5 mg of 4CRC in 8 mL of DI water) was 157 ppm. Again, TOC removal was not as high as disappearance of starting material (4CRC). TOC removal trend was similar to previous experiment with 4-methoxyoresorcinol. In both cases, hydroxylation products are major

degradation intermediates as shown by GC-MS study in initial photo catalytic degradation. Thus relatively low TOC removal compared to total conversion is correlated to this earlier reaction with slow ring opening followed my further decomposition.

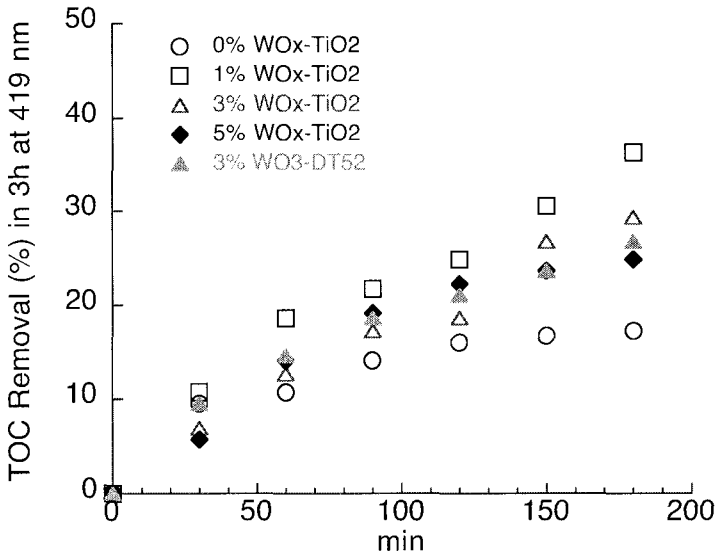

Figure 12. TOC Study from photocatalytic degradation of 4-chlororesorcinol.

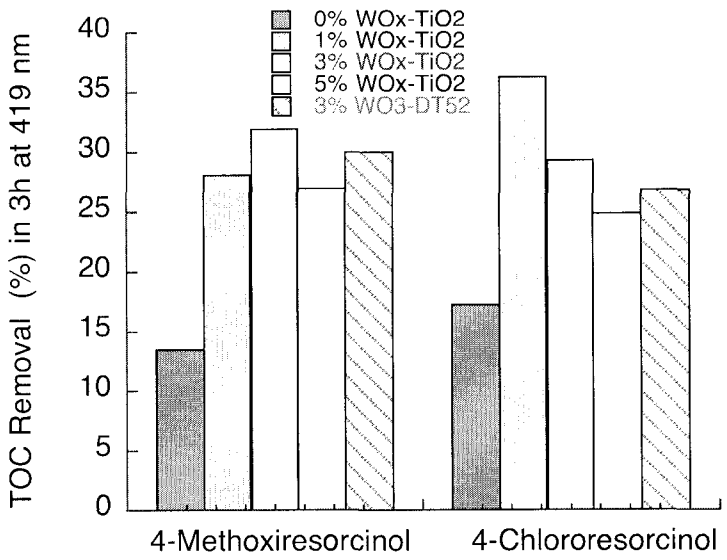

(a) PCD efficiency from photocatalytic degradation of 4-MRC and 4-CRC.

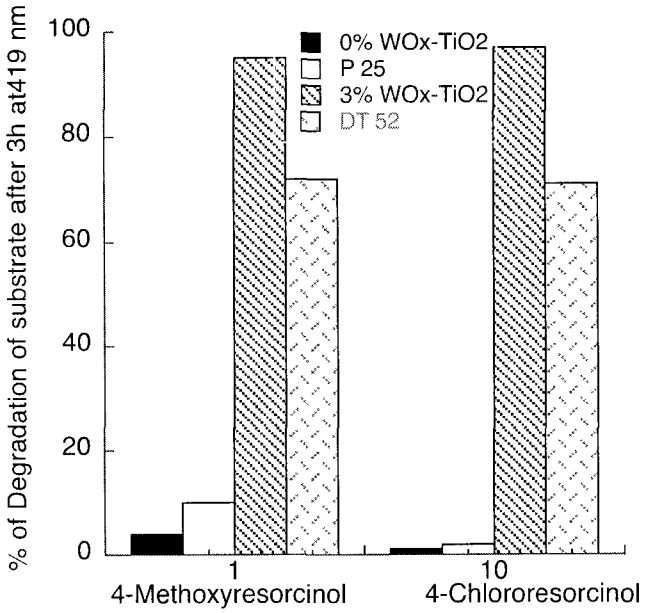

(b) TOC Study from photocatalytic degradation of 4-MRC and 4-CRC.

Figure 13. (a) PCD efficiency and (b) TOC Study from photocatalytic degradation of 4-methoxyresorcinol(4-MRC) and 4-chlororesorcinol(4-CRC).

Degradation efficiency comparison Differently prepared WO_x-TiO_2.

Differently prepared (incipient wetness method for P25 Degussa and PC 50 Millennium Chemical) WO_x-TiO_2 also shows similar effect of photo-activation by visible light. For comparing photocatalytic degradation efficiency, 7 mg of 4-methoxyresorcinol and 12.5mg of catalyst in 25 mL of DI water was irradiated visible light of (419 nm, 4 x 8W) for 12 h. Following the removal of water, the intermediate degradation products were identified and quantified as their trimethylsilyl (TMS) derivatives, using GC-MS procedures reported in our earlier work. The removal of TOC was analyzed by Shimadzu 5000A TOC analyzer as usual. WO_x-TiO_2 by sol-gel method consistently shows higher degradation efficiency (10~20%) shown in Figure 14 and 15. There was no significant difference in detected degradation products shown in Figure 16.

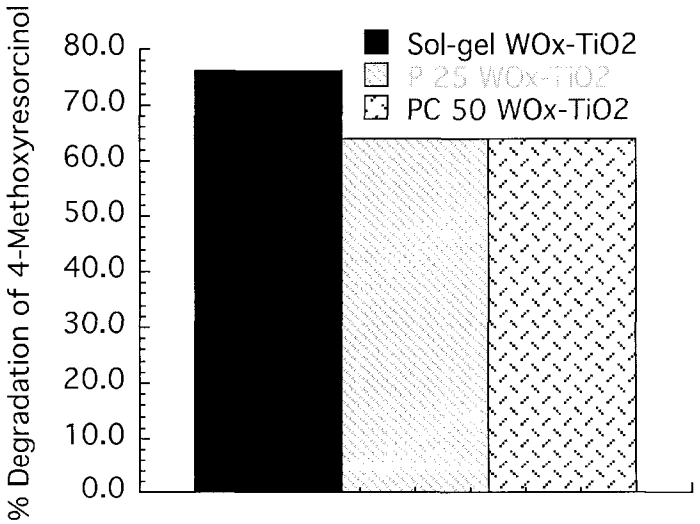

Figure 14. Degradation of 4-methoxyresorcinol comparison by using differently prepared WO_x-TiO_2 with 419 nm irradiation.

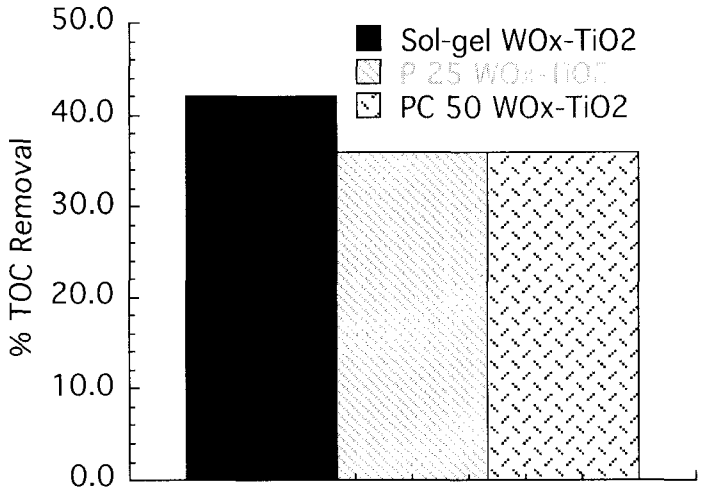

Figure 15. TOC removal comparison from the photocatalytic degradation of 4MRC by using differently prepared WO_x-TiO_2 with 419 nm irradiation.

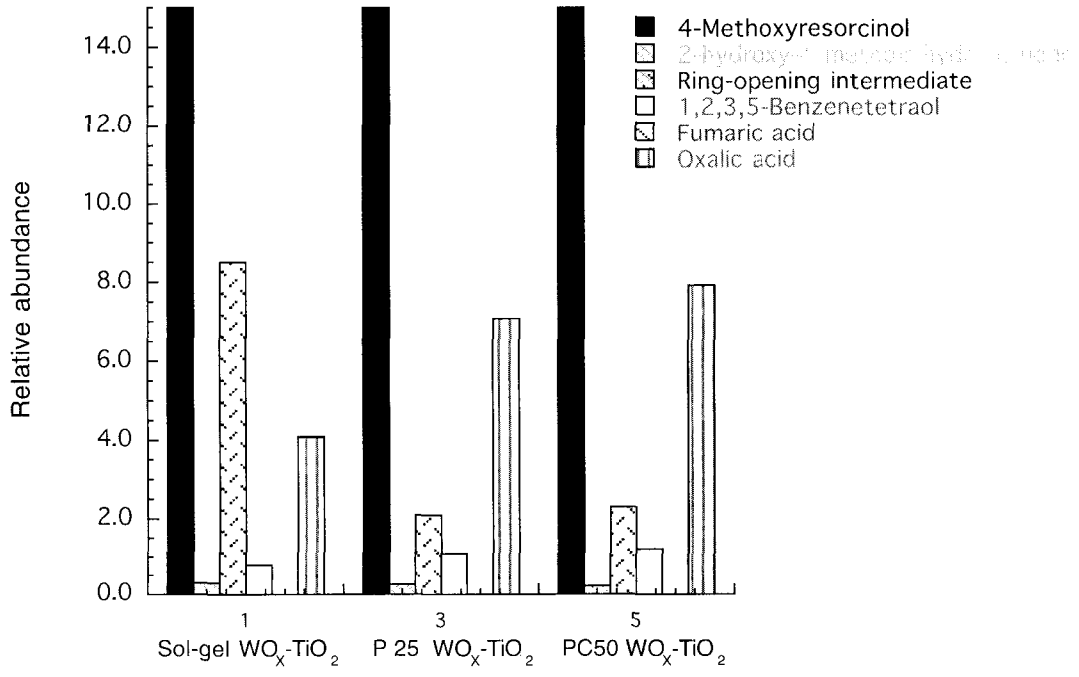

Figure 16. Products distribution from photocatalytic degradation of 4MRC with differently prepared WOx-TiO_2 (containing 3% WO_x). 4MRC is off scale.

5. 4. Discussion

Li and coworkers carried out systematic approach to characterize tungstated titania (WO_x-TiO_2) prepared by sol-gel method. They also test the photodegradation efficiency of methylene blue (MB) using WO_x-TiO_2 under visible light irradiation [2]. The photocatalytic activity (chemical composition and optical absorption) of WO_x-TiO_2 was examined by XRD, UV-VIS absorption spectra, XPS, photoluminescence spectra (PL), and electron-field-induced surface photo voltage spectra (EFISPS). The order of photo activity from weak to strong had a good agreement with that of PL intensity and that of EFISPS intensity from strong to weak. They reported that MB in aqueous solution was successfully photo-degraded using WO_x-TiO_2 under visible light irradiation. They proposed that tungsten oxides doping into TiO_2 could shift the light absorption band from near UV range to visible range.

We hypothesize that this visible light excitation of WO_x-TiO_2 facilitates the photo-catalytic degradation of 4-methoxyresorcinol (4MRC), and 4-chlororesorcinol (4CRC). This hypothesis is consistent with the data in figure 8~15. We observed that the photo activity of WO_x-TiO_2 is significantly higher than that of pure TiO_2, and sol-gel prepared WO_x-TiO_2 also shows higher photo activity than that of tungsten oxide coated TiO_2 (DT 52 from Millennium Chemical).

Based on basic conception for modification of photo activity of TiO_2 as mentioned previously, We prepared WO_x-TiO_2 by a sol-gel method with an attempt to activate the modified TiO_2 photocatalysts by the visible light, and to decrease the rapid recombination of excited electrons/holes during photoreaction. The WO_x-TiO_2

catalysts were characterized by XRD, XPS, and SEM-EDX. Our XRD result is in very good agreement with the result by Li et al [2]. Obviously, tungsten oxides hindered the phase transformation from anatase to rutile during sintering. We applied even lower sintering temperature (923 K) than Li's experiment (973 K) to further inhibit the phase transformation to rutile to better approach the successful mix of phase seen in P25 DeGussa.

Under the visible light irradiation with photocatalyst, photoactivation of the photoctalysts will be through visible light activation due to doping or sub-bandgap activation due to charge transfer complex formation [2, 30]. 4MRC would form charge-transfer complex intermediate more easily than 4CRC, which has electron withdrawing group. It would result in higher initial degradation on pure TiO_2 with MRC than CRC through electron transfer pathways by forming charge transfer complex (Figure. 9 & 10) [30]. However, overall photocatalytic degradation of these probe molecules with WO_x-TiO_2 shows similar degree due to major hydroxyl radical mediated degradation under visible light photo activation.

Experiments for evaluating degradation efficiency between homemade WO_x-TiO_2 (particle size 20-100 nm) with DT 52 from Millennium Chemical (particle size 15-25 nm), shows that particle size is not the only factor that decides the efficiency of photo catalysts. Larger particle sized homemade WO_x-TiO_2 results better photo catalytic degradation efficiency than DT 52. Differently prepared (incipient wetness method for P25 Degussa and PC 50 Millennium Chemical) WO_x-TiO_2 also shows similar effect of photo-activation by visible light. WO_x-TiO_2 by sol-gel method

consistently shows higher degradation efficiency (c.a. 20%). It is difficult to explain thoroughly this result at this point because photocatalytic activity is affected by much more factors than simply particle size i.e., agglomerate size, crystallization condition, surface property also affect to photocatalytic activity. One possible speculation for better photocatalytic activity of WO_x-TiO_2 by sol-gel method may due to less formation of aggregate by WO_x-TiO_2 from sol-gel method. Future work could refine the degradation efficiency precisely by controlling the particle sizes, defective sites of TiO_2, agglomerate size etc.

5. 5. Conclusion

With an attempt to activate the modified TiO_2 photocatalysts by the visible light and decrease the rapid recombination of excited electrons/holes during photoreaction, WO_x-TiO_2 powder was prepared by a sol-gel method.

The WO_x-TiO_2 catalysts were characterized by XRD, XPS, and SEM-EDX. The attempt to decompose 4-methoxyresorcinol and 4-chlororesorcinol in aqueous solution by using WO_x-TiO_2 under visible light was successfully achieved. The removal of TOC was lower than the degree of degradation of probe molecules. It is correlated that the hydroxylation reaction is the major initial reaction.

The modification of TiO_2 by W shows its benefit of utilizing visible light for photocatalytic degradation of organic compounds. Differently prepared (incipient wetness method for P25 Degussa and PC 50 Millennium Chemical) WO_x-TiO_2 also

shows similar effect of photo-activation by visible light. WO_x-TiO_2 by sol-gel method consistently shows higher degradation efficiency

5. 6. References

[1] A. Mills, S. Le Hunte, J. Photochem. Photobiol. A 108 (1997) 1.

[2] X. Z. Li, F. B. Li, J. Photochem. Photobiol. A 141 (2001) 209.

[3] Y. R. Do, W. Lee, K. Dwight, A. Wold, J. Solid State Chem. 108 (1994) 198.

[4] G. Ramis, G. Busca, C. Cristiani, Langmuir 8 (1992) 1744.

[5] H. V. Damme, Photocatalysis-Fundamentals and Applications, ed. N. Serpon, E. Pelizzetti (1989) New York: Wiley.

[6] H. Harada, T. Ueda, Chem. Phys. Lett. 106 (1984) 229.

[7] H. Gerischer, A. Heller, J. Phys. Chem. 95 (1991) 5261.

[8] R. I. Bickley, T. Gonzalex-Carreno, J. Solid State Chem. 92 (1991) 178.

[9] K. Kobayakawa, Y. Nakazawa, M. Ikeda, Y. Sato, A. Fujishima, Berichte der Bunsen-Gesellschaft 94 (1990) 1439.

[10] E. Borgarello, N. Serpone, G. Emo, R. Harris, E. Pelizzetti, C. Minero, Inorg. Chem. 25 (1986) 4499.

[11] I. Izumi, W. W. Dunn, K. O. Wilbourn, F. F. Fan, A. J. Bard, J. Phys. Chem. 84 (1980) 3207.

[12] Z. Goren, I. Wilner, A. J. Nelson, A. J. Frank, J. Phys. Chem. 94 (1990) 3784.

[13] Y. M. Gao, W. Lee, R. Trehan, K. Dwight, A. Wold, Materials Research Bulletin 26 (1991) 1247.

[14] J. M. Herrmann, J. Disdier, P. Pichat, A. Fernandez, A. Gonzalez-Elipe, G. Munuera, C. Leclerq, J. Catalysis 132 (1991) 490.

[15] A. Fujishima, K. Itho, R. Baba, Kenkyu Hokoku Asahi Garasu Kogyo Gijutsu Shoreikai 55 (1989) 347.

[16] D. Liu, P. V. Kamat, J. Phys. Chem. 97 (1993) 10769.

[17] C. Nasr, P. V. Kamat, S. Hotchandani, J. Electroanal. Chem. 420 (1997) 201.

[18] C. Nasr, S. Hotchandani, P.V. Kamat, Proceedings - Electrochemical Society, 97-20 (1997) 130.

[19] S. Hotchandani, P.V. Kamat, Chem. Phys. Lett. 191 (1992) 320.

[20] L. K. Vinodgopal, I. Bedja, P. V. Kamat, Chem. Mater. 8 (1996) 2180.

[21] X. Li, J. W. Cubbage, W. S. Jenks, J. Photochem. Photobiol. A 143 (2001) 69.

[22] M. Andersson, L. Oesterlund, S. Ljungstroem, A. Palmqvist, J. Phys. Chem. B 106 (2002) 10674.

[23] J. Engweiler, J. Harf, A. Baiker, J. Catalysis 159 (1996) 259.

[24] A. L. Linsebigler, G. Lu, J. T. Yates, Jr., Chem. Rev. 95 (1995) 735.

[25] S. Eibl, B. C. Gates, H. Knoezinger, Langmuir 17 (2001) 107.

[26] A. Scholz, B. Schnyder, A. Wokaun, J. Molecular Cat. A 138 (1999) 249.

[27] L. Su, Z. Lu, J. Physics and Chemistry of Solids 59 (1998)1175.

[28] J. F. Moulder, W. F. Stickle, P. E. Sobol, K. D. Bomben, Handbook of X-ray Photoelectron Spectroscopy, ed. J. Chastin (1992) Eden Prairie, MN: Perkin-Elmer.

[29] J. H. Scofield, J. Elec. Spec. and Related Phenomena, 8 (1976) 129.

[30] A. G. Agrios, K. A. Gray, E. Weitz, Langmuir 19 (2003)1402.

Chapter 6

GENERAL CONCLUSION

Photocatalytic degradation of organic contaminants in water was investigated by aqueous suspension of TiO_2 and modified-TiO_2. The objectives of these studies are composed of elucidation of degradation mechanisms of organic contaminants under various photo-catalysis environment, optimization of degradation efficiency, and enhancement of the activity of photo-catalysts.

The partial photocatalytic degradation of maleic acid has been investigated with the purpose of elucidating the mechanism of catalyst action for some of the early transformations. In particular, it is proposed that the photo-catalytically induced *cis-trans* isomerization of maleic acid and fumaric acid is initiated by adsorption-dependent reductive electron transfer. The bases for this conclusion include the acid's superior adsorption at low pH, the near exclusivity of this process in the absence of O_2 (which usually acts as an electron acceptor), the increase in observed isomerization rate in the absence of O_2 (contrary to almost any other known photocatalytic degradation process), and the suppression of isomerization with the addition of fluoride to the system. An investigation into the involvement of superoxide in the oxygenation reactions observed near neutral and higher pH clearly demonstrates that superoxide does not initiate the chemistry. Photocatalytic degradation of maleic acid in aqueous TiO_2 suspension provides an important insight

into the degradation mechanism of major aromatic pollutants due to maleic acid is one of major four carbon intermediates from the photocatalysis of 4-chlorophenol and other aromatic organic contaminants in water. The aliphatic intermediates most frequently encountered during the degradation of aromatic compounds are short-chain carboxylic diacids, as maleic, fumaric and oxalic acids, which have been detected during the mineralization of a variety of organic chemicals. Thus, the understanding of the mechanism of degradation of these compounds can assist us for the ascertaining of the better conditions to perform the mineralization of recalcitrant organic compounds. HO• and O_2 play significant roles in the photocatalytic degradation of aliphatic acids. An investigation into the possibility that other reactions begin with the reaction of maleic acid with superoxide in a similar electron/nucleophile-accepting mode produced results in clear contradiction with this idea. It is presumed that the formation of tartaric acid and dihydroxyfumaric acid – along with other smaller intermediates – occurs by conventional mechanisms beginning with hydroxyl attack on the substrate. OH radical adding to the unsaturated bond to form a carbon-centered radical. In the presence of oxygen such carbon-centered radicals are converted into the corresponding peroxy radicals. Then, peroxy radicals undergo decay by a bimolecular mechanism by forming tetroxide radical and decayed by Russell process.

The challenge to decompose a cyanuric acid, a recalcitrant species, by modifying TiO_2 suspension was carried out in TiO_2/F aqueous suspensions. The addition of fluoride to aqueous suspensions of TiO_2 has proved to be an important mechanistic tool in unraveling a long-standing conundrum in photocatalytic degradation. By using this method in parallel with other methods for producing homogeneous hydroxyl-type reagents, it is shown that cyanuric acid is susceptible to degradation under easily accessible conditions. There is another supportive evidence that TiO_2/F method was successfully applied to degrade 4-*t*-butylpyridine (which is also almost untouched by ordinary TiO_2 photolysis condition. It gives predictable hydroxylated intermediates, and thus supports the hypothesis that the induced reactivity is due to the formation of homogeneous HO•. The reason that cyanuric acid is ordinary inert to TiO_2-mediated photocatalytic degradation appears to be that simply is not bound to the reactive portions of the TiO_2 surface to any measurable extent, perhaps in combination with its lower reactivity evident from other reactions. Its inherent chemical resistance to degradation is still exhibited in the inability to observe intermediate degradation products, regardless of degradation methods, because the intermediates are consumed more rapidly than they are formed.

An important unsettled mechanistic point is the degradation mechanism of phosphonate was investigated by isotope studies from the degradation of dimethyl phenyl phosphonate (DMPP). Exposure of DMPP and related simple phosphonates to TiO_2-mediated photocatalytic conditions results first in the loss of one of the

methyl esters. The unsettled mechanistic point is the mechanism by which the methyl is removed. The question is whether attack occurs at the methyl or at the phosphorus or both. Through the isotope studies of TiO_2-mediated photocatalytic degradation of phosphonates, now we can well understand including removal of the alkyl ester portion of the compounds to produce phosphonic acid monoesters among the primary steps. While there is ambiguity in the interpretation of small H/D selectivity in the dealkylation of DMPP by TIO_2 photocatalysis and various other methods, the results of ^{18}O labeling are clear. They do not rely on any kinetic effect. The retention of ^{18}O in the formation of MMPP by demethylation of DMPP clearly demonstrates that the dealkylation mechanism involves degradation of the methyl group exclusively, and neither attack at phosphorus by $HO\bullet_{ads}$ or a related species, nor photoinduced hydrolysis.

The Modification of TiO_2 is aims to increases activity with an attempt to activate the modified TiO_2 photocatalysts by the visible light and decrease the rapid recombination. Photocatalytic degradation of 4-methoxy resorcinol by using modified composite photo catalyst, WO_x-TiO_2 was carried out for evaluation of photocatalysis characteristics. There has been recent interest in WO_3-coated DeGussa P25 TiO_2 because it has higher activity than native material. With an attempt to activate the modified TiO_2 photocatalysts by the visible light and decrease the rapid recombination of excited electrons/holes during photoreaction, WO_x-TiO_2 powder was prepared by a sol-gel method. The WO_x-TiO_2 catalysts were characterized by XRD, XPS, SEM and SEM-EDX. The degradation of 4-methoxy-resorcinol by using

WO_x-TiO_2 under visible light irradiation was observed. Modified catalyst shows significant degradation efficiency under 419 nm light and longer wavelength (> 435 nm). The modification of TiO_2 by W shows its benefit of utilizing visible light for photocatalytic degradation of organic compounds. Differently prepared (incipient wetness method for P25 Degussa and PC 50 Millennium Chemical) WO_x-TiO_2 also shows similar effect of photo-activation by visible light. This is the first repot that directly compared the photocatalytic degradation efficiency between WO_x-TiO_2 prepared by traditional incipient wetness method and WO_x-TiO_2 by sol-gel method. WO_x-TiO_2 by sol-gel method consistently shows higher degradation efficiency (c.a. 20 %). This is possibly due to less formation of aggregate by WO_x-TiO_2 from sol-gel method. The future work could refine the degradation efficiency precisely by controlling the particle sizes, defective sites of TiO_2 and agglomerate size etc.

As we explored the photo-catalytic degradation of organic pollutants in aqueous system, we tried to maximize the advantageous approaching method from chemistry. Our research interest is different from engineering aspects, which mainly concern about optimizing degradation efficiency. Here, we tried to collect information about mechanisms of photo-catalytic degradation and degradation intermediates. The understanding of mechanisms of degradation of organic contaminants can assist us for the ascertaining of the better conditions to perform the mineralization of recalcitrant organic compounds. The photo-catalytic degradation of organic pollutants generally produces still harmful intermediates

before total mineralization. Therefore, the information of the degradation intermediates is also necessary to understand and characterize photo-catalytic degradation process. In addition to these mechanism and intermediate study, we could utilize various kinds of control experiments to clarify the major reactive species under photo-catalytic degradation conditions. This information is critically useful to propose reasonable degradation mechanism. We took advantage of chemical modification of TiO_2 based photo-catalysts was carried out in two ways. In one way, we modified adsorbed surface functional groups on TiO_2 from OH to F by adding fluoride ions in aqueous suspension at low pH. The addition of fluoride to aqueous suspensions of titania has proved to be an important mechanistic tool in unraveling a long-standing conundrum in photocatalytic degradation of cyanuric acid which was degraded only by free hydroxyl radical. In the other way, we modified TiO_2 by making composite semiconductor with W. This modification results in both retardation of fast recombination of photo activated electron/hole and absorption of visible light for activation of this composite semiconductor photo-catalyst. All above-mentioned strategies are well representing the characteristics of approaching method from chemistry.

APPENDIX

Millennium Inorganic chemical TiO_2

	Composition TiO_2 (%)	Specific surface area (BET), m^2/g	Average particle size	Agglomerate size	pH (10% aqueous slurry
PC 10	> 99	10.6	1.5 μm	N.A.	4.5-6.5
PC 50	98.2	50.1	20-30 nm	1.5 μm	2.5-4.5
PC 100	97.9 (anatase >99)	87	15-25 nm	1.2 μm	1.5-3.5
PC 500	82.8 (anatase >99)	335	5-10 nm	1.2-1.7 μm	4.0-8.0
DT 52	90 (TiO_2) (anatase) 10 (WO_3)	89	15-25 nm	0.5-2.9 μm	1.2-3.0

ACKNOWLEDGMENTS

I would like to thank Professor William S. Jenks for his support and guidance during my stay at Iowa State University. I appreciate his personal attention to my work and development of my career. His critical idea and thoughtful advice was guiding light for my research from the beginning and to the end.

I would like to express my thanks to Mrinmoy Nag, Ryan McCullar,Yun Bao, and Dr. Xiaoxing Li. Mrinmoy and Ryan were good friends to help me to survive from our Lab. They are exceptionally gentle and nice guys make me happy to be together. Dr. Li and Yun Bao lead my research with their previous wonderful work. Without their previous great work, I could not finish my thesis within allowed time.

I would also like to thank my family for their immeasurable support. Finally, I would like to thank my wife, Heaseong, for helping me and raising two kids, Seungjun and Jennifer wonderfully under difficult situation.